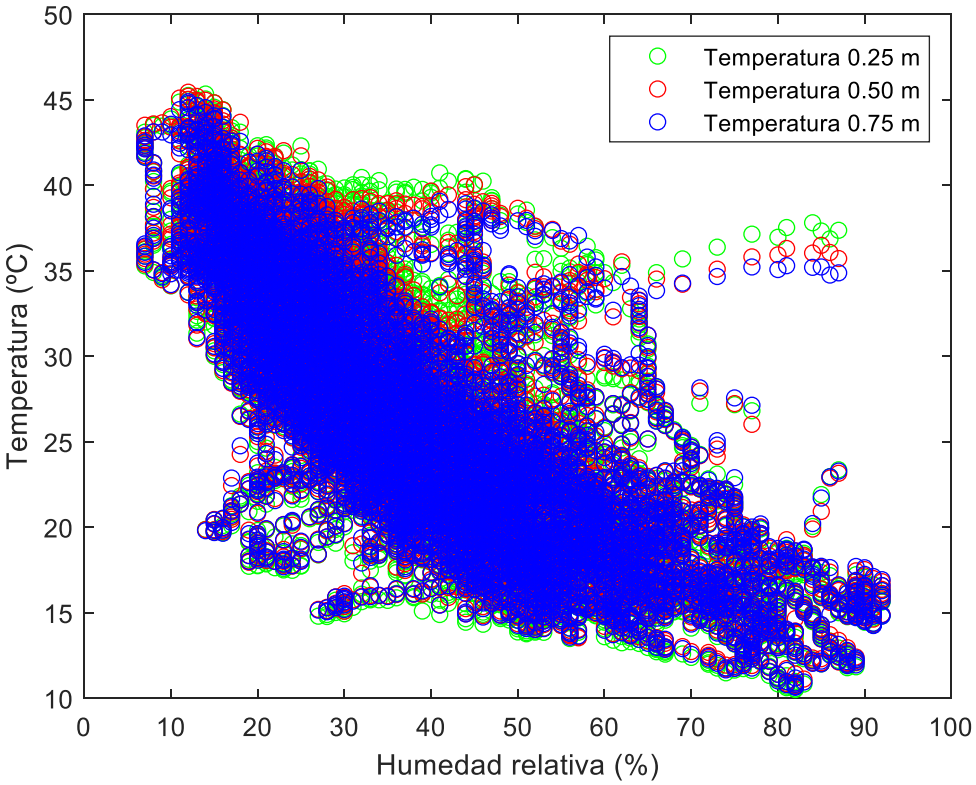

S-T: Fachada sur base de datos de temperatura diurnos y nocturnos

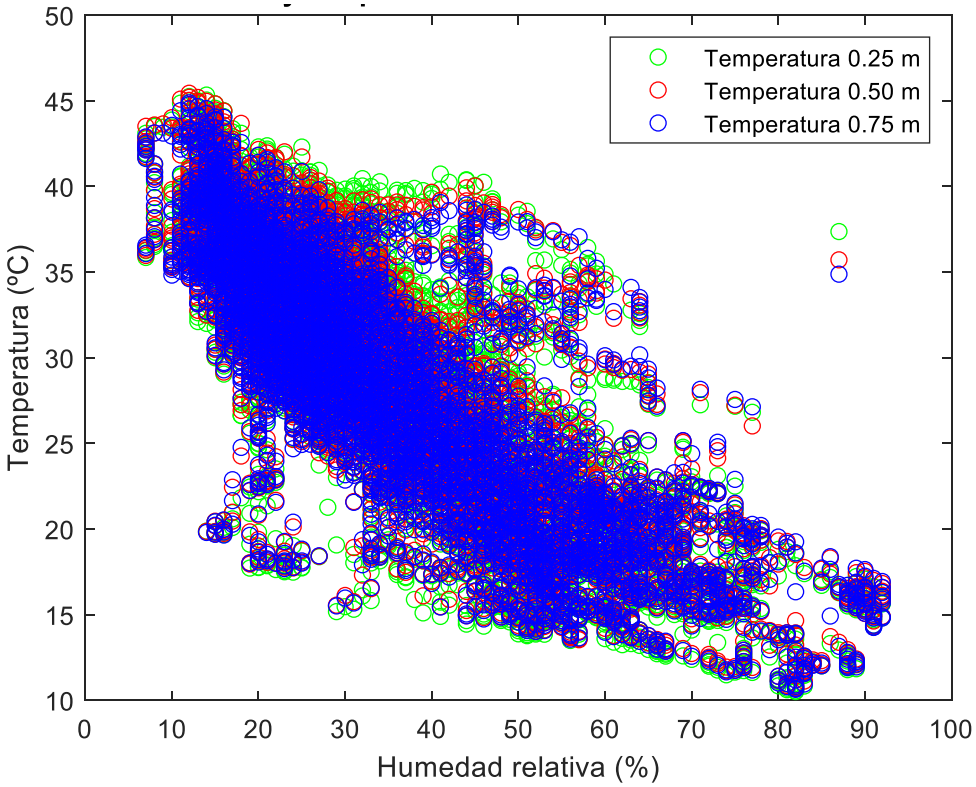

S-D: Fachada sur base de datos de temperatura diurnos (irradiancia > 0)

Figura 25: Correlaciones entre la humedad relativa y la temperatura de los sensores durante el verano

Tabla 9: Correlaciones entre la humedad relativa y la temperatura de los sensores durante el verano. Datos diurnos y nocturnos

	x	f(x)	Función	Coeficientes	R^2
Fachada Sur -Verano	HR	T 0.25 m	f(x) = p1*x^2 + p2*x + p3	p1 = 0.004718 p2 = -0.7851 p3 = 48.61	0.7311
	HR	T 0.50 m	f(x) = p1*x^2 + p2*x + p3	p1 = 0.004703 p2 = -0.7739 p3 = 48.07	0.7469
	HR	T 1.00 m	f(x) = p1*x^2 + p2*x + p3	p1 = 0.004576 p2 = -0.7528 p3 = 47.25	0.7548
Fachada Oeste - Verano	HR	T 0.25 m	f(x) = p1*x^2 + p2*x + p3	p1 = 0.005628 p2 = -0.8488 p3 = 48.21	0.7400
	HR	T 0.50 m	f(x) = p1*x^2 + p2*x + p3	p1 = 0.005223 p2 = -0.802 p3 = 47.32	0.7452
	HR	T 0.75 m	f(x) = p1*x^2 + p2*x + p3	p1 = 0.00512 p2 = -0.7974 p3 = 47.46	0.8870
	HR	T 1.00 m	f(x) = p1*x^2 + p2*x + p3	p1 = 0.005271 p2 = -0.818 p3 = 48.25	0.7475

Tabla 10: Correlaciones entre la humedad relativa y la temperatura de los sensores durante el verano. Datos diurnos.

	x	f(x)	Función	Coeficientes	R^2
Fachada Sur -Verano (solo día)	HR	T 0.25 m	f(x) = p1*x^2 + p2*x + p3	p1 = 0.00312 p2 = -0.6537 p3 = 47.41	0.7418
	HR	T 0.50 m	f(x) = p1*x^2 + p2*x + p3	p1 = 0.003706 p2 = -0.6931 p3 = 47.66	0.8106
	HR	T 1.00 m	f(x) = p1*x^2 + p2*x + p3	p1 = 0.003648 p2 = -0.6765 p3 = 46.84	0.8808
Fachada Oeste – Verano (solo día)	HR	T 0.25 m	f(x) = p1*x^2 + p2*x + p3	p1 = 0.004159 p2 = -0.7607 p3 = 41.51	0.2916
	HR	T 0.50 m	f(x) = p1*x^2 + p2*x + p3	p1 = 0.003757 p2 = -0.6886 p3 = 38.18	0.2760
	HR	T 0.75 m	f(x) = p1*x^2 + p2*x + p3	p1 = 0.003663 p2 = -0.6696 p3 = 37.27	0.2641
	HR	T 1.00 m	f(x) = p1*x^2 + p2*x + p3	p1 = 0.003566 p2 = -0.6511 p3 = 36.35	0.2538

- *Correlación entre la irradiancia y la temperatura de los sensores* en este caso, solo existe correlación entre la temperatura del aire y la irradiancia en el caso de la fachada sur en invierno (figura 26). En el resto de los casos los R^2 son inferiores a 0.5, no viéndose tendencias claras (tablas 11 – 14).

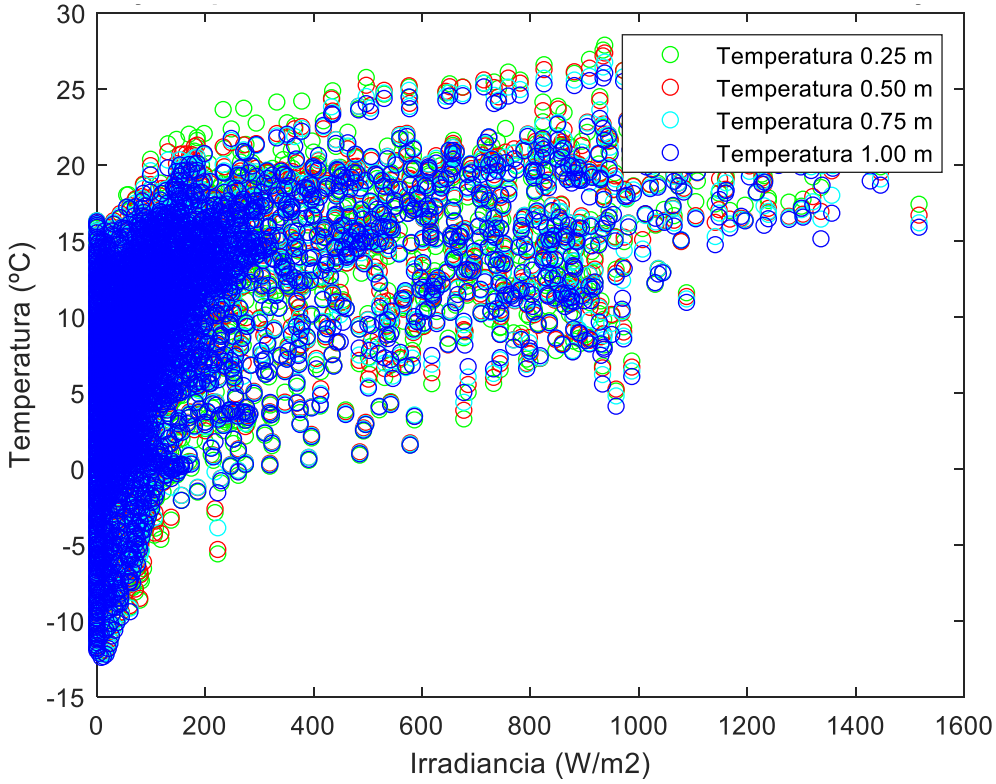

O-T: Fachada oeste base de datos de temperatura diurnos y nocturnos

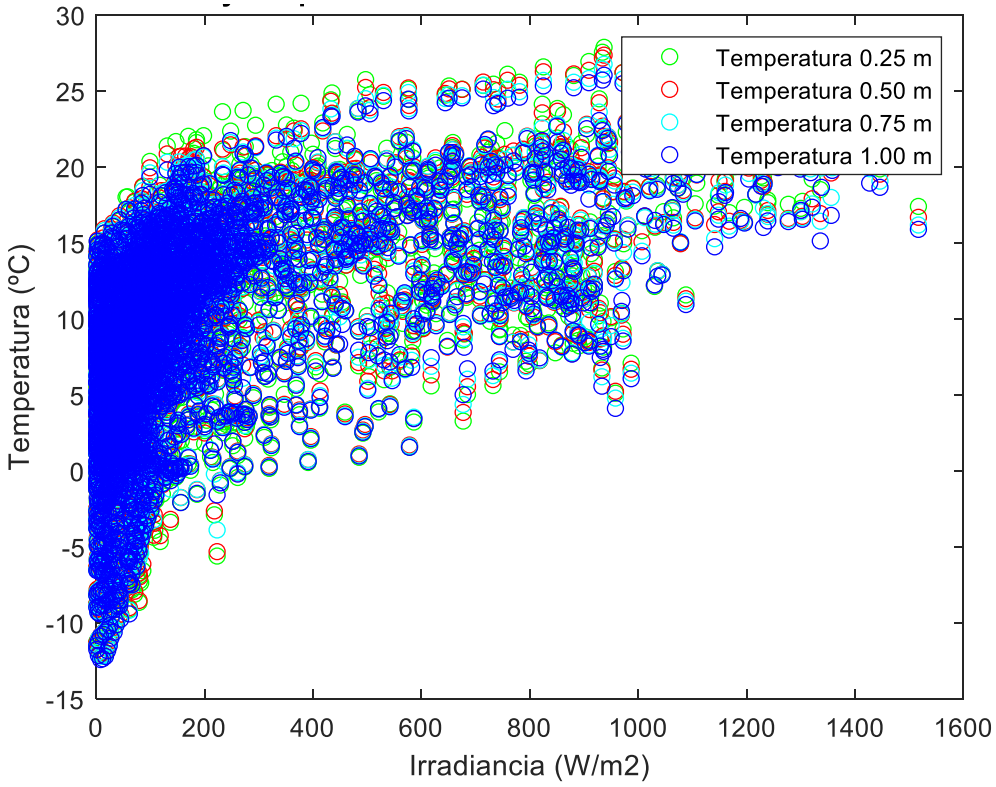

O-D: Fachada oeste base de datos de temperatura diurnos (irradiancia > 0)

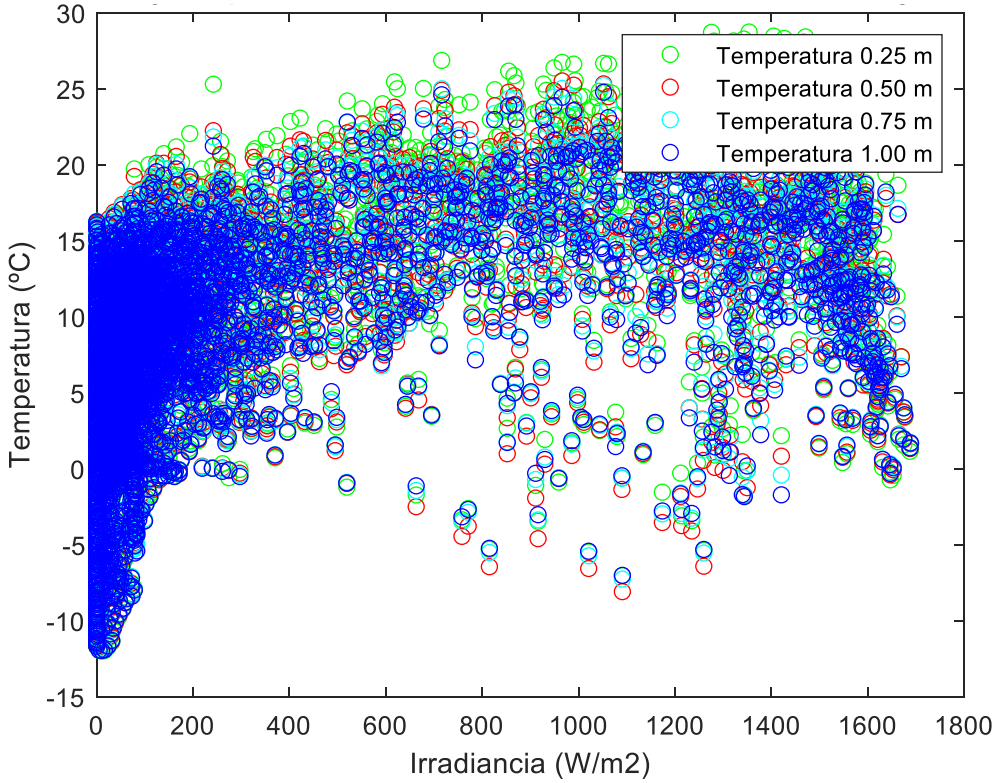

S-T: Fachada sur base de datos de temperatura diurnos y nocturnos

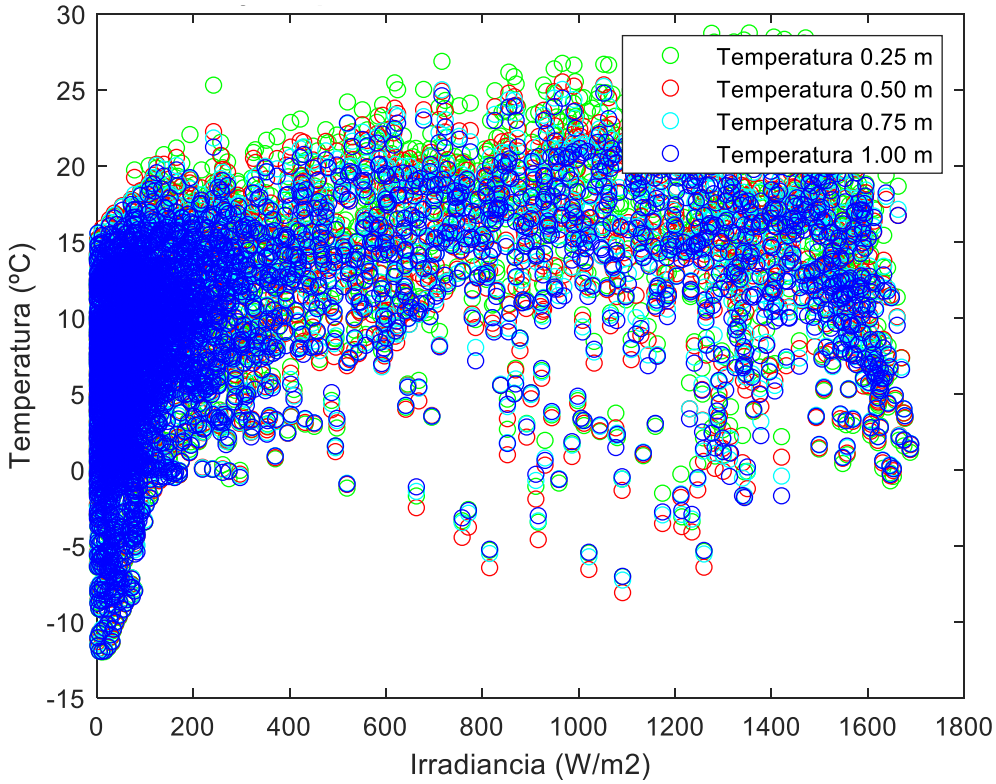

S-D: Fachada sur base de datos de temperatura diurnos (irradiancia > 0)

Figura 26: Correlaciones entre la irradiancia y la temperatura de los sensores durante el invierno

Tabla 11: Correlaciones entre la irradiancia y la temperatura de los sensores durante el invierno.

Datos diurnos y nocturnos.

	x	f(x)	Función	Coeficientes	R^2
Fachada Oeste - Invierno	Irradiancia	T 0.25 m	f(x) = p1*x^2 + p2*x + p3	p1 = -1.934e-05 p2 = 0.03232 p3 = 4.782	0.2548
	Irradiancia	T 0.50 m	f(x) = p1*x^2 + p2*x + p3	p1 = -1.968e-05 p2 = 0.03234 p3 = 4.953	0.2510
	Irradiancia	T 0.75 m	f(x) = p1*x^2 + p2*x + p3	p1 = -2.067e-05 p2 = 0.03309 p3 = 4.946	0.2520
	Irradiancia	T 1.00 m	f(x) = p1*x^2 + p2*x + p3	p1 = -2.109e-05 p2 = 0.03328 p3 = 4.902	0.2490
Fachada Sur - Invierno	Irradiancia	T 0.25	f(x) = p1*x^2 + p2*x + p3	p1 = -1.346e-05 p2 = 0.02769 p3 = 5.26	0.3247
	Irradiancia	T 0.50	f(x) = p1*x^2 + p2*x + p3	p1 = -1.183e-05 p2 = 0.02337 p3 = 6.176	0.7297
	Irradiancia	T 0.75	f(x) = p1*x^2 + p2*x + p3	p1 = -1.202e-05 p2 = 0.02345 p3 = 6.166	0.8453
	Irradiancia	T 1.00	f(x) = p1*x^2 + p2*x + p3	p1 = -1.202e-05 p2 = 0.02319 p3 = 6.125	0.3738

Tabla 12: Correlaciones entre la irradiancia y la temperatura de los sensores durante el invierno.

Datos diurnos.

	x	f(x)	Función	Coeficientes	R^2
Fachada Oeste - Invierno	Irradiancia	T 0.25 m	f(x) = p1*x^2 + p2*x + p3	p1 = -1.559e-05 p2 = 0.02784 p3 = 5.848	0.3457
	Irradiancia	T 0.50 m	f(x) = p1*x^2 + p2*x + p3	p1 = -1.567e-05 p2 = 0.02754 p3 = 6.072	0.3383
	Irradiancia	T 0.75 m	f(x) = p1*x^2 + p2*x + p3	p1 = -1.628e-05 p2 = 0.02787 p3 = 6.125	0.3271
	Irradiancia	T 1.00 m	f(x) = p1*x^2 + p2*x + p3	p1 = -1.665e-05 p2 = 0.028 p3 = 6.104	0.3235
Fachada Sur - Invierno	Irradiancia	T 0.25 m	f(x) = p1*x^2 + p2*x + p3	p1 = -1.14e-05 p2 = 0.02398 p3 = 6.429	0.8699
	Irradiancia	T 0.50 m	f(x) = p1*x^2 + p2*x + p3	p1 = -1.064e-05 p2 = 0.0215 p3 = 6.567	0.9017
	Irradiancia	T 0.75 m	f(x) = p1*x^2 + p2*x + p3	p1 = -1.08e-05 p2 = 0.02159 p3 = 6.56	0.7703
	Irradiancia	T 1.00 m	f(x) = p1*x^2 + p2*x + p3	p1 = -1.109e-05 p2 = 0.02159 p3 = 6.508	0.8951

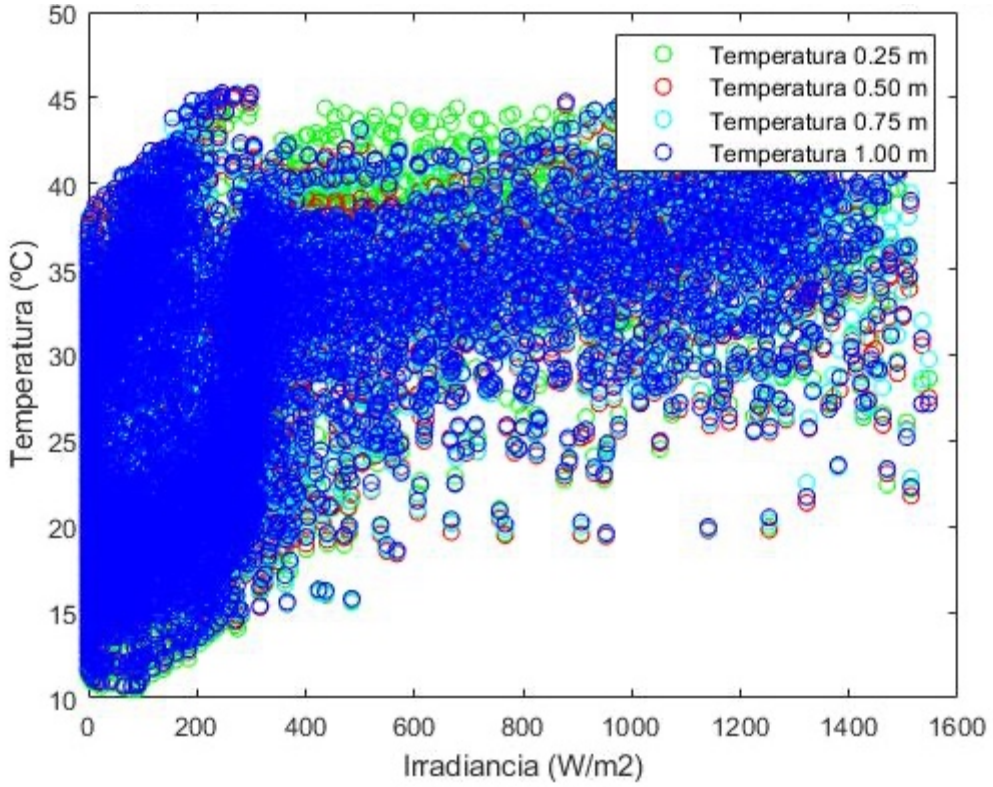

O-T: Fachada oeste base de datos de temperatura diurnos y nocturnos

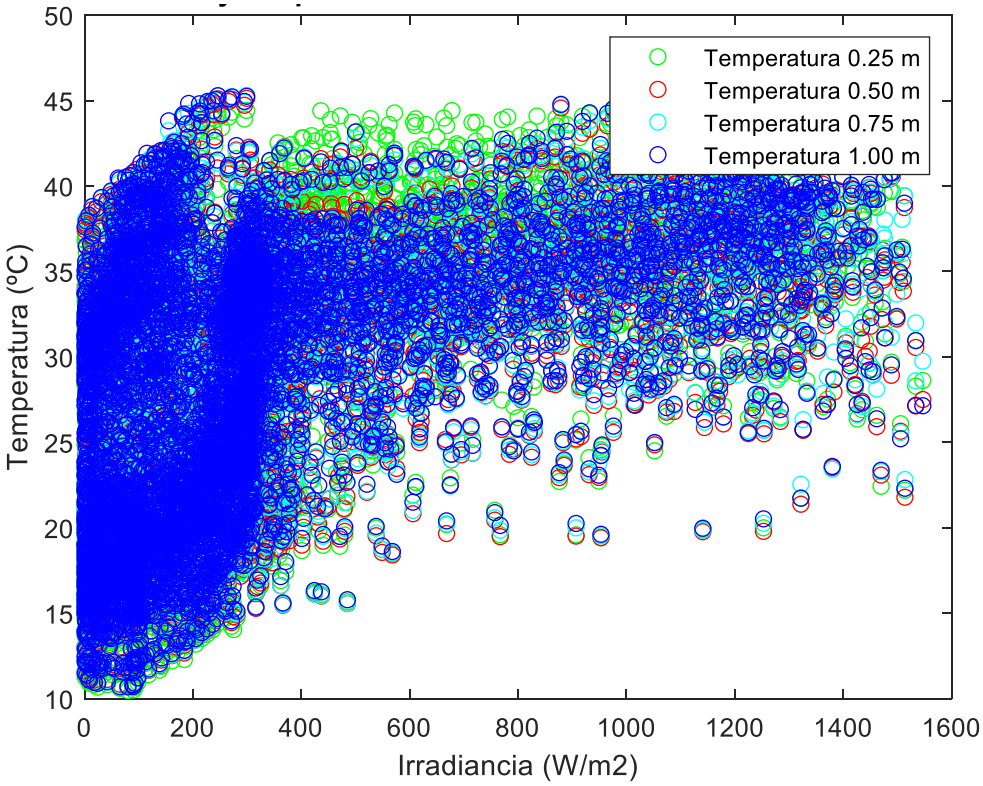

O-D: Fachada oeste base de datos de temperatura diurnos (irradiancia > 0)

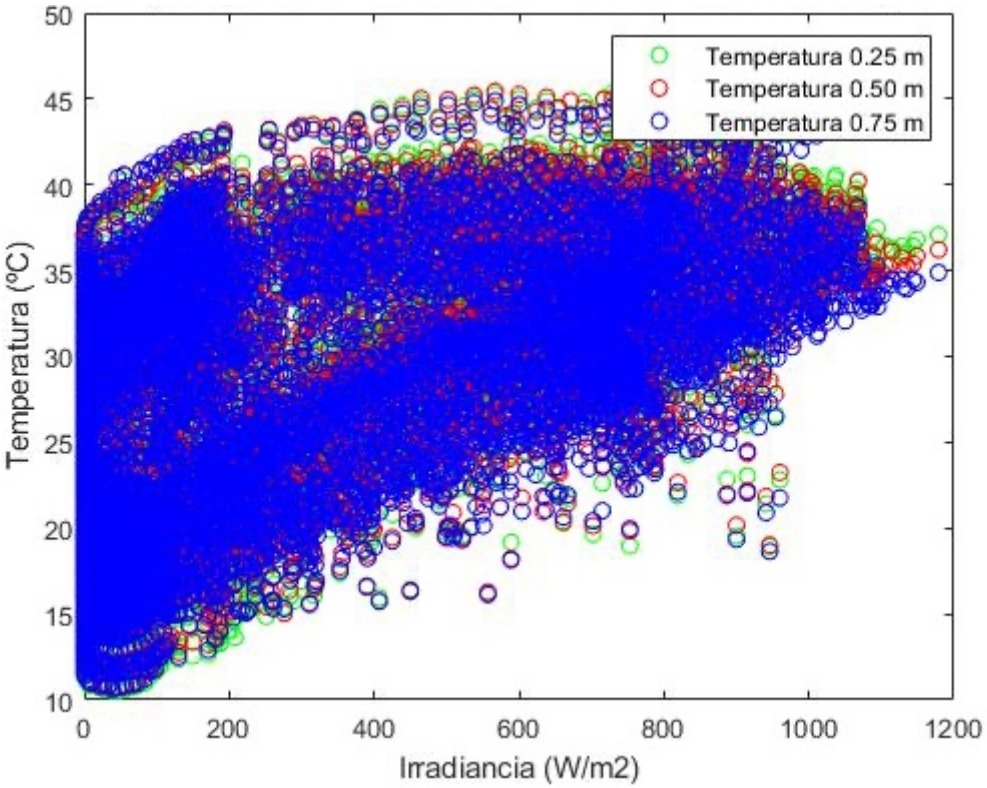

S-T: Fachada sur base de datos de temperatura diurnos y nocturnos

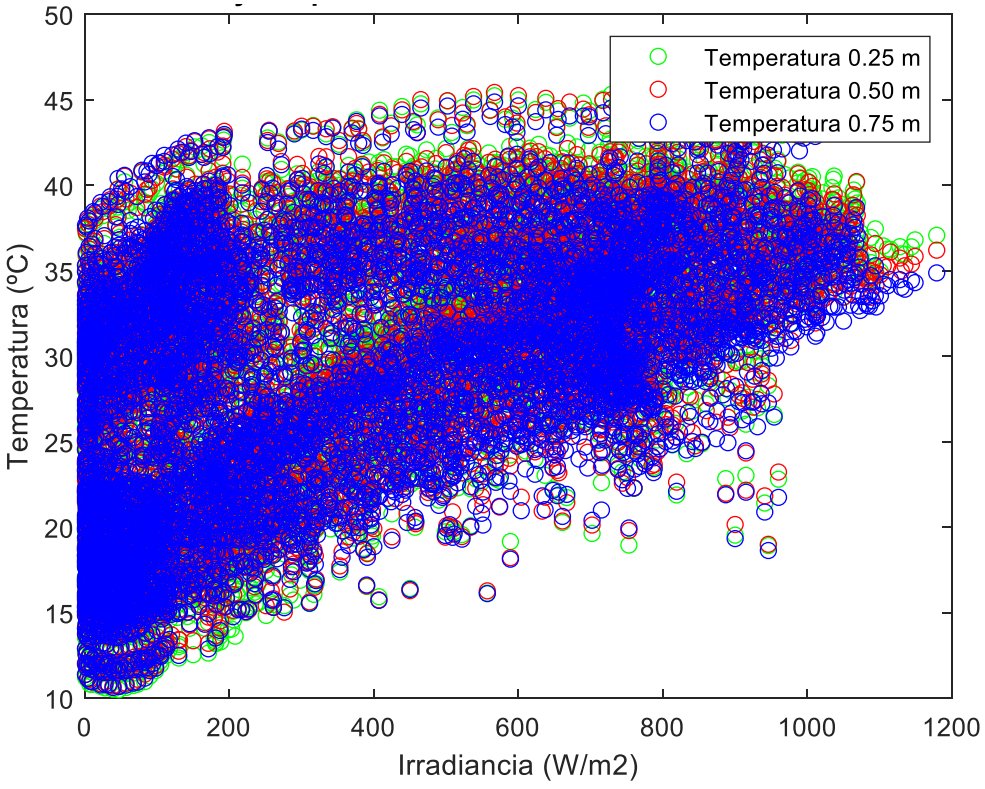

S-D: Fachada sur base de datos de temperatura diurnos (irradiancia > 0)

Figura 27: Correlaciones entre la irradiancia y la temperatura de los sensores durante el verano

Tabla 13: Correlaciones entre la irradiancia y la temperatura de los sensores durante el verano.

Datos diurnos y nocturnos

	x	f(x)	Función	Coeficientes	R^2
Fachada Oeste - Verano	Irradiancia	T 0.25 m	f(x) = p1*x^2 + p2*x + p3	p1 = -1.098e-05 p2 = 0.02589 p3 = 21.74	0.3913
	Irradiancia	T 0.50 m	f(x) = p1*x^2 + p2*x + p3	p1 = -8.631e-06 p2 = 0.02205 p3 = 22.29	0.3474
	Irradiancia	T 0.75 m	f(x) = p1*x^2 + p2*x + p3	p1 = -9.54e-06 p2 = 0.02319 p3 = 22.39	0.3512
	Irradiancia	T 1.00 m	f(x) = p1*x^2 + p2*x + p3	p1 = -1.113e-05 p2 = 0.02502 p3 = 22.43	0.3557
Fachada Sur - Verano	Irradiancia	T 0.25 m	f(x) = p1*x^2 + p2*x + p3	p1 = -1.417e-05 p2 = 0.02809 p3 = 22.13	0.4677
	Irradiancia	T 0.50 m	f(x) = p1*x^2 + p2*x + p3	p1 = -1.33e-05 p2 = 0.02613 p3 = 22.33	0.4280
	Irradiancia	T 1.00	f(x) = p1*x^2 + p2*x + p3	p1 = -1.285e-05 p2 = 0.02441 p3 = 22.43	0.3815

Tabla 14: Correlaciones entre la irradiancia y la temperatura de los sensores durante el verano.

Datos diurnos.

	x	f(x)	Función	Coeficientes	R^2
Fachada Oeste - Verano	Irradiancia	T 0.25 m	f(x) = p1*x^2 + p2*x + p3	p1 = -1.16e-05 p2 = 0.0268 p3 = 21.52	0.3396
	Irradiancia	T 0.50 m	f(x) = p1*x^2 + p2*x + p3	p1 = -8.109e-06 p2 = 0.02128 p3 = 22.48	0.2925
	Irradiancia	T 0.75 m	f(x) = p1*x^2 + p2*x + p3	p1 = -8.626e-06 p2 = 0.02184 p3 = 22.71	0.2870
	Irradiancia	T 1.00 m	f(x) = p1*x^2 + p2*x + p3	p1 = -9.927e-06 p2 = 0.02324 p3 = 22.86	0.2801
Fachada Sur - Verano	Irradiancia	T 0.25 m	f(x) = p1*x^2 + p2*x + p3	p1 = -1.33e-05 p2 = 0.02712 p3 = 22.35	0.3824
	Irradiancia	T 0.50 m	f(x) = p1*x^2 + p2*x + p3	p1 = -1.111e-05 p2 = 0.02367 p3 = 22.87	0.3311
	Irradiancia	T 1.00 m	f(x) = p1*x^2 + p2*x + p3	p1 = -9.873e-06 p2 = 0.02106 p3 = 23.17	0.2791

Los resultados de esta segunda fase del estudio demostraron correlaciones fuertes entre la temperatura de los sensores y la temperatura del aire, especialmente durante el verano. En el caso de la humedad relativa, las correlaciones no son significativas y, en algunos casos, negativas, lo que explica la reducción de temperaturas debido al aumento de la humedad relativa. Finalmente, en el caso de la irradiancia, no existen correlaciones estadísticamente significativas, lo que demuestra que no es una variable que condicione el comportamiento de la fachada y se descarta en los siguientes análisis. Este estudio no cuantifica la influencia de una variable sobre otra, por lo que se estimó necesario realizar un análisis de varianza (ANOVA).

- ***ANOVA simple***

  El tercer paso de este estudio comprende el desarrollo de un análisis de varianza simple (ANOVA), el cual compara la media de tres o más grupos de datos de forma cuantitativa, comprobando la igualdad de medias de la variable independiente. En este estudio la variable independiente es la distancia, mientras que la variable dependiente será la temperatura y la humedad relativa.

  Los resultados de este análisis nos permiten comparar los distintos valores medios de temperatura y humedad relativa para determinar si difieren significativamente del resto, y, por tanto, resolver la pregunta del estudio sobre la influencia de la distancia en la capacidad de reducción de temperaturas. Estas hipótesis se comprueban a partir de dos valores:

  - *Coeficiente F:* muestra cuán dispersos están los datos con respecto a la media. Los valores más altos representan mayor dispersión.

- *P-valor:* es un valor de probabilidad que oscila entre 0 y 1. Ayuda a diferenciar resultados que son producto del azar del muestreo, de resultados que son estadísticamente significativos. Por ejemplo, cuando el valor es inferior a 0.05, demuestra que no se cumple la hipótesis nula con una probabilidad superior al 95% y, por tanto, los resultados son estadísticamente significativos con ese nivel de confianza del 95%.

A continuación, se explican los resultados obtenidos a partir de ambos ANOVA:

- *ANOVA de temperatura*

En este primer análisis de varianza el coeficiente F oscila entre 1.73 y 13.99, lo que muestra una varianza significativa entre las medias de cada distribución. Por otro lado, el P-valor es inferior a 0.001, lo que significa que la diferencia estadística es significativa con una confianza del 99.9%.

En la (Tabla 15) se muestra un procedimiento de comparación múltiple para determinar qué medias son significativamente diferentes de las demás, y cuál es la diferencia cuantitativa. Los resultados muestran que, para la fachada sur, las temperaturas disminuyen con la distancia para todas las estaciones, siendo estadísticamente significativas para todas las distancias en verano, y para los casos de 0.25 - 0.50m y 0.25 - 1.00m en invierno.

Tabla 15: Diferencias de temperatura para cada distancia, incluida su significación estadística, en las fachadas sur y oeste *(se coloca un asterisco junto a los pares que no muestran diferencias estadísticamente significativas)*

	ΔT (°C) (0.25-0.50)	**ΔT (°C) (0.50-0.75)**	**ΔT (°C) (0.50-1.00)**	**ΔT (°C) (0.75-1.00)**	**ΔT (°C) (0.25-1.00)**
Fachada oeste (verano)	0.050*	-0.30	-0.61	-0.31	-0.56
Fachada oeste (invierno)	-0.17*	-0.07*	-0.03*	0.04*	-0.20*
Fachada sur (verano)	0.24	-	0.38	-	0.63
Fachada sur (invierno)	0.36	0.05*	0.18*	0.13*	0.54

Estos resultados llevan a concluir que el jardín vertical reduce las temperaturas hasta 1.00 m de distancia durante invierno y verano; la fachada sur registra durante el verano reducciones de hasta 0.63 ºC entre el sensor a 0.25 m y el situado a 1.00 m, mientras que en el invierno se alcanzan reducciones de 0.54 ºC; en la fachada oeste las temperaturas aumentan tanto en invierno como en verano, con significación estadística en verano para todas las distancias menos entre 0.25 y 0.50 m. El aumento entre el sensor a 0.25 y 1.00 m es de 0.56 ºC.

- *ANOVA de humedad relativa (HR)*

  En este análisis dado que los coeficientes F son elevados en todos los casos, y el P-valor es también inferior a 0.0000, puede concluirse que el jardín vertical influye en la humedad relativa con significación estadística en ambas estaciones y en ambas orientaciones.

  En la fachada sur en invierno, la HR disminuye con la distancia con una reducción total del 2.3% entre los sensores a 0.25 y 1.00 m, lo que constituye una mejora del confort térmico. En verano, se produce un aumento de la HR del 0.66% en el

primer tramo evaluado (0.25 – 0.50 m), mientras que en los tramos subsiguientes (0.5 – 1.00 m) se produce una disminución significativa del 1.52%, produciendo una reducción total del 0.9% entre los extremos (Tabla 16)

En la fachada oeste, el comportamiento es el contrario, ya que, tanto en invierno como en verano, la HR aumenta con la distancia, probablemente debido al menor número de horas de radiación solar directa. En verano, se produce un aumento estadísticamente significativo del 1.5% entre 0.25 y 0.5m, mientras que la HR disminuye un 0.9% en los siguientes tramos analizados (0.5 – 1.00 m), lo que supone un aumento total del 0.6% entre los extremos. Del mismo modo, en invierno, la HR aumenta 1.9% entre 0.25 y 0.5 m, mientras que disminuye un 0.9% en el último tramo (0.5 – 1.00 m), con un aumento total de 1% entre 0.25 y 1.00 m (Tabla 16)

Tabla 16: Diferencias de humedad relativa para cada distancia, incluida su significación estadística, en las fachadas sur y oeste *(se coloca un asterisco junto a los pares que no muestran diferencias estadísticamente significativas)*

	ΔHR (%) (0.25-0.50)	**ΔHR (%) (0.25-0.75)**	**ΔHR (%) (0.50-0.75)**	**ΔHR (%) (0.50-1.00)**	**ΔHR (%) (0.75-1.00)**	**ΔHR (%) (0.25-1.00)**
Fachada oeste (verano)	1.46245	0.946474	-0.515971*	-0.905041	-0.38907*	0.557404*
Fachada oeste (invierno)	1.90672	1.44352	-0.463206*	-0.859108	-0.395901*	1.04761
Fachada sur (verano)	0.663387	-	-	-1.52276	-	-0.859369
Fachada sur (invierno)	-0.761241	-1.10295	-0.34171*	-1.53717	-1.19546	-2.29841

Estos resultados llevan a concluir que el jardín vertical condiciona el porcentaje de humedad relativa hasta 1.00 m de distancia. En el caso de la fachada sur, se reduce en ambas estaciones, y en la fachada oeste aumenta.

Se concluye que el jardín vertical reduce la temperatura con significación estadística, siendo mayor en la fachada sur. Esta reducción se traduce a 0.63 °C en verano y 0.54 °C en invierno, entre el sensor situado a 0.25 y el sensor a 1.00 m del jardín vertical, mientras que en la fachada oeste se encontraron reducciones de 0.56 °C en verano. Los resultados obtenidos a partir de esta investigación demuestran que el módulo de jardinería vertical puede mejorar el microclima urbano y, por ende, el confort a nivel peatonal sobre todo durante el verano.

Artículo 5

Assessment of the impact of green walls on urban thermal comfort in a Mediterranean climate

Valentina Oquendo-Di Cosola, Francesca Olivieri, Lorenzo Olivieri, Luis Ruiz-García.

Energy and Building, 296, 113375.

DOI: https://doi.org/10.1016/j.enbuild.2023.113375

Q1 (JCR)

Assessment of the impact of green walls on urban thermal comfort in a Mediterranean climate

Authors: Oquendo-Di Cosola Valentina.[1]*, Olivieri Francesca.[1], Olivieri Lorenzo.[1], Ruiz-García Luis.[2].

[1]: Departamento de Construcción y Tecnología Arquitectónicas, Escuela Técnica Superior de Arquitectura, Universidad Politécnica de Madrid, Av. Juan de Herrera 4, 28040, Madrid, Spain.
[2]: Departamento de Ingeniería Agroforestal, Universidad Politécnica de Madrid, Av. Complutense s/n, 28040, Madrid, Spain.

Abstract: A study has been performed to quantify the impact of a green wall temperature reduction in a continental Mediterranean climate. This paper presents the results of a monitoring campaign during the summer and winter of 2021-2022. First, a database was elaborated with information on air temperature and relative humidity at four different distances from the wall (0.25, 0.50, 0.75, and 1 m) and irradiance in the vertical plane. Secondly, a statistical analysis was carried out to determine whether there is a correlation between these variables and whether there are statistically significant differences between them at different distances from the wall. Results show a strong positive correlation between air temperature recorded by sensors and the ambient air temperature for all seasons and between air temperature and relative humidity in summer. The ANOVA shows that the green wall reduces the temperature and relative humidity with statistical significance for most of the cases. These results confirmed the great capacity of green walls to improve the urban microclimate, especially during summer, by reducing air temperatures, providing evidence that greening the building envelope can complement conventional city green infrastructure and provide multiple ecosystem services to dense urban contexts.

Keywords: Vegetation; Green wall; Urban microclimate; Outdoor thermal comfort; Temperature reduction.

1. Introduction

The accelerated urbanisation of territories has led to the concentration of most of the world's population in cities. The associated urban development and population growth have resulted in significant public health consequences linked to climate change. It has triggered a strong interest in finding solutions to help overcome the adverse effects of air pollution, environmental noise, or thermal conditions in cities.

The urban heat island effect (UHI) is urbanization's most apparent climate consequence, contributing to increased city temperatures. Recent studies on air temperature variation in urban environments have shown that this phenomenon can occur in isolation with greater or lesser intensity at specific locations in the same space, with a significant difference between air temperature and land temperature of up to 4.2 °C for air temperature and 8 °C for land temperature. Furthermore, it has been shown that the temperature increase is conditioned by the landscape and climatological parameters of the location, which play an essential role in temperature regulation (Amani-Beni et al., 2022). It affects urban comfort (Chun and Guldmann, 2018), energy consumption in buildings (Zhang et al., 2019), and pollutant concentration (Charoenkit and Yiemwattana, 2016b). Moreover, actions to create cool-summer urban microclimates should take into account that each type of urban development is thermally affected by different sets of spatial variables (Chen et al., 2023).

The growing interest in outdoor thermal comfort research is mainly due to the high health risks caused by climate change and the increase in global temperatures. The correlation between thermal comfort and mortality rates in a city has been more than proven (Shafiee et al., 2020). An example may be the heat waves suffered in Spain during the summer of 2022, which, according to the World Health Organisation, left a death toll of 4000 and 15000 in Europe. Despite this reality, the complex interaction between several variables in outdoor spaces, where conditions are not controllable, poses a significant challenge in finding a pattern of behaviour and practical solutions to improve the thermal conditions of the urban environment.

If we consider that thermal comfort can be defined from the psychological aspect (the mental expression of satisfaction with the thermal conditions of the environment); the thermophysiological aspect (contributing to the biological reactions and thermal receptors of the skin to the environment); and the energetic aspect (light flow to and from the human body), it could be stated that hygrothermal comfort can be modified using materials and surfaces that contribute to balancing the thermal balance of urban space.

The relationship between urban design and thermal comfort has been the subject of much research in recent years, some of which have focused on the effect that several aspects of urban space have on the magnitude of solar radiation and its effect on pedestrian comfort (Castaldo et al., 2018). The contribution of vegetation to this balance has been studied in urban parks, gardens, roofs, and green walls (Taleghani, 2018b). It has resulted in developing solutions that create comfortable urban areas, including green walls that can absorb large amounts of solar radiation to grow plants and their biological functions (Krusche, P., Krusche, M., Althaus, D., Gabriel, 1982).

The thermoregulatory capacity of the vegetation will depend on factors such as climate, type and mass of vegetation, and proper irrigation, among others. Irrespective of the characteristics and configuration of the vegetation, this is mainly due to two mechanisms: shading, which reduces the solar radiation, and evapotranspiration, in which the heat absorbed by plants and the substrate is dissipated through water loss by transpiration and evaporation (Charoenkit and Yiemwattana, 2016b). Regarding the specific effect of plant leaves, studies have shown that the development of the plant and its percentage cover is statistically decisive for the reduction of temperatures (Koyama et al., 2013).

As shown by (Oquendo-Di Cosola et al., 2022), the combined effect of shade and evapotranspiration can reduce the air temperature by up to 3 °C, depending on the climate and substrate conditions (Wong et al., 2016). Similarly, in a humid subtropical climate, the effect of shade on reducing the temperature of the adjacent environment could be between 1.1 and 1.5 °C compared to the air temperature. (Zhang et al., 2019) estimated the thermal effect of plant

physiological activities and evaluated the overall effects in indoor and outdoor environments in humid subtropical climates through research on the thermal equilibrium of vegetation, showing a reduction of 2.7 °C compared to the air temperature. The main reasons were: (i) solar radiation absorption, (ii) heat transfer by convection between foliage and air, (iii) transpiration in plant leaves, and (iv) thermal effects of photosynthesis. However, most studies were conducted only during the summer.

Studying the influence of green walls on the adjacent microclimate requires an accurate assessment of the orientation and type of walls and the distance at which the data are collected. Previous studies concluded the following:

- Green walls may not have any cooling effect on the surrounding microenvironment at a distance greater than 1 m (Razzaghmanesh and Razzaghmanesh, 2017b).
- A decrease of up to 3.3 °C can be reached at 15 cm from the plant façade due to evapotranspiration (Nyuk Hien Wong et al., 2010a).
- Temperature differences between a green wall (in three façades of different plants) and a bare wall were up to 1.7 °C for direct systems and up to 8.4 °C for living wall systems (modular) after 8 hours of solar incidence (Ottelé and Perini, 2017).
- Reduction of up to 8 °C in the air cavity after vegetation and a reduction of an air temperature of up to 4 °C in humid and warm climates such as Malaysia (Safikhani et al., 2014).
- The shade generated by green walls on the walls of buildings and the microclimate generated in the cavity between the green wall and the building impacts temperature reduction in the Mediterranean climate (Pérez et al., 2011).
- Continuous green walls can achieve temperature reduction of the adjacent air between 2 °C and 5 °C, while modular green walls with substrate reach much higher reductions between 10 °C and 14 °C (Oquendo-Di Cosola et al., 2022).
- Other variables can affect the behaviour of green walls both in terms of performance and environmental sustainability (Oquendo-Di Cosola et al., 2020): climate (Olivieri et al., 2017), system design and components (Jim, 2015b), irrigation and fertilisation system

(Charoenkit and Yiemwattana, 2016b), and type of plants and substrate (Charoenkit et al., 2020).

1.1 Scope of the study

Most of the studies reviewed have concentrated on analysing the evidence on the cooling effects of green infrastructure (green walls, green roofs, trees, and shrubs), providing general suggestions for more effective implementation strategies. For green walls, most studies are experiments with prototypes developed for data collection and testing of surface temperature reduction and the effect this has indoors.

Considering the limited knowledge of the influence of distance as a determining variable in assessing the impact of green walls on urban comfort in a Mediterranean climate and the evaluation of its performance at scale and in real conditions, the objectives of this study were: (1) to determine if a green wall can improve the urban microclimate at the pedestrian level in a Mediterranean climate, and (2) to identify if the distance from the green wall is a variable that affects the impact of temperature reduction at the pedestrian level.

In order to achieve the proposed objectives, this research analyses real data obtained from façade monitoring. The results aim to quantify the impact of green walls on temperature reduction at the pedestrian level, considering the effect of some parameters such as temperature, relative humidity, and irradiance.

2. Materials and methods

2.1. itdUPM building

The Innovation and Technology for Development Center (itdUPM) building at the Technical University of Madrid (UPM) was developed to create the first building with almost zero energy consumption inside the campus. The building includes a drilled metal plate skin covering all façades, leaving an air gap between the concrete wall and the mentioned skin of 20 cm. Additionally, some parts of the skin are covered by a green wall. The building uses passive strategies to reduce energy consumption and increase thermal comfort indoors and outdoors.

The integration of a green wall in the south (11.25 m^2), east (6.25 m^2), and west (10 m^2) façade was part of these strategies (see Fig.1).

Figure 1: Green walls installed in the itdUPM building used for the study

The green wall installed is a modular system called BIOFIVER (Morales, 2012). It comprises two three-dimensional structures of polypropylene cells, separated by a hydrophilic polyester fabric (see Table 1 for a detailed list of the components). The dimension of each module is 50 cm x 50 cm x 10 cm and is filled in with organic substrate enriched for the cultivation of plants selected based on their adaptation to the climate in which they are located.

Table 1: Characteristics of the green wall module used in (BIOFIVER)

System components and characteristics	Description
Polyethylene module	50 cm x 50 cm x 10 cm
Weight without plants	2 kg/module
Weight at half saturation	3.40 kg/module
Weight at total saturation	5.60 kg/module
Number of plants	12 per module
External finishing layer	Polyester
Bearing structure	Polypropylene boxes
Hydrophilic layer	Polyester
Growing medium	Coconut fibre, turf, and humus
Hooking system	Hooking brackets in aluminium and galvanised steel

The plants selected for the itdUPM building were: *Heuchera americana "dale's strain"; Sedum acre "golden carpet; Sedum album "coral carpet"; Thymus communis; Lonicera nitida "maigrun"; Heuchera americana "palace purple"; Carex oshimensis; Delosperma cooperi; Gazania rigens; Thymus vulgaris*. They are precultivated and inserted into gaps. The rear structure remains empty, generating a hollow space for air circulation (Fig. 2). The green wall has an exudation irrigation system that allows the entire surface to have the same amount of water at any point. It favours that the necessary irrigation for the green wall can be easily calculated. The number of plants installed per module is 16, i.e., 64 per m^2.

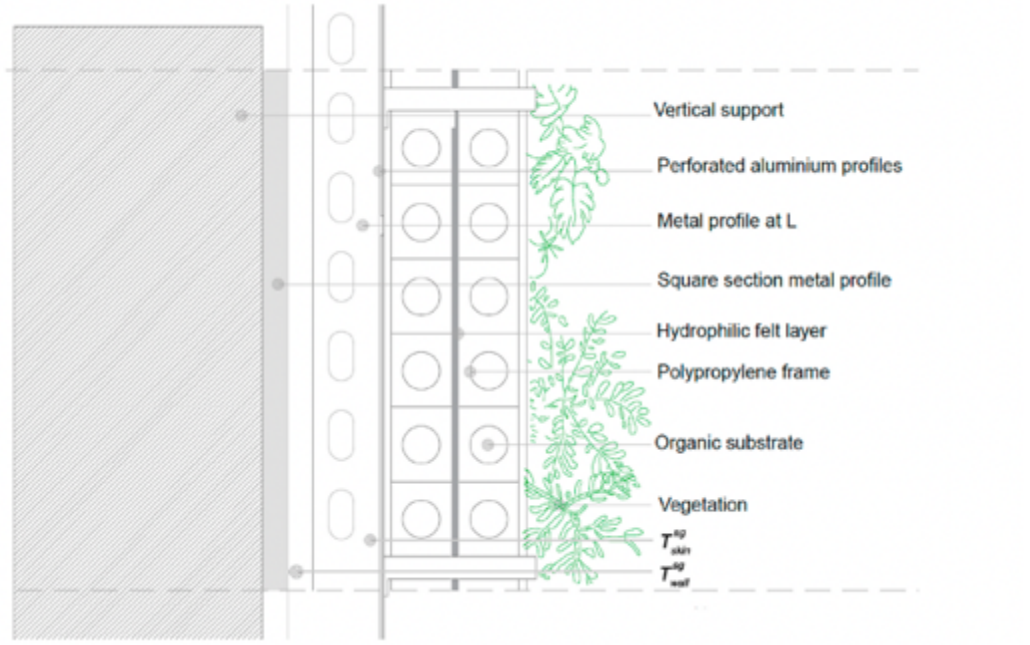

Figure 2: Section detail of the green wall installed in the itdUPM used for the study

2.2 Monitoring system

A real-time distributed monitoring system has been installed to analyse the behaviour of the south and west façades. The monitoring system is based on eight sets of HOBO MX2301 data loggers with internal temperature and relative humidity probes, with a temperature precision of ±0.25 °C from -40 to 0 °C; ±0.2 °C from 0 to 70 °C; and ±0.25 °C from 70 to 100 °C, and a relative humidity precision of ±2.5% from 10% to 90% (typical) to a maximum of ±3.5% including hysteresis at 25 °C; below 10% RH and above 90% RH ±5% typical.

Two solar radiation sensors (pyranometers), series SP-100 and SP-200 from Sensovat were installed on both façades to measure the solar radiation incident on the vertical surface. Lastly, a weather station was set up nearby to collect the meteorological parameters, including ambient air temperature, relative humidity, solar radiation, wind speed, wind direction, and rainfall.

The data obtained from the analysis performed in Section 3 are gathered from December 2020 until February 2021 for winter and from June until August 2021 for summer, although monitoring is still ongoing. The time series data set comprises more than 50.000 samples with 10 minutes sampling period. Measurements of air temperature and relative humidity are taken at 4 points in

each façade. Data loggers were placed in front of the green wall and secured to a customised structure at intervals of 0.25m, 0.50m, 0.75m, and 1.00 m away from the vegetation (Fig. 3).

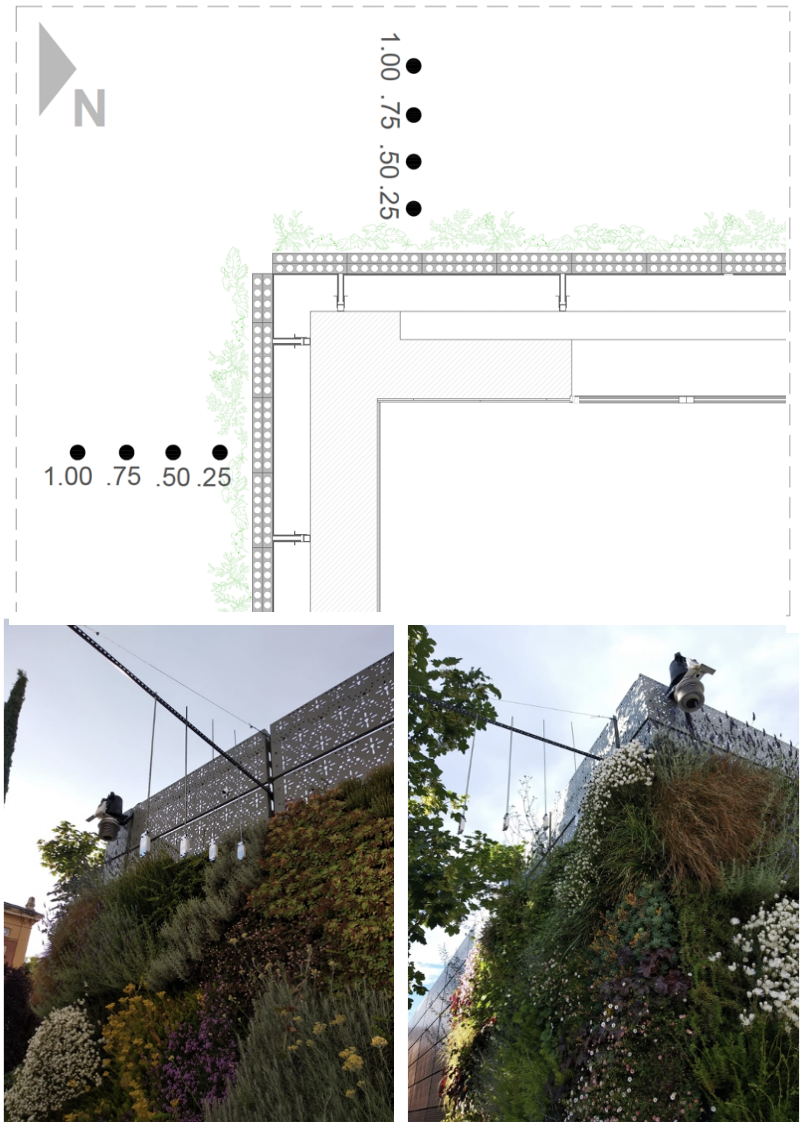

Figure 3: Distribution of sensors, pyranometers, and weather station on the west and south façades of the itdUPM building

2.3 Methods for data analysis

The data analysis of the study is structured in 3 phases (Figure 4): (i) a descriptive analysis of the entire database; (ii) several correlations between the temperatures recorded by the sensors and other variables such as relative humidity and irradiance; and (iii) a *One-way Analysis of Variance* (ANOVA). These are explained in the following chart.

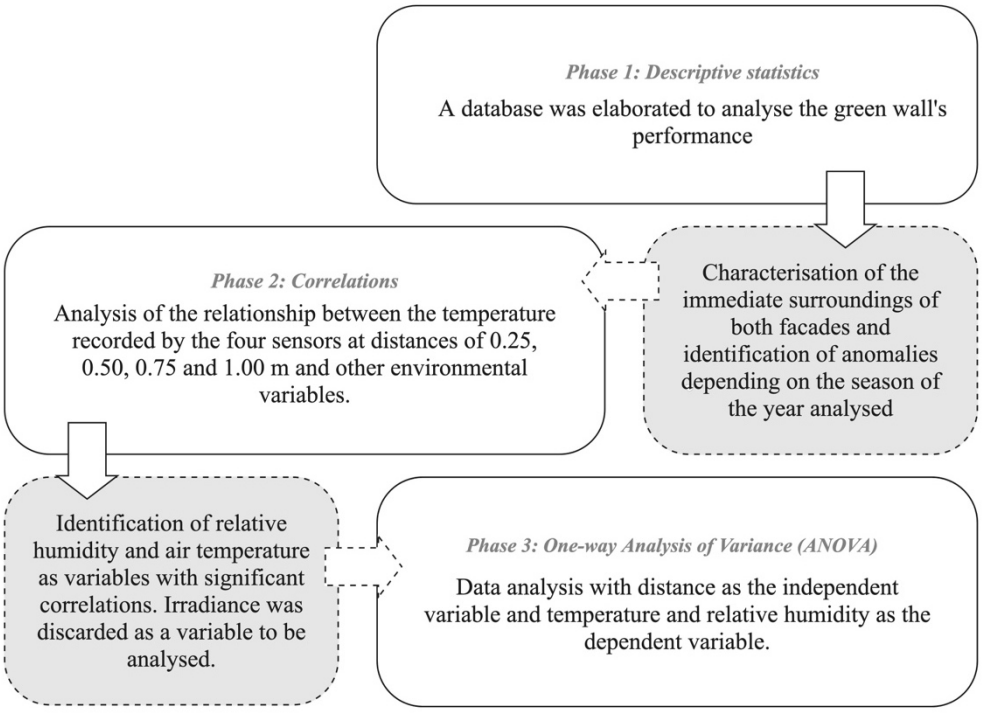

2.3.1 Descriptive statistics

A database was elaborated to analyse the green wall's performance. It provides information on air temperature and relative humidity at the different distances the sensors are located (0.25, 0.50, 0.75, and 1.00m). It also contains the irradiance values recorded by a pyranometer installed on each building façades studied. The objective was to build a profile with the main parameters to characterise both facades' immediate environment and to identify anomalies according to the year's season analysed.

2.3.2 *Correlations*

A *correlation* is a statistical measure that expresses the extent to which two variables are related. They can be linearly related (i.e., change together at a constant rate) or related by any other mathematical function. It is a standard tool for describing simple relationships without stating cause and effect. The sample correlation coefficient, R^2, quantifies the strength of the relationship being 1 maximum value, and the correlation is tested for statistical significance.

This study has used this methodology to analyse the relationship between the temperature recorded by the four sensors at distances of 0.25, 0.50, 0.75, and 1.00 m and other environmental variables during the winter and summer seasons. The results define the behaviour of the façade and the degree of influence of variables such as relative humidity and irradiance on the temperature recorded at the established distances.

The sample has been analysed from two data sets: one that considers all recorded data (day and night) and another that considers only the data recorded when irradiance is above 0 W/m^2. This distinction aims to study the variability of temperature and relative humidity according to irradiance.

2.3.3 *One-way Analysis of Variance (ANOVA)*

ANOVA (ANalysis Of VAriance) is a statistical analysis that quantitatively compares the mean of three or more groups of data, testing the equality of means of the independent variables. A one-way ANOVA uses one independent variable, while a two-way ANOVA uses two independent variables that affect the behaviour of another variable (dependent variable).

To perform the one-way ANOVA it is necessary to collect data about one categorical independent variable and one quantitative dependent variable. In our case, the independent variable is the distance, while the dependent variable is the temperature and relative humidity. As we have sensors located at four different distances from the wall, using the analysis, we

can compare the various mean values for temperature and relative humidity to determine whether they differ significantly from the rest. If so, we can estimate the maximum distance at which the green wall influences air temperature and humidity.

3. Results and discussion

3.1. Descriptive statistics of the south and west façade

3.1.1. Temperature database

Table 2 shows the summary statistics for the south and west façade from the entire temperature database used for the study (winter and summer). There is less data for the south, as one of the sensors (at 0.75 m) did not work correctly during the monitoring summer period. The study has a comprehensive database of 40.641 data for the south façade and 54.216 data for the west façade. In both cases, the average temperature is 20-21 °C, with a similar coefficient of variation (around 58%), showing that both façades have a similar temperature pattern and with the minimum temperature reaching -12 °C and the maximum temperature reaching 46 °C. The distribution cannot be assimilated to a normal distribution, as standardised skewness and standardised kurtosis are outside the range of -2 to 2, indicating a significant departure from normality.

Table 2: Statistics for temperature data in the south and west façades over winter and summer

Statistic	South façade	West façade
Count (amount of data)	40.641	54.216
Average	20.95 ºC	20.09 ºC
Standard deviations	12.04 ºC	11.74 ºC
Coefficient of variation	57.45%	58.47%
Minimum	-11.99 ºC	-12.41 ºC
Maximum	45.44 ºC	46.35 ºC
Range	57.43 ºC	58.76 ºC
Standardised skewness	-9.49	1.85
Standardised kurtosis	-43.66	-43.54

Figure 5 shows the histogram for both façades, where the two temperature data series for winter (89 days between December 1, 2020, and February 28, 2021) and summer (91 days between June 1, 2021, and August 31, 2021) are distinguished. The combined pattern for winter and summer is trinomial, like a mixture of three normal distributions. This can be confirmed by the individual histograms for both façades shown in Figure 5. In winter, both the south and west façades present a normal distribution with a mean of 9°C while in summer, the distributions are simple binomial, with a combination of two normal distributions with means of 20°C and 35°C for the west façade, and 20°C and 36°C for the south façade.

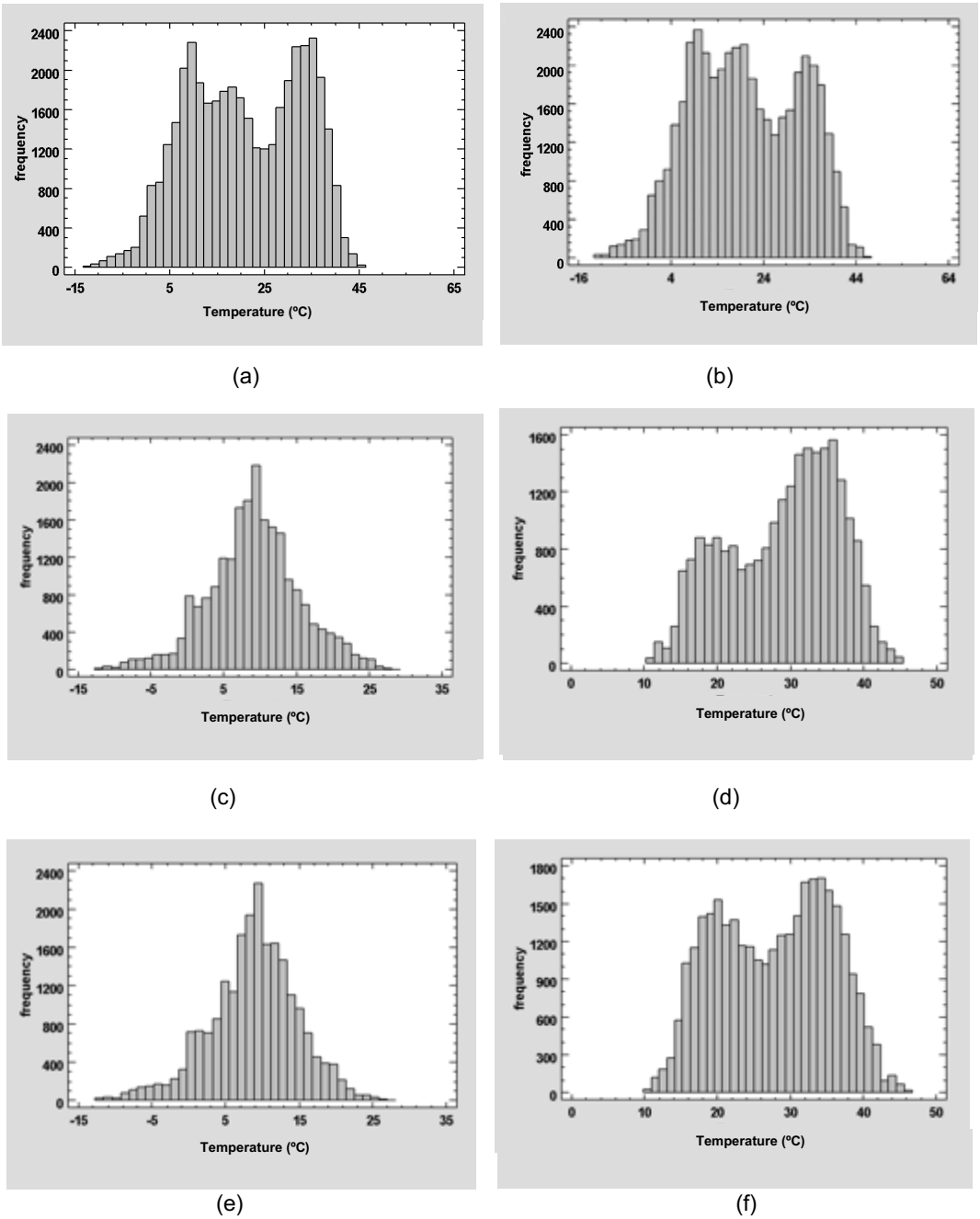

Figure 5: Temperature histograms for the south (a) and west façades (b); temperature histogram for the south facade in winter (c), the south façade in summer (d), the west facade in winter (e), and west façade in summer (f).

3.1.2 Relative humidity database

Table 3 shows the summary statistics for the south and west façade from the entire relative humidity database used for the study (winter and summer). As with the temperature dataset, the difference in the number of data is due to sensor running errors. The study has a comprehensive database of 46.143 data for the south façade and 54.216 data for the west façade. In both cases,

the average is 54-55%, with a similar coefficient of variation (around 43%). The relative humidity of the green walls varies between 8 and 100% in both seasons. In this case, the standardised skewness and kurtosis value are also not within the expected range for data from a normal distribution.

Table 3: Statistics for relative humidity data in the south and west façades during winter and summer

Statistics	South façade	West façade
Count (amount of data)	46.143	54.216
Average	54.92%	55.98%
Standard deviations	24.65%	23.54%
Coefficient of variation	44.89%	42.06%
Minimum	8.63%	11.48%
Maximum	100%	100%
Range	91.37%	88.52%
Standardized skewness	14.34	-31.02
Standardized kurtosis	-53.44	-53.90

Figure 6 shows the histogram for both façades, where the two relative humidity data series for winter (89 days between December 1, 2020, and February 28, 2021) and summer (91 days between June 1, 2021, and August 31, 2021) are distinguished. The distribution also looks like a trimodal distribution with more distinguished normal distributions. This distribution can be confirmed by the individual histograms for both façades shown in Figure 7. In winter, the south and west façades present a normal distribution with a mean of 90%, while in summer is 30%.

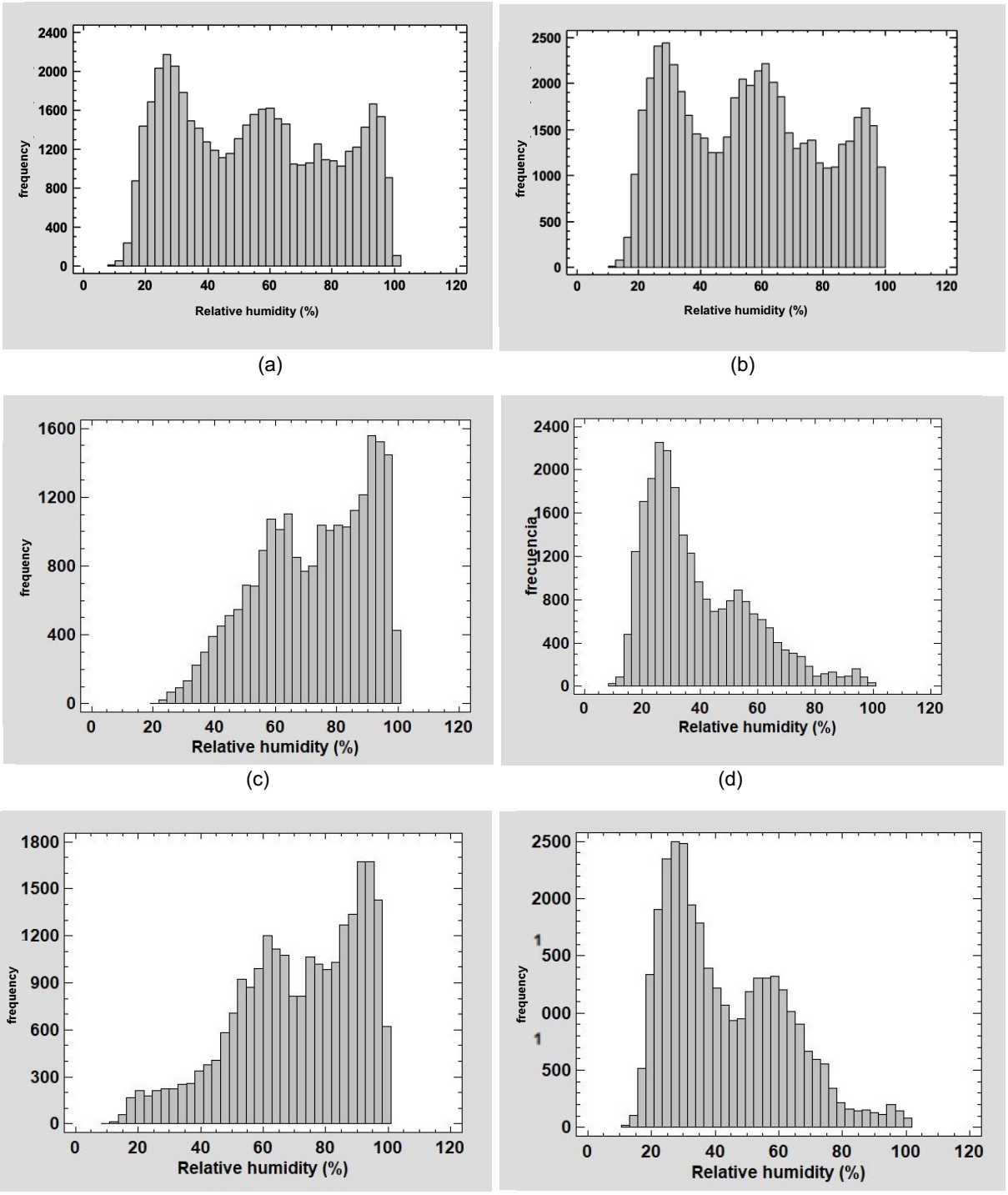

Figure 6: Relative humidity histograms for the south (a) and west façade (b); relative humidity histogram for the south facade in winter (c), the south façade in summer (d), the west facade in winter (e), and west façade in summer (f).

3.1.3 Irradiance database

Table 4 shows the summary statistics for the south and west facades of the entire irradiance database (winter and summer) used for the study. The study has a comprehensive database of 25.967 data for the south façade and 25.967 for the west façade. The average irradiance ranges between 179 and 339 W/m^2, with a coefficient of variation between 180-194%. Therefore, the variance is more significant than for temperature and relative humidity. The two facades have a significant difference in the mean and maximum irradiation values due to the orientation. The south façade receives more direct radiation from the sun (therefore showing a higher mean and maximum). The standardised skewness and kurtosis value are not within the expected range for data from a normal distribution.

Table 4: Irradiance data statistics for the south and west façades over winter and summer

Statistic	South façade	West façade
Count (amount of data)	25.967	54.216
Average	179.24 W/m^2	134.83 W/m^2
Standard deviations	323.16 W/m^2	262.39 W/m^2
Coefficient of variation	180.29%	194.60%
Minimum	0 W/m^2	0 W/m^2
Maximum	1702 W/m^2	1547 W/m^2
Range	1702 W/m^2	1547 W/m^2
Standardized skewness	144.71	185.25
Standardized kurtosis	150.19	265.55

Figure 7 shows the histogram for both façades, where the two irradiance data series for winter (89 days between December 1, 2020, and February 28, 2021) and summer (91 days between June 1, 2021, and August 31, 2021) are distinguished. In this case, both distributions are similar to gamma distributions.

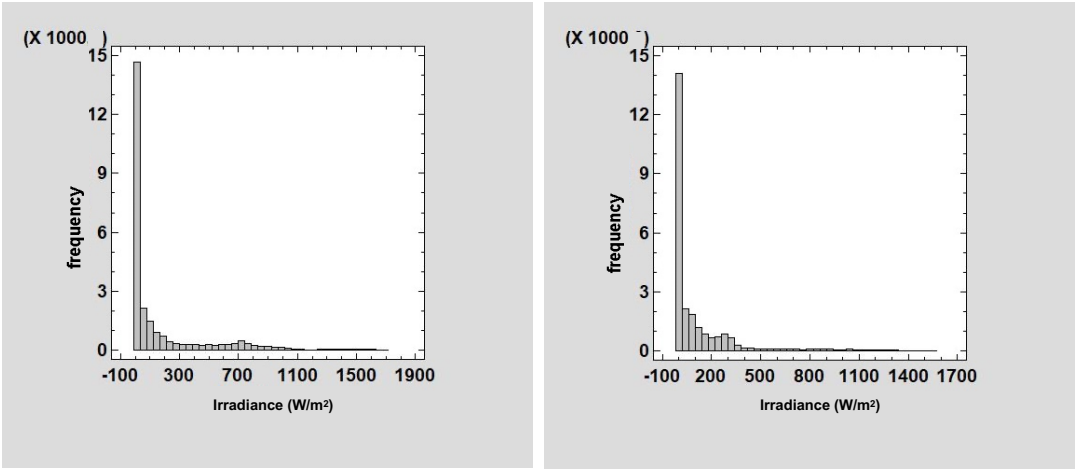

(a) (b)

Figure 7: Irradiance histograms for the South (a) and West (b) façades

The descriptive analysis of the data sample shows that the green walls studied are under continentalized Mediterranean climate conditions (Csa) (Kottek et al., 2006), with typical summer temperatures averaging 29 °C and winter temperatures 8 °C. In some cases, the minimum temperatures in this study have reached unusually low values due to a deep squall (Filomena) that affected Spain between 6 and 11 January 2021.

3.2. Correlations between sensor temperatures at four distances from the green wall and relative humidity, irradiance, and air temperature of the south and west façade

3.2.1 Correlations between air temperatures at different distances from the green wall and ambient temperature

Figure 8 and 9 shows the correlation between air temperature measured by the weather station and sensor temperatures for both façades. There is a strong positive correlation between air temperature and sensor temperature at all distances, with R^2 greater than 0.7. The correlation is stronger when the data is from the whole day than when only daytime data are analysed, indicating that facades have a more visible effect during the day. The correlations are higher in summer than in winter. As the sensors are farther away from the wall, the temperature tends to coincide with the air temperature. In summer, there is a stronger correlation between ambient

temperature and sensor temperature than in winter; it suggests that the effect of the green façade is more significant in winter than in summer.

W-T: West façade daytime and night-time temperature data base

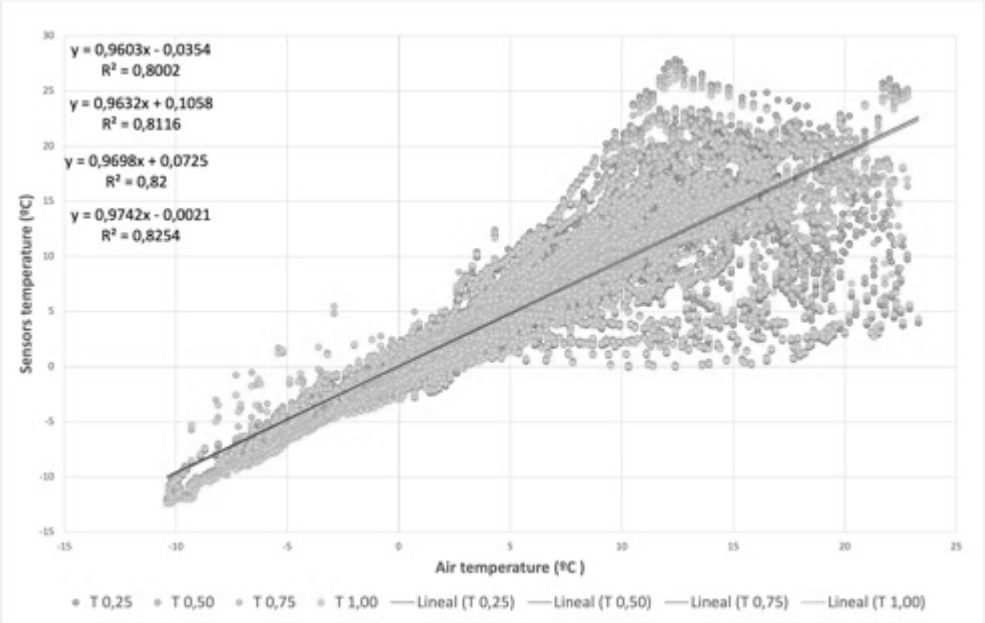

W-D: West façade diurnal temperature database (irradiance > 0)

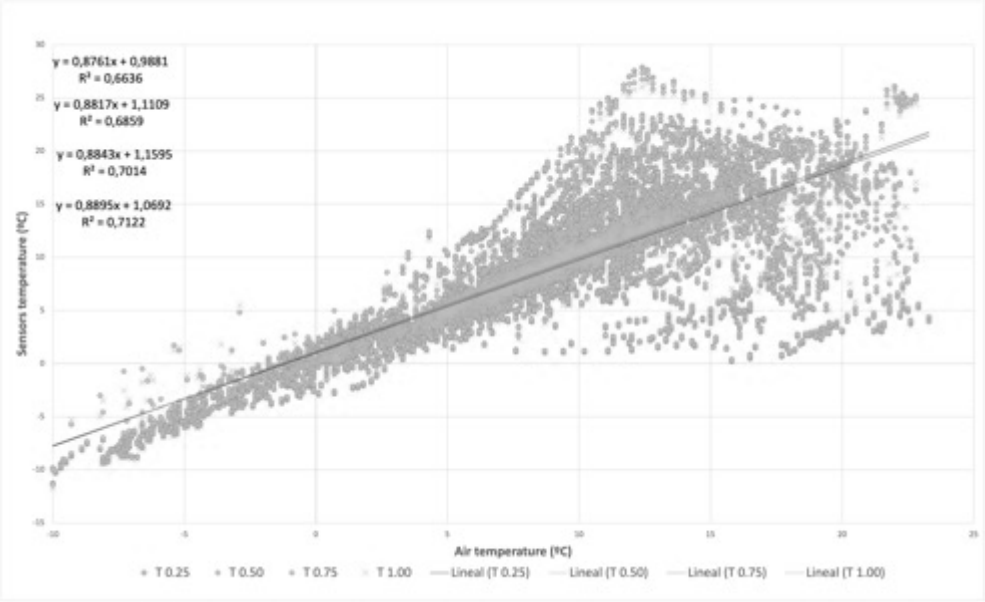

S-T: South façade daytime and night-time temperature database

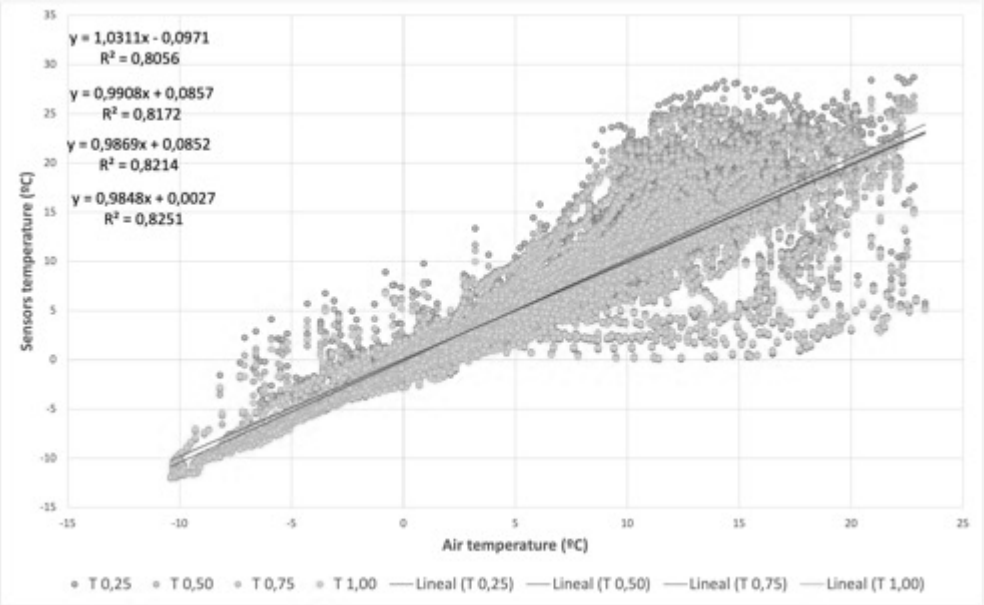

S-D: South façade diurnal temperature database (irradiance > 0)

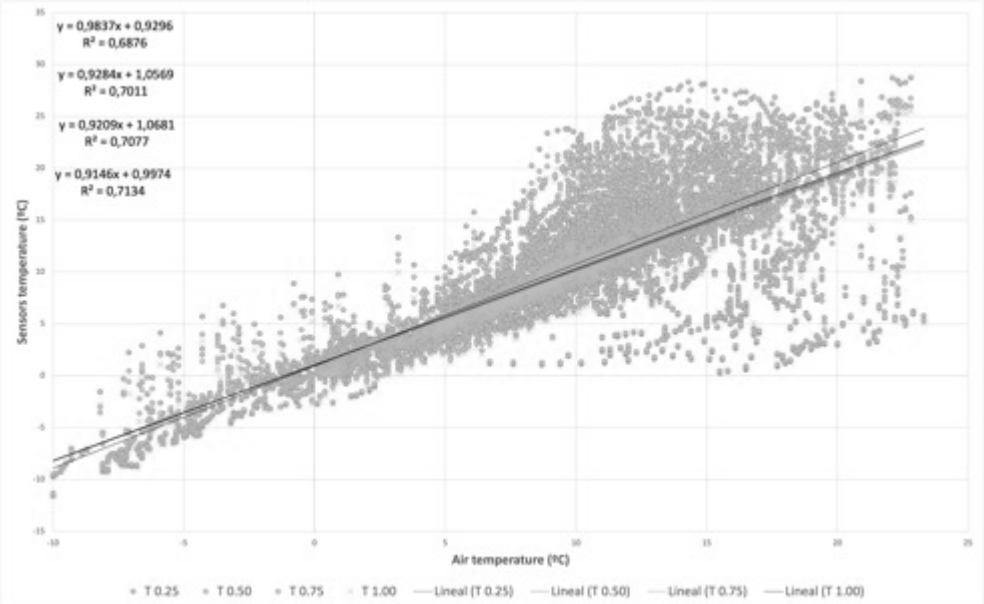

Figure 8: Correlations between sensor temperature and air temperature during winter on both facades (south – west)

W-T: West façade daytime and night-time temperature data base

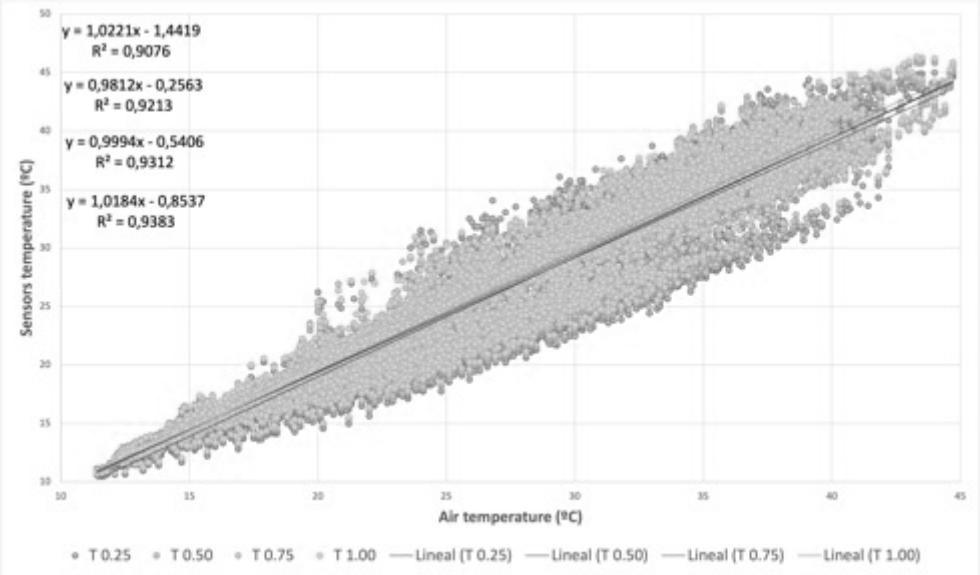

W-D: West façade diurnal temperature database (irradiance > 0)

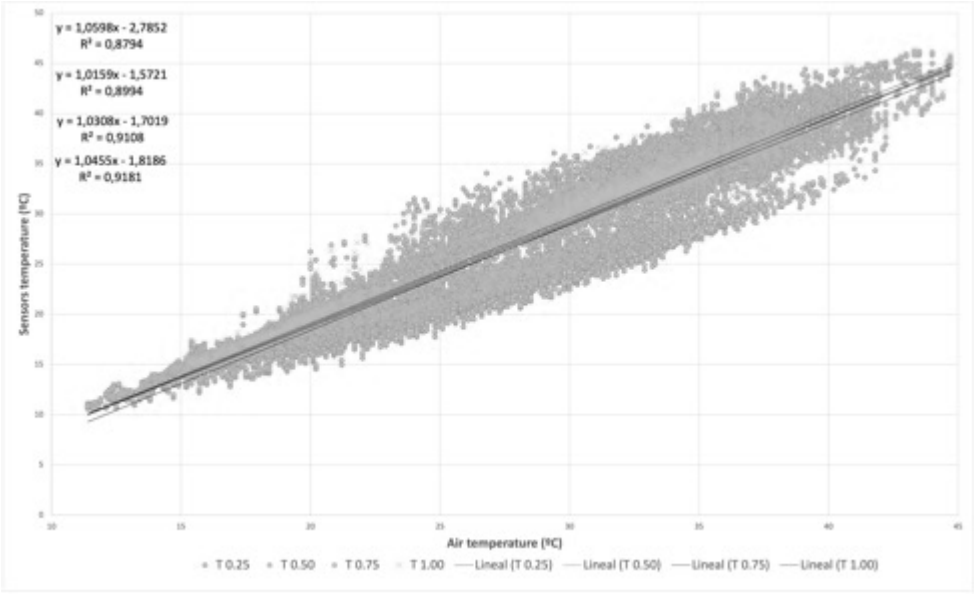

S-T: South façade daytime and night-time temperature database

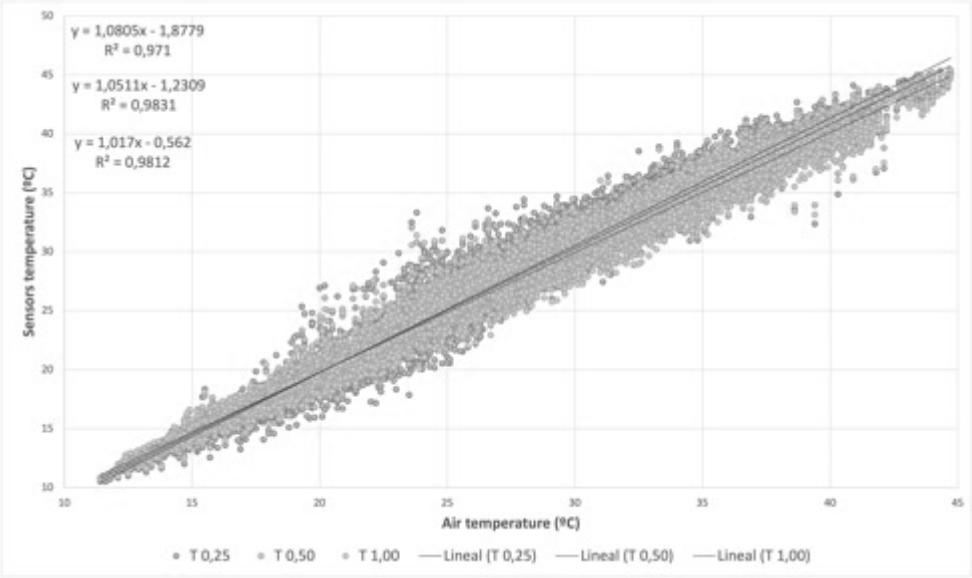

S-D: South façade diurnal temperature database (irradiance > 0)

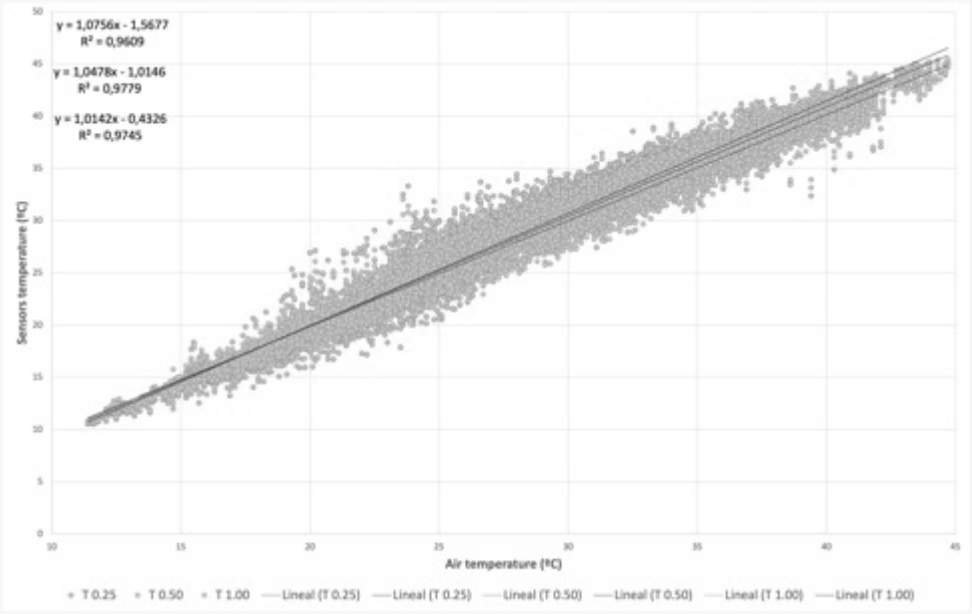

Figure 9: Correlations between sensor temperature and air temperature during summer on both facades (south – west)

Table 5 summarises the regression formulae in Figures 9 and 10 to visualise the correlation between the air temperature measured at the weather station and the temperature measured by each sensor at different distances. In addition, to see an example of the effect of the façade in terms of temperature reduction or increase, the formulas are applied to calculate the temperature at the different distances using concrete air temperature values. These values are 9 °C for winter

and 35 °C for summer, which have been identified as the mode value from the descriptive analysis of the database for each season.

Table 5: Correlation between air temperature and sensor temperature for the south and west façades.

Distance from wall		Winter				Summer			
		W-T	W-D	S-T	S-D	W-T	W-D	S-T	S-D
0.25	Formula	y=0,9603 x-0,0354	y=0,8761x +0,9881	y=1,0311x-0,0971	y=0,9837x+ 0,9296	y=1,0221x-1,4419	y=1,0598x-2,7852	y=1,0805x-1,8779	y=1,0756x-1,5677
	R^2	0,8002	0,6636	0,8056	0,6876	0,9076	0,8794	0,971	0,9609
	Example	8,6073	8,873	9,1828	9,7829	34,3316	34,3078	35,9396	36,0783
0.50	Formula	y=0,9632 x+0,1058	y=0,8817x+ 1,1109	y=0,9908x+ 0,0857	y=0,9284x+ 1,0569	y=0,9812x-0,2563	y=1,0159x – 1,52721	y=1,0511x-1,2309	y=1,0478x-1,0146
	R^2	0,8116	0,6859	0,8172	0,7011	0,9213	0,8994	0,9831	0,9779
	Example	8,7746	9,0462	9,0029	9,4125	34,0857	34,02929	35,5576	35,6584
0.75	Formula	y=0,9698 x+0,0725	y=0,8843x+ 1,1595	y=0,9869x+ 0,0852	y=0,9209x+ 1,0681	y=0,9994x-0,5406	y=1,0308x-1,7019	*No data*	*No data*
	R^2	0,82	0,7014	0,8214	0,7077	0,9312	0,9108		
	Example	8,8007	9,1182	8,9673	9,3562	34,4384	34,3761		
1.00	Formula	y=0,9742 x-0,0021	y=0,8895x+ 1,0692	y=0,9848x+ 0,0027	y=0,9146x+ 0,9974	y=1,0184x-0,8537	y=1,0455x-1,8186	y=1,017x-0,562	y=1,0142x-0,4326
	R^2	0,8254	0,7122	0,8251	0,7134	0,9383	0,9181	0,9812	0,9745
	Example	8,7657	9,0747	8,8659	9,2288	34,7903	34,7739	35,033	35,0644

W-T: West façade for all-day
W-D: West façade only when sunlight (irradiance > 0)
S-T: South façade for all-day
S-D: South façade only when sunlight (irradiance > 0)
Example: sensor temperature estimated at each distance applying the corresponding formula using the ambient temperature of 9 ºC for winter and 35 ºC for summer (mode values for each season)

3.2.2 Correlations between relative humidity and air temperature at different distances from the green wall

Figure 10 and 11 shows the correlation between relative humidity and sensor temperature for both façades. There is no strong correlation for any façade during winter. However, there is a negative correlation for summer, especially during the day, for both façades, with R^2 between 0.6 and 0.65. It indicates the effect of the increase in relative humidity on the reduction of sensors' temperature in summer, particularly during daylight hours.

W-T: West façade daytime and night-time temperature data base

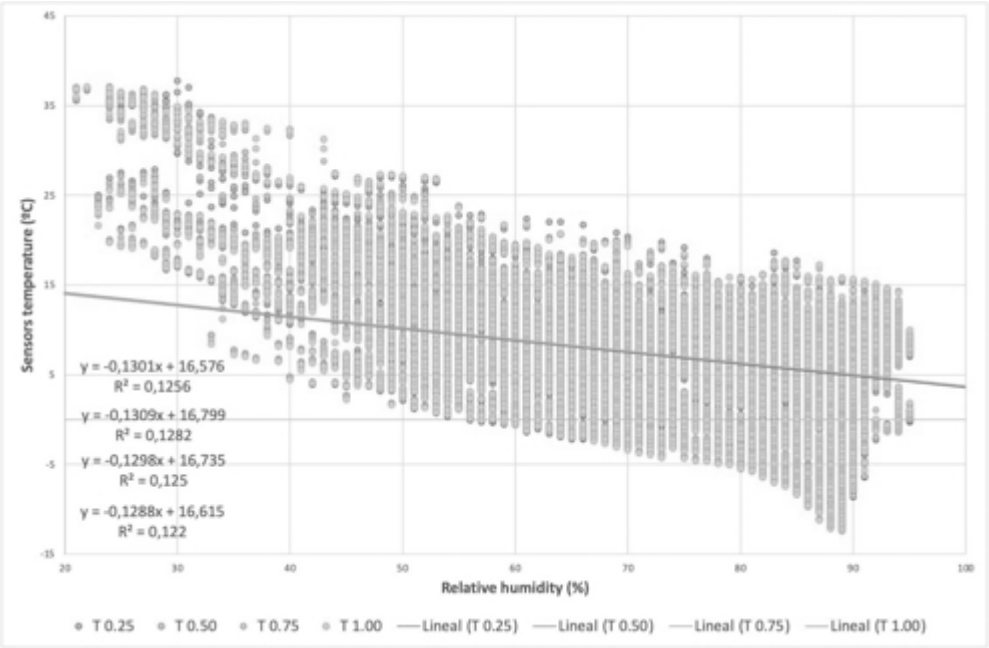

W-D: West façade diurnal temperature database (irradiance > 0)

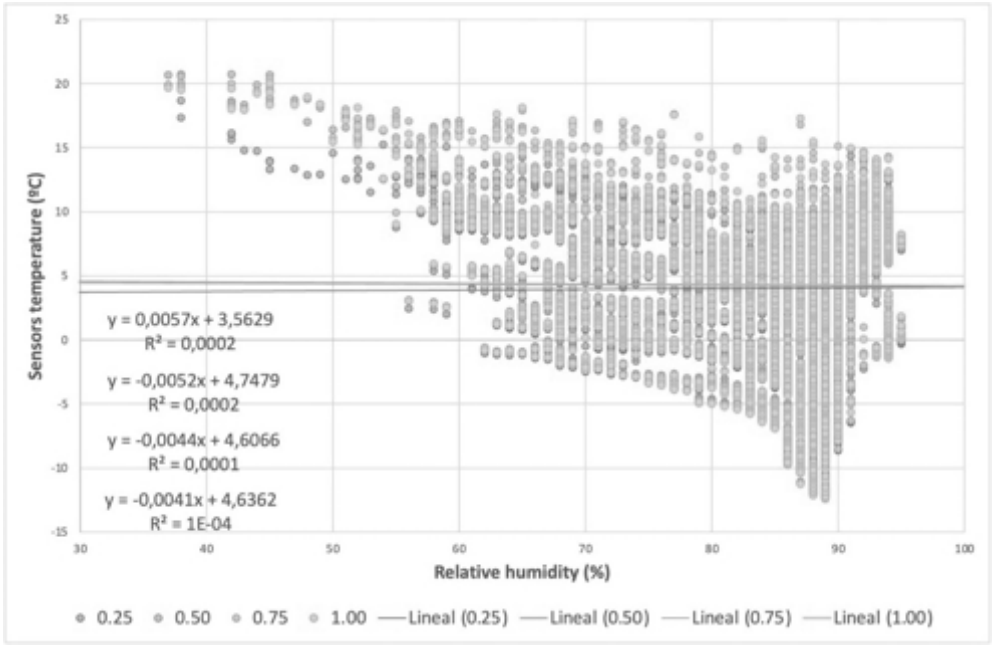

S-T: South façade daytime and night-time temperature database

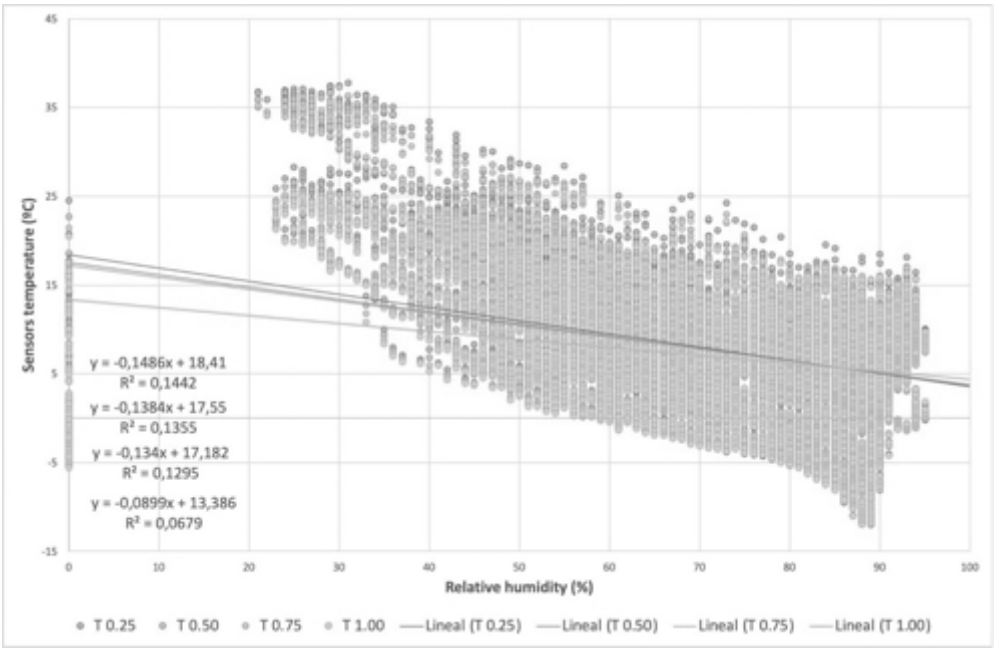

S-D: South façade diurnal temperature database (irradiance > 0)

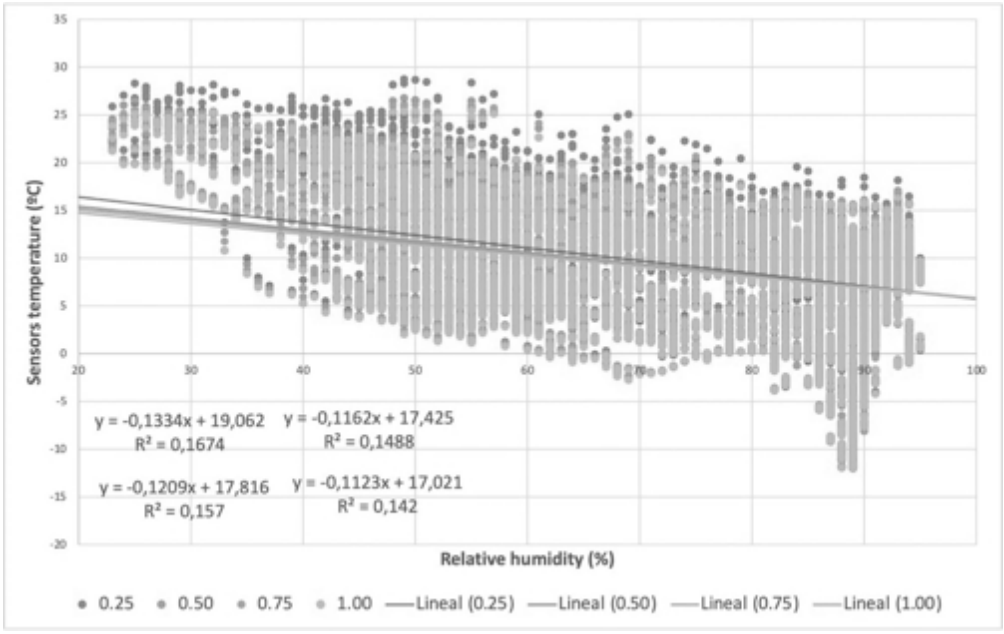

Figure 10: Correlations between relative humidity and sensor temperature during winter on both facades (south – west)

W-T: West façade daytime and night-time temperature data base

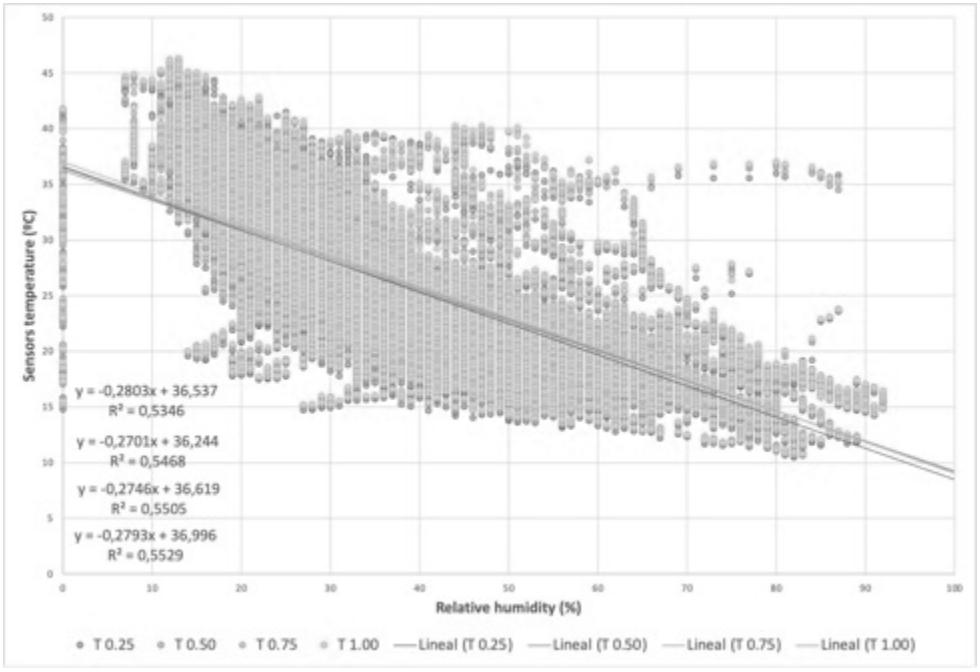

W-D: West façade diurnal temperature database (irradiance > 0)

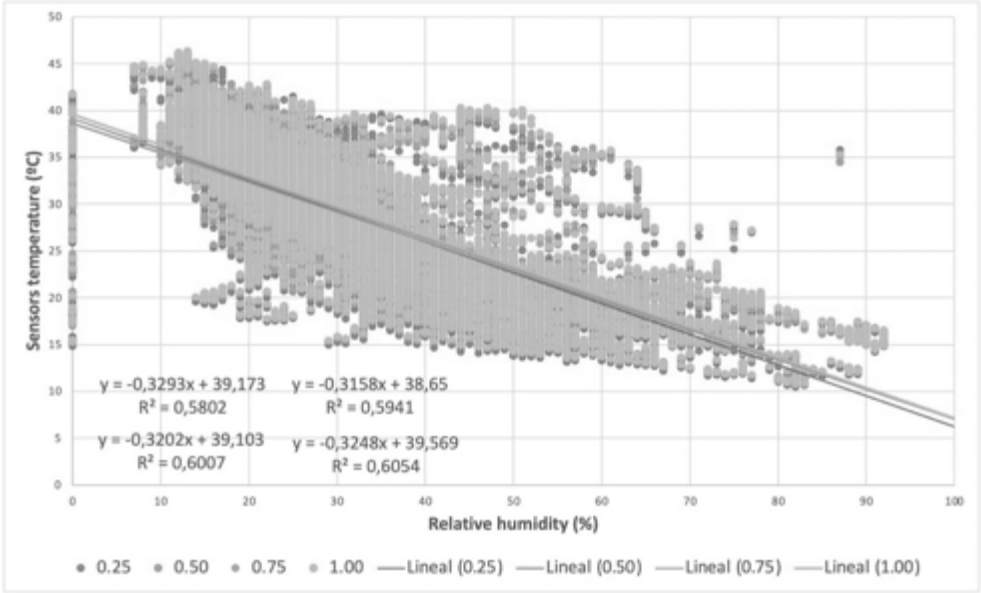

S-T: South façade daytime and night-time temperature database

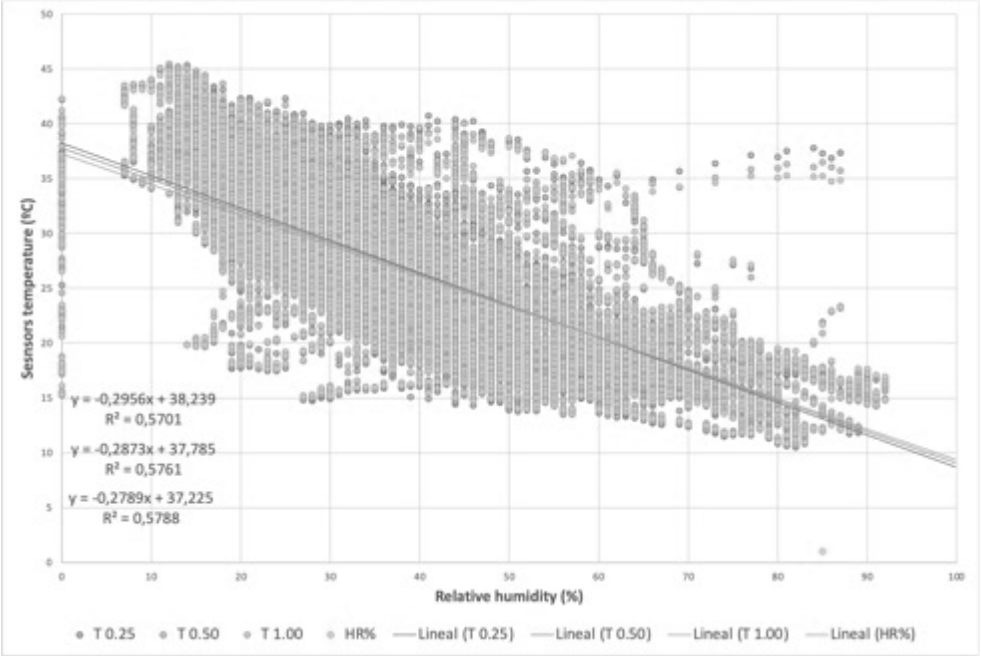

S-D: South façade diurnal temperature database (irradiance > 0)

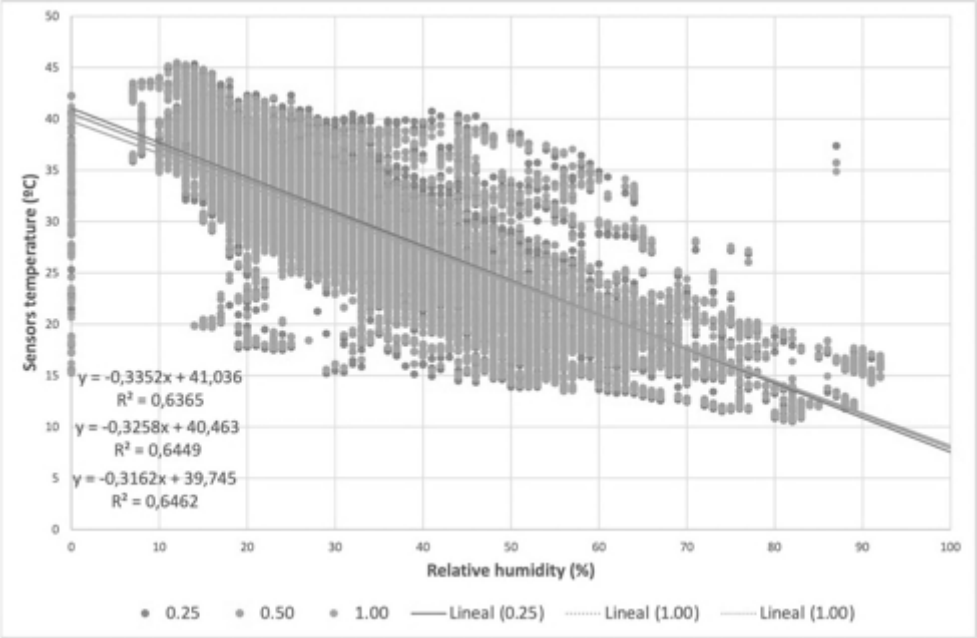

Figure 11: Correlations between relative humidity and sensor temperature during summer on both facades (south – west)

Table 6 summarizes the regression formulae in Figures 9 and 10 to visualise the correlation between relative humidity and temperature measured by each sensor at different distances. In addition, the formulas are applied to calculate the relative humidity at different distances using specific values to see an example of the effect of the façade in terms of reduction or increase of relative humidity. These values are RH 90% for winter and RH 30% for summer, which have been identified as the mode values from the descriptive analysis of the database for each season.

Table 6: Correlation between relative humidity and sensor temperature for the south and west façade

Distance from wall		Winter				Summer			
		W-T	W-D	S-T	S-D	W-T	W-D	S-T	S-D
0.25	Formula	y=-0,1301x+16,576	y=0,0057x+3,5629	y=-0,1486x+18,41	y=-0,1334x+19,062	y=-0,2803x+36,537	y=-0,3293x+39,173	y=-0,2956x+39,239	y=-0,3352x+41,036
	R^2	0,1256	0,0002	0,1442	0,1674	0,5346	0,5802	0,5701	0,6365
	Example	4,867	4,0759	5,036	7,056	28,128	29,294	30,371	30,98
0.50	Formula	y=-0,1309x+16,799	y=-0,0052x+4,7479	y=-0,1384x+17,55	y=-0,1209x+17,816	y=-0,2701x+36,244	y=-0,3158x+38,65	y=-0,2873x+37,785	y=-0,3258x+40,463
	R^2	0,1282	0,0002	0,1355	0,157	0,5468	0,5941	0,5761	0,6449
	Example	5,018	4,2799	5,094	6,935	28,141	29,176	29,166	30,689
0.75	Formula	y=-0,1298x+16,735	y=-0,0044x+4,6066	y=-0,134x+17,182	y=-0,1162x+17,425	y=-0,2746x+36,619	y=-0,3202x+39,103	No data	No data
	R^2	0,125	0,0001	0,1295	0,1488	0,5505	0,6007		
	Example	5,053	4,2106	5,122	6,967	28,381	29,497		
1.00	Formula	y=-0,1288x+16,615	y=-0,0041x+4,6362	y=-0,0899x+13,386	y=-0,1123x+17,021	y=0,2793x+39,996	y=-0,3248x+39.569	y=-0.2789x+37,225	y=-0,3162x+39,745
	R^2	0,122	0,0001	0,0679	0,142	0,5529	0,6054	0,5788	0,6462
	Example	5,023	4,2672	5,295	6,914	48,375	29,825	28,858	30,259

W-T: West façade for all-day
W-D: West façade only when sunlight (irradiance > 0)
S-T: South façade for all-day
S-D: South façade only when sunlight (irradiance > 0)
Example: temperature estimated at each sensor applying the correlation formula and using 90% for winter and 30% for summer as the mode value of the relative humidity for each season.

3.2.3 Correlations between irradiance and air temperature at different distances from the green wall

Table 7 shows the correlation between irradiance and sensor temperatures for both façades. There is no strong correlation between air temperature and irradiance, as R^2 are lower than 0.5 for all cases. There is also no trend on which façade or season has stronger correlations, although summer tends to produce higher R^2 values for all cases.

It means that in summer, higher irradiations produce higher temperatures except for the west façade, perhaps because the irradiation is less direct, so its influences sensor temperatures.

W-T: West façade daytime and night-time temperature data base

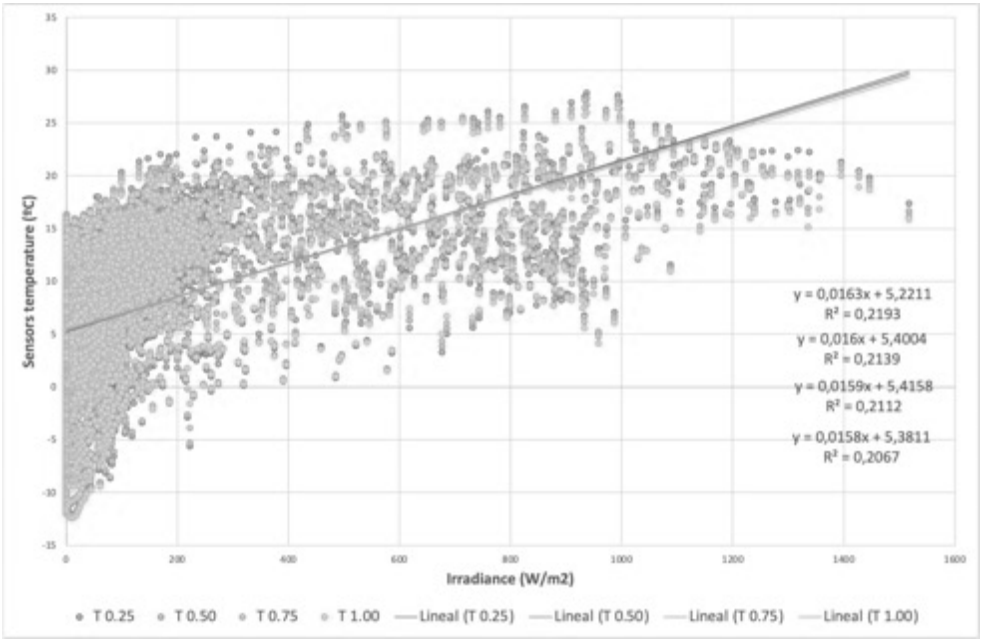

W-D: West façade diurnal temperature database (irradiance > 0)

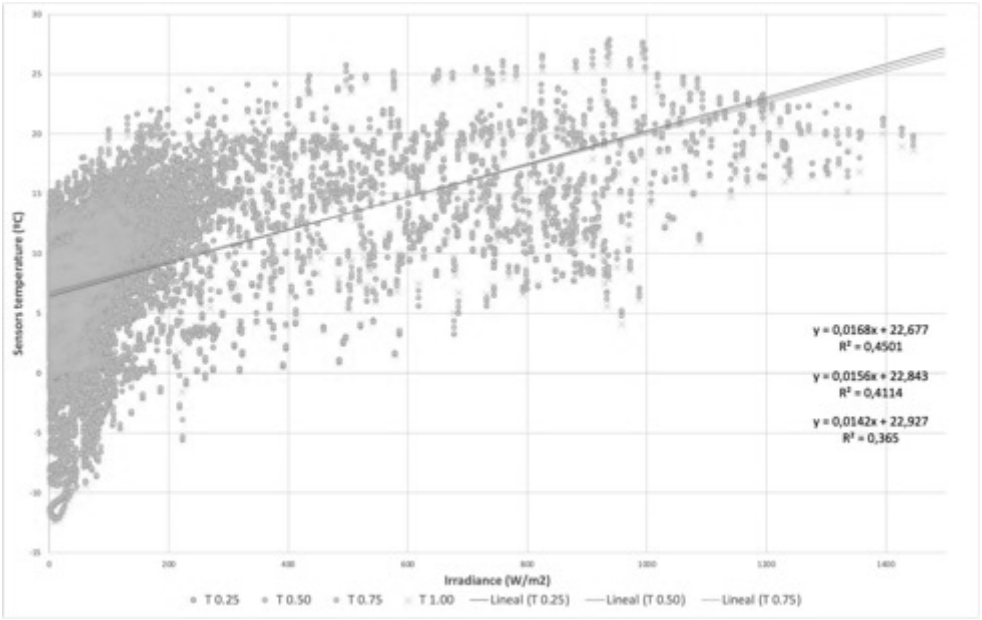

S-T: South façade daytime and night-time temperature database

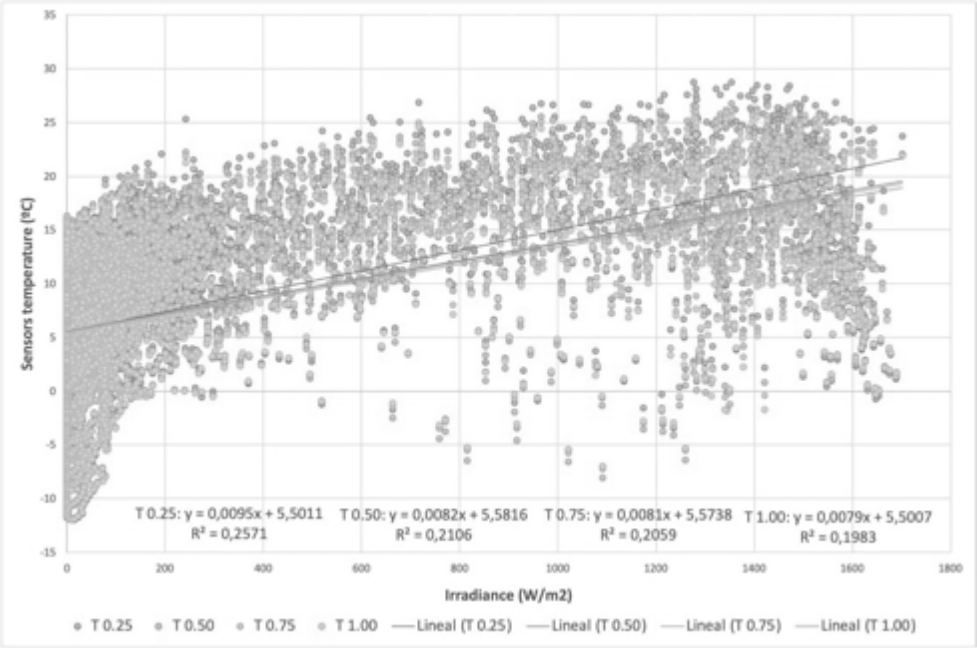

S-D: South façade diurnal temperature database (irradiance > 0)

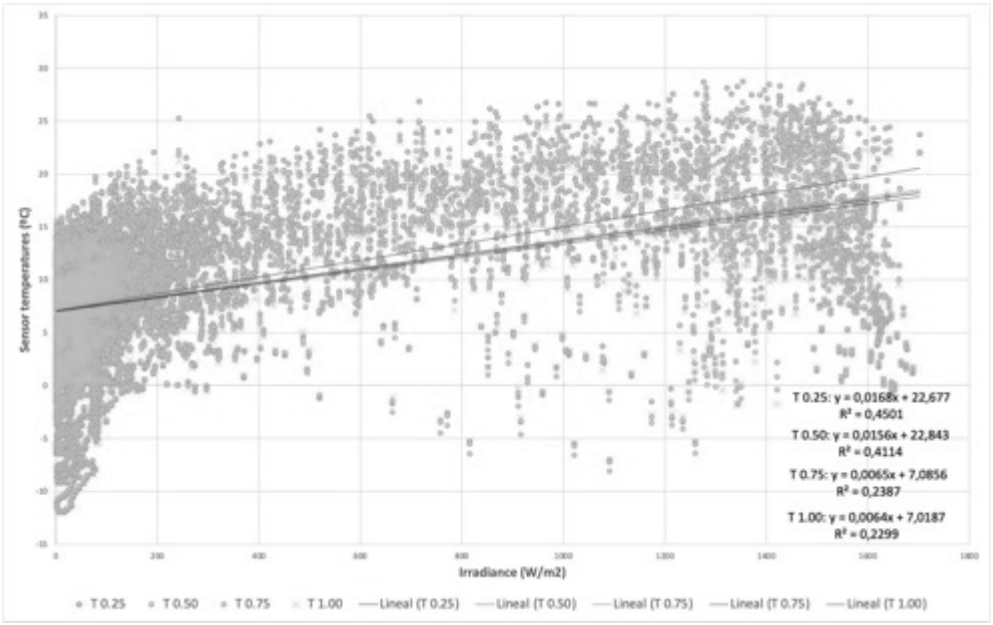

Figure 12: Correlations between irradiance and sensor temperature during winter for both façades (south – west)

W-T: West façade daytime and night-time temperature data base

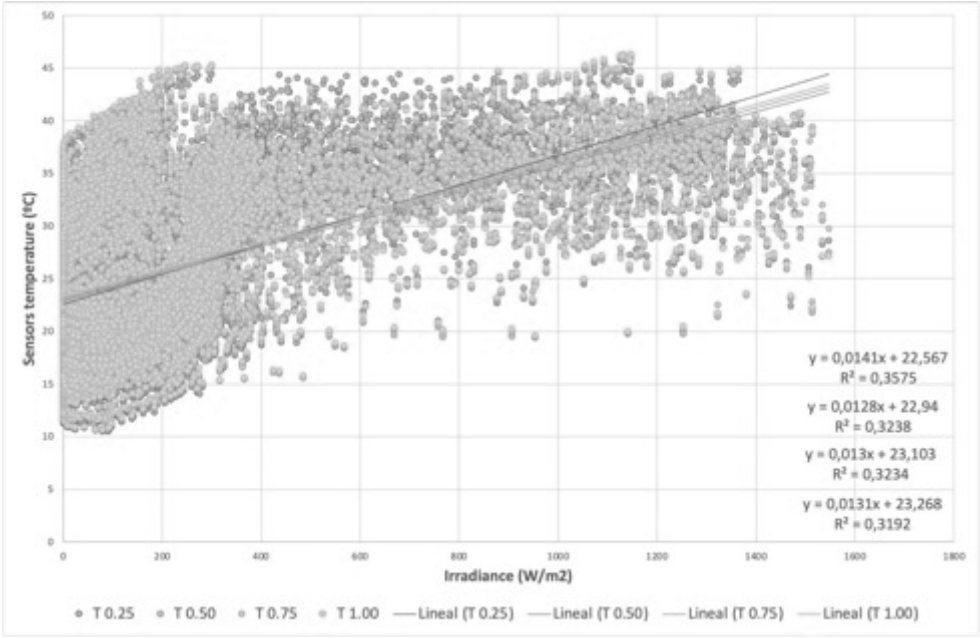

W-D: West façade diurnal temperature database (irradiance > 0)

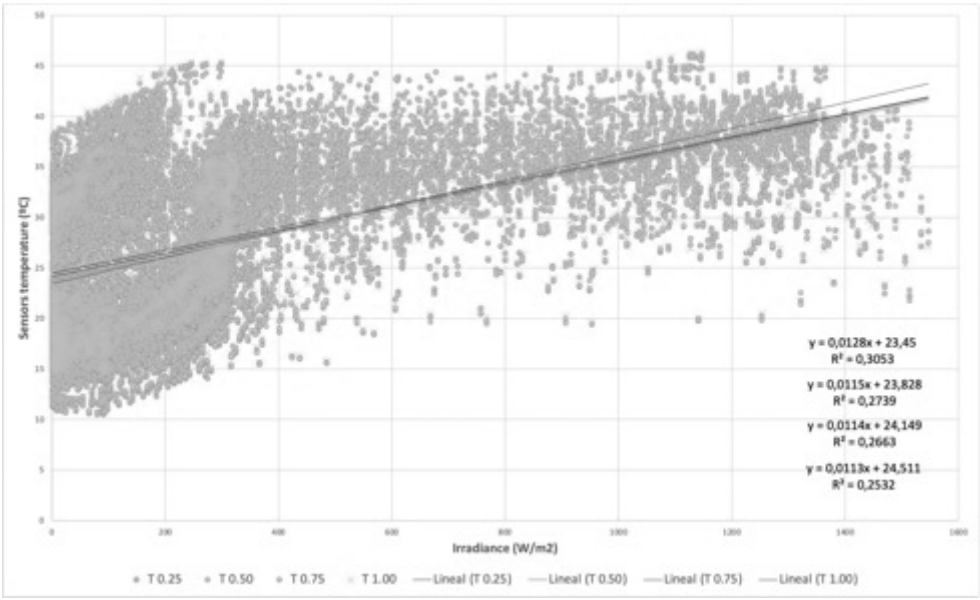

S-T: South façade daytime and night-time temperature database

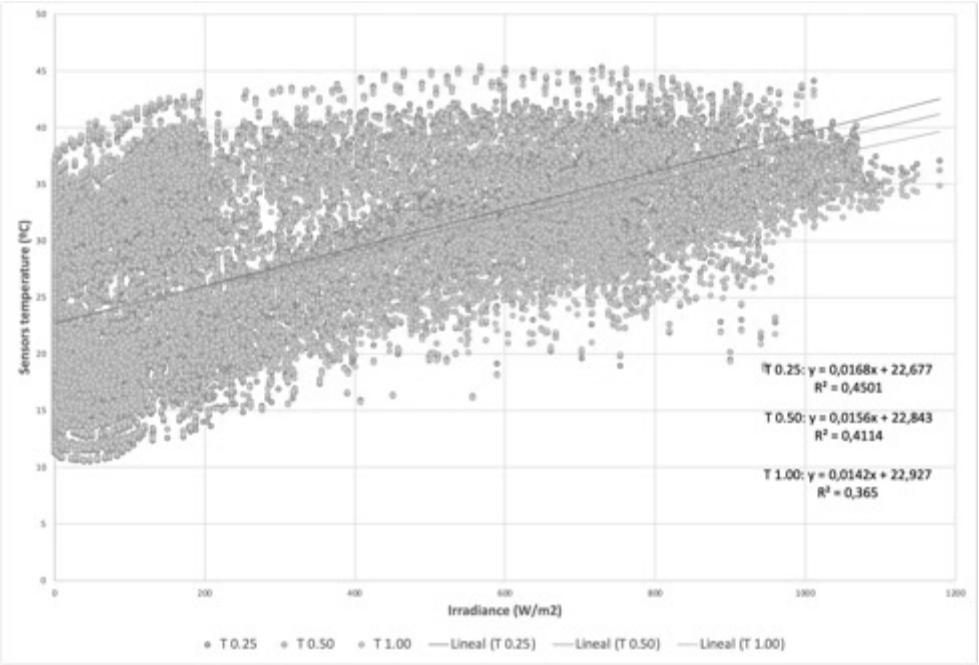

S-D: South façade diurnal temperature database (irradiance > 0)

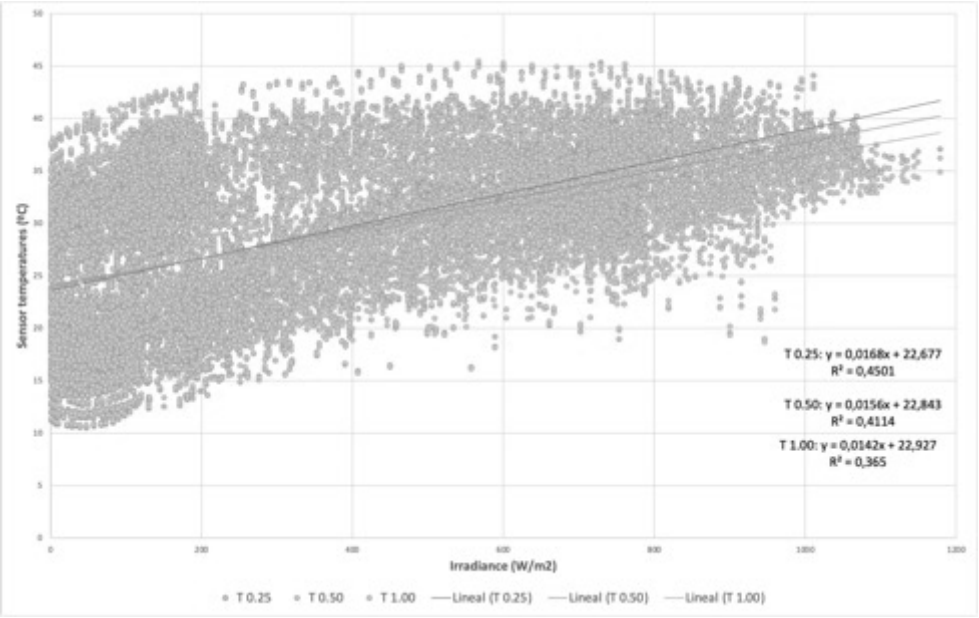

Figure 13: Correlations between irradiance and sensor temperature during summer for both façades (south – west)

Table 7 summarizes the regression formulas in Figures 12 and 13 to visualise the correlation between the irradiance measured in the vertical plane of the green wall and the temperature measured by each sensor at different distances.

Table 7: Correlation between irradiance and sensor temperature for the south and west façades

Distance from wall		Winter				Summer			
		W-T	W-D	S-T	S-D	W-T	W-D	S-T	S-D
0.25	Formula	y=0,0163x+ 5,2211	y=0,0168x + 22,677	y=0,0095x+ 5,5011	y=0,0079x + 7,0781	y=0,0141x+ 22,567	y=0,0128x + 23,441	y=0,0168x+2 2,677	y=0,0153x + 23,621
	R^2	0,2193	0,4501	0,2571	0,2976	0,3575	0,30571	0,4501	0,3655
0.50	Formula	y=0,016x+5 ,4004	y=0,0156x + 22,843	y=0,0082x+ 5,5816	y=0,0067x + 7,0985	y=0,0128x+ 22,94	y=0,0115x + 23,819	y=0,0156x+2 2,843	y=0,0138x + 23,934
	R^2	0,2139	0,4114	0,2106	0,2426	0,3238	0,2744	0,4114	0,3186
0.75	Formula	y=0,0159x+ 5,4158	y=0,0135x + 6,6625	y=0,0081x+ 5,5738	y=0,0065x + 7,0856	y=0,013x+2 3,103	y=0,0114x + 24,14	*No data*	*No data*
	R^2	0,2112	0,2668	0,2059	0,2387	0,3234	0,2667		
1.00	Formula	y=0,0158x+ 5,3811	y=0,0142x + 22,927	y=0,0079x+ 5.5007	y=0,0064x + 7,0187	y=0,0131x+ 23,268	y=0,0113x + 24,502	y=0,0142x+2 2,927	y=0,0123x + 24,111
	R^2	0,2067	0,365	0,1983	0,2299	0,3192	0,2535	0,365	0,2686

W-T: West façade for all-day
W-D: West façade only when sunlight (irradiance > 0)
S-T: South façade for all-day
S-D: South façade only when sunlight (irradiance > 0)

In summary, the results show a strong correlation between the temperature recorded by the sensors and the air temperature, especially during the summer, which increases proportionally as the ambient temperature increases. It does not directly show whether there is a relevant influence of the façade on the immediate surroundings, so an analysis of variance (ANOVA) must be performed, which is explained below. In the case of relative humidity, the correlations are not significant and, in some cases, negative, which explains the reduction in temperatures due to the increase in relative humidity. As for irradiance, there is no correlation, which shows that it is not a variable that conditions the behaviour of the façade.

3.3 One-way Analysis of Variance (ANOVA) of the south and west façade

Table 8 shows the one-way ANOVA results for the temperature as the dependent variable. It ranges from 1.73 to 13.99, showing a significant variance between means for each distribution. The F-ratio determines if the variability between the group means is

greater than the variability of the observations within the groups. If that ratio is large enough, it can be concluded that not all means are equal. Another way to know if the differences between means are statistically significant is by analyzing the P-value. The hypothesis behind the ANOVA test is that all means are equal, and that the P-value evaluates whether this is true or whether the null hypothesis should be discarded. If the P-value is lower than 0.05, the means are different, with a statistical significance of 95%. In this case, the P-values are less than 0.05 for all façades and all seasons, except the west façade in winter. Therefore, the green wall reduces the temperature, with more statistical significance in the south façade. For all cases, the P-value is lower than 0.001, meaning the statistical difference is significant with 99.9% confidence.

Table 8: ANOVA for sensor temperatures of the south and west façades

Statistics	Mean square	F-ratio	P-value
West façade (all seasons)	494.806	3.59	0.0131
West façade (summer)	619.084	10.20	0.0000
West façade (winter)	62.1636	1.73	0.1577
South façade (all seasons)	1179.07	8.14	0.0003
South façade (summer)	802.214	13.99	0.0000
South façade (winter)	291.359	7.33	0.0001

To analyze the differences in more detail, Table 9 shows a multiple comparison procedure to determine which means are significantly different from which others and what is the quantitative difference. Columns represent the temperature difference between distances. For instance, ΔT (0.25-0.50) represents the difference in temperature between the sensor located at 0.25 m from the façade and the sensor located at 0.5 m. An asterisk is placed next to those pairs that do not show statistically significant differences at the 95% confidence level. For the south façade, temperatures

decrease with distance for all seasons, being statistically significant at all distances in summer and for the cases of 0.25-0.5 and 0.25-1.00 in winter. Therefore, it could be concluded that the green wall reduces temperatures during all seasons in the south façade with a total decrease of 0.63 °C between the sensor at 0.25 m and the one at 1m in summer and 0.54 °C in winter. On the contrary, temperatures increase in the west façade in winter and summer, with statistical significance in summer for all distances but between 0.25 m and 0.5 m. The increase between the sensor at 0.25 m and the sensor at 1.00 m in summer is 0.56 °C.

Table 9: Differences in temperature for each distance, including its statistical significance, in the south and west façades.

Statistics	ΔT (°C) (0.25-0.50)	ΔT (°C) (0.50-0.75)	ΔT (°C) (0.50-1.00)	ΔT (°C) (0.75-1.00)	ΔT (°C) (0.25-1.00)
West façade (summer)	0.050*	-0.30	-0.61	-0.31	-0.56
West façade (winter)	-0.17*	-0.07*	-0.03*	0.04*	-0.20*
South façade (summer)	0.24	-	0.38	-	0.63
South façade (winter)	0.36	0.05*	0.18*	0.13*	0.54

Table 10 shows the one-way ANOVA results for relative humidity as the dependent variable. As F-ratios are high for all cases, and all p-values are below 0.0000, it can be concluded that the green wall influences the relative humidity with statistical significance for all seasons and all façades.

Table 10: ANOVA for relative humidity of the south and west façades

Statistics	Mean square	F-ratio	P-value
West façade (all seasons)	6520.79	11.77	0.0000
West façade (summer)	3074.5	8.96	0.0000
West façade (winter)	3634.15	12.60	0.0000
South façade (all seasons)	647144.	1143.80	0.0000
South façade (summer)	4689.41	14.35	0.0000
South façade (winter)	5037.75	15.21	0.0000

Table 11 shows the detailed comparison of HR means at each distance. An asterisk is placed next to those pairs that do not show statistically significant differences at the 95% confidence level. For the south façade, HR decreases with distance in winter, with a total reduction of 2.3% between the sensors at 0.25 and 1m, which improves thermal comfort. In summer, there is an increase in HR of 0.66% in the zone closer to the wall (between 0.25 m and 0.5 m), while a decrease of 1.52% occurs between 0.5 m and 1 m, producing a total reduction of 0.9% between the extremes. In the west façade, the behaviour is the opposite. In winter and summer, the RH increases with distance, probably due to the lower number of hours of direct solar radiation. In summer, there is a statistically significant increase of 1.5% between 0.25 m and 0.5 m, while the RH decreases 0.9% in the second part of the wall (between 0.5 m and 1 m), leading to a total increase of 0.6% between the extremes. Similarly, in winter, the HR increases by 1.9% between 0.25 m and 0.5 m, while it decreases a 0.9% during the last section (0.5-1 m), with a total increase of 1.0% between 0.25 m and 1 m. Therefore, it could be concluded that the green wall reduces RH during all seasons in the south façade and increases the RH in the west façade.

Table 11: Differences in relative humidity for each distance, including its statistical significance in the south and west façades.

Statistics	ΔRH (%) (0.25-0.50)	ΔRH (%) (0.25-0.75)	ΔRH (%) (0.50-0.75)	ΔRH (%) (0.50-1.00)	ΔRH (%) (0.75-1.00)	ΔRH (%) (0.25-1.00)
West façade (summer)	1.46245	0.946474	-0.515971*	-0.905041	-0.38907*	0.557404*
West façade (winter)	1.90672	1.44352	-0.463206*	-0.859108	-0.395901*	1.04761
South façade (summer)	0.663387	-	-	-1.52276	-	-0.859369
South façade (winter)	-0.761241	-1.10295	-0.34171*	-1.53717	-1.19546	-2.29841

3.4 Overall discussion

This study has shown the effectiveness of green walls towards reducing temperatures in the urban environment and improving thermal comfort. From a microclimate perspective, green walls can help lower air temperatures, especially during hot summers, by providing shade and evapotranspiration (Yang et al., 2018). More importantly, through the ANOVA results, this study has confirmed that the green wall reduces the temperature with statistical significance, with greater significance on the south façade.

The mentioned reduction translates to 0.63 ºC in summer and 0.54 ºC in winter, between the sensor at 0.25 and 1.00 m. The P-value is less than 0.001 in all cases, meaning the statistical difference is significant with 99.9% confidence. These results are similar to other studies that have shown that south orientation in a Mediterranean climate enhances the temperature reduction impact of a green wall (Sendra-Arranz et al., 2020). In contrast, on the west façade, temperatures increase in winter and summer, with statistical significance in summer for all distances except between 0.25 and 0.5 m. The increase translates to 0.56 ºC between the sensor at 0.25 and 1.00 m.

Analysis conducted has verified that, as well as the results obtained in other studies on the non-significant impact of green walls in winter on urban comfort [24], there are no significant correlations between the relative humidity and the temperatures recorded by the sensors in front of the wall during the winter, showing that there is no significant effect in wintertime.

No strong correlation was found between irradiance and air temperature recorded by the sensors in none of the seasons tested. However, there are negative correlations during the summer, which is evidence of the effect of irradiance on the green wall, which increases the air temperature and reduces the relative humidity, especially during daylight hours (Cameron et al., 2014). Based on these results, irradiance is discarded as a variable that conditions the behaviour of the façade and the reduction of adjacent temperatures.

This study revealed that the green wall influences relative humidity with statistical significance in all seasons and both orientations. On the south façade, relative humidity decreases with distance during the winter, with a total reduction of RH 2.3% between the sensors at 0.25 and 1.00m and increases during the summer RH 0.66% in the area closest to the green wall. In contrast, between 0.5m and 1m, there is a decrease of 1.52%, producing a total reduction of 0.9% between the extremes. On the west façade, the behaviour is the opposite. RH increases with distance in winter and summer, probably due to the lower number of hours of direct solar radiation.

The positive correlation between the air temperature recorded by the sensors in front of the wall and the air temperature recorded by the weather station, especially during the summer, demonstrates that the green wall affects the thermal conditions in its immediate surroundings. It is similar to a study conducted by (Tan et al., 2014b), where the ambient temperature range recorded did not fluctuate wildly, with a slight increase of 1.5 ºC.

Improving the urban microclimate has increasingly become a priority for living in cities. Recent studies have focused on studying how meteorological parameters affect outdoor thermal perception. (Wei et al., 2022) showed the relation between local climate, human comfort, and well-being through results demonstrating that thermal comfort varies considerably depending on the season and the type of landscape. It highlights the relevance of using green walls in reducing temperatures in urban contexts and how the climate in which they are located influences their effects on the urban microclimate.

4. Conclusions

The effect of distance on the temperature reduction of a green wall in real Mediterranean climate conditions has been evaluated by developing an experimental analysis, which advances the present knowledge as there are no specific studies in situ and in the Mediterranean climate. The experimental approach provided valuable data to evaluate the performance of a green wall at four different distances from the wall: 0.25, 0.50, 0.75 and 1m. Four main variables were used for the analysis:

- air temperature (registered by the weather station)
- air temperature at four different distances from the green wall
- relative humidity at four different distances from the green wall
- irradiance (registered by pyranometers installed on the vertical plane of the green wall)

The study has a database recorded during winter and summer 2021-2022 on two green walls facing south and west, consisting of 94.857 air temperature data, 100.359 relative humidity data and 51.934 data of irradiance in the vertical plane. The dataset provides evidence of the effect of a green wall improving the urban microclimate at the pedestrian level in a Mediterranean climate and the impact of distance to the green wall to reduce the temperature at the pedestrian level.

Therefore, the results show that a green wall can improve the urban microclimate at the pedestrian level in a Mediterranean climate during summer, which is novel in the field. However, it cannot be concluded that distance is a significant variable influencing the temperature reduction of a green wall in dense urban environments, as the maximum difference found is 0.6 ºC for temperature and 2.3% for relative humidity.

The applicability of these conclusions to other climates is not direct, as the study showed a significant influence of wall orientation and weather conditions on the results. Therefore, results can only be extrapolated to other contexts with a field campaign, which limits the findings. However, they are aligned with previous literature, confirming the impact a green wall can have on improving urban comfort, especially in the summertime.

Another limitation is related to the experimentation approach. There is a need for an enormous data set to obtain statistically significant conclusions, which is costly and difficult to obtain in an accurate site, such as the building used in the study. Moreover, the need to use a building already built where all equipment can be located could prevent obtaining data corresponding to specific conditions representative of the built environment (wall orientation, radiation impact, wind profiles, etc.)

Furthermore, many factors such as the physical structure, substrate and plant species, materials, dimensions of the green wall modules, and moisture content impact the green wall's performance. These factors are not analysed separately, and future studies can be tailored to study the impact of these factors individually in a Mediterranean climate.

Other future lines of research are related to the following:

- Replicate the methodology to other buildings to avoid the influence of some façade characteristics and to get more data representative from the built environment;

- Analyses the influence of additional variables, such as wind speed, on the performance of the façade; and
- Assess the combined effects of the main parameters to evaluate the impact of green walls on thermal comfort at the urban level.

Furthermore, this study provides compelling evidence that greening the building envelope can complement conventional city green infrastructure and provide multiple ecosystem services to dense urban contexts where the available ground-level area is limited.

References

[1] M. Amani-Beni, Y. Chen, M. Vasileva, B. Zhang, G. di Xie, Quantitative-spatial relationships between air and surface temperature, a proxy for microclimate studies in fine-scale intra-urban areas?, Sustain. Cities Soc. 77 (2022) 103584. doi:10.1016/j.scs.2021.103584.

[2] B. Chun, J.M.J.-M. Guldmann, Impact of greening on the urban heat island: Seasonal variations and mitigation strategies, Comput. Environ. Urban Syst. 71 (2018) 165–176. doi:10.1016/j.compenvurbsys.2018.05.006.

[3] L. Zhang, Z. Deng, L. Liang, Y. Zhang, Q. Meng, J. Wang, M. Santamouris, Thermal behavior of a vertical green facade and its impact on the indoor and outdoor thermal environment, Energy Build. 204 (2019). doi:10.1016/j.enbuild.2019.109502.

[4] S. Charoenkit, S. Yiemwattana, Living walls and their contribution to improved thermal comfort and carbon emission reduction: A review, Build. Environ. 105 (2016) 82–94. doi:10.1016/j.buildenv.2016.05.031.

[5] Y. Chen, B. Shu, R. Zhang, M. Amani-Beni, LST determination of different urban growth patterns: A modeling procedure to identify the dominant spatial metrics, Sustain. Cities Soc. 92 (2023) 104459. doi:10.1016/j.scs.2023.104459.

[6] E. Shafiee, M. Faizi, S.A. Yazdanfar, M.A. Khanmohammadi, Assessment of the effect of living wall systems on the improvement of the urban heat island phenomenon, Build.

Environ. 181 (2020) 106923. doi:10.1016/j.buildenv.2020.106923.

[7] V.L. Castaldo, A.L. Pisello, C. Piselli, C. Fabiani, F. Cotana, M. Santamouris, How outdoor microclimate mitigation affects building thermal-energy performance: A new design-stage method for energy saving in residential near-zero energy settlements in Italy, Renew. Energy. 127 (2018) 920–935. doi:10.1016/j.renene.2018.04.090.

[8] M. Taleghani, Outdoor thermal comfort by different heat mitigation strategies- A review, Renew. Sustain. Energy Rev. 81 (2018) 2011–2018. doi:10.1016/j.rser.2017.06.010.

[9] I. Krusche, P., Krusche, M., Althaus, D., Gabriel, Ökologisches Bauen Umweltbundesamt. Vieweg Friedr. + Sohn Ver, Deutschland., (1982).

[10] T. Koyama, M. Yoshinaga, H. Hayashi, K. ichiro Maeda, A. Yamauchi, Identification of key plant traits contributing to the cooling effects ofgreen façades using freestanding walls, Build. Environ. 66 (2013) 96–103. doi:10.1016/j.buildenv.2013.04.020.

[11] V. Oquendo-Di Cosola, F. Olivieri, L. Ruiz-García, A systematic review of the impact of green walls on urban comfort: temperature reduction and noise attenuation, Renew. Sustain. Energy Rev. 162 (2022) 112463. doi:10.1016/j.rser.2022.112463.

[12] P.P.-Y. Wong, P.-C. Lai, C.-T. Low, S. Chen, M. Hart, The impact of environmental and human factors on urban heat and microclimate variability, Build. Environ. 95 (2016) 199–208. doi:10.1016/j.buildenv.2015.09.024.

[13] M. Razzaghmanesh, M. Razzaghmanesh, Thermal performance investigation of a living wall in a dry climate of Australia, Build. Environ. 112 (2017) 45–62. doi:10.1016/j.buildenv.2016.11.023.

[14] N.H. Wong, A.Y. Kwang Tan, Y. Chen, K. Sekar, P.Y. Tan, D. Chan, K. Chiang, N.C. Wong, Thermal evaluation of vertical greenery systems for building walls, Build. Environ. 45 (2010) 663–672. doi:10.1016/j.buildenv.2009.08.005.

[15] M. Ottelé, K. Perini, Comparative experimental approach to investigate the thermal behaviour of vertical greened façades of buildings, Ecol. Eng. 108 (2017) 152–161. doi:https://doi.org/10.1016/j.ecoleng.2017.08.016.

[16] T. Safikhani, A.M. Abdullah, D.R. Ossen, M. Baharvand, Thermal impacts of vertical greenery systems, Environ. Clim. Technol. 14 (2014) 5–11. doi:10.1515/rtuect-2014-0007.

[17] G. Pérez, L. Rincón, A. Vila, J.M. González, L.F. Cabeza, Behaviour of green facades in Mediterranean Continental climate, Energy Convers. Manag. 52 (2011) 1861–1867. doi:10.1016/j.enconman.2010.11.008.

[18] V. Oquendo-Di Cosola, F. Olivieri, L. Ruiz-García, J. Bacenetti, An environmental Life Cycle Assessment of Living Wall Systems, J. Environ. Manage. 254 (2020) 109743. doi:10.1016/j.jenvman.2019.109743.

[19] F. Olivieri, R.C. Grifoni, D. Redondas, J.A. Sánchez-Reséndiz, S. Tascini, An experimental method to quantitatively analyse the effect of thermal insulation thickness on the summer performance of a vertical green wall, Energy Build. 150 (2017) 132–148. doi:10.1016/j.enbuild.2017.05.068.

[20] C.Y. Jim, Thermal performance of climber greenwalls: Effects of solar irradiance and orientation, Appl. Energy. 154 (2015) 631–643. doi:https://doi.org/10.1016/j.apenergy.2015.05.077.

[21] S. Charoenkit, S. Yiemwattana, N. Rachapradit, Plant characteristics and the potential for living walls to reduce temperatures and sequester carbon, Energy Build. 225 (2020) 110286. doi:10.1016/j.enbuild.2020.110286.

[22] P.F.H.Ó.D.R.D.S. Morales, Sistema JARDIN VERTICAL BIOFIVER ®, 2012.

[23] M. Kottek, J. Grieser, C. Beck, B. Rudolf, F. Rubel, World Map of the Köppen-Geiger climate classification updated, Meteorol. Zeitschrift. 15 (2006) 259–263. doi:10.1127/0941-2948/2006/0130.

[24] F. Yang, F. Yuan, F. Qian, Z. Zhuang, J. Yao, Summertime thermal and energy performance of a double-skin green facade: A case study in Shanghai, Sustain. Cities Soc. 39 (2018) 43–51. doi:10.1016/j.scs.2018.01.049.

[25] R. Sendra-Arranz, V. Oquendo, L. Olivieri, F. Olivieri, C. Bedoya, A. Gutiérrez, Monitorization and statistical analysis of south and west green walls in a retrofitted building in Madrid, Build. Environ. 183 (2020). doi:10.1016/j.buildenv.2020.107049.

[26] C. Piselli, V.L. Castaldo, I. Pigliautile, A.L. Pisello, F. Cotana, Outdoor comfort conditions in urban areas: On citizens' perspective about microclimate mitigation of urban transit areas, Sustain. Cities Soc. 39 (2018) 16–36. doi:10.1016/j.scs.2018.02.004.

[27] R.W.F. Cameron, J.E. Taylor, M.R. Emmett, What's "cool" in the world of green

façades? How plant choice influences the cooling properties of green walls, Build. Environ. 73 (2014) 198–207. doi:10.1016/j.buildenv.2013.12.005.

[28] C.L. Tan, N.H. Wong, S.K. Jusuf, Effects of vertical greenery on mean radiant temperature in the tropical urban environment, Landsc. Urban Plan. 127 (2014) 52–64. doi:10.1016/j.landurbplan.2014.04.005.

[29] D. Wei, L. Yang, Z. Bao, Y. Lu, H. Yang, Variations in outdoor thermal comfort in an urban park in the hot-summer and cold-winter region of China, Sustain. Cities Soc. 77 (2022). doi:10.1016/j.scs.2021.103535.

Artículo 6

Monitorization and statistical analysis of south and west green walls in a retrofitted building in Madrid

Rafael Sendra-Arranz, Valentina Oquendo-Di Cosola, Lorenzo Olivieri, Francesca Olivieri, César Bedoya, Álvaro Gutiérrez (2020).

Building and Environment, 183, 107049.

DOI: 10.1016/j.buildenv.2020.107049

Q1 (JCR)

Monitorization and statistical analysis of south and west green walls in a retrofitted building in Madrid

Authors: R. Sendra-Arranza, V. Oquendo-Di Cosola[b,c], L. Olivieri[b,c], F. Olivieri[b,c], C. Bedoya[b,c,] A. Gutiérrez[a,c]

[a] E.T.S. Ingenieros de Telecomunicación, Universidad Politécnica de Madrid, Av. Complutense 30, 28040 Madrid, Spain

[b] E.T.S. Arquitectura, Universidad Politécnica de Madrid, Av. Juan de Herrera 4, 28040 Madrid, Spain

[c] Innovation and Technology for Development Center, Universidad Politécnica de Madrid, Av. Complutense, 28040 Madrid, Spain

Abstract: Green walls can act as natural thermal regulators, reducing solar radiation on surfaces and providing cooling due to shading and evapotranspiration. Several studies have investigated the cooling effects of a bare wall, in contrast to a vegetated wall, as well as the correlation between temperature reduction and system characteristics. In the present work, we analyse the influence of the orientation of a green wall on its ability to reduce surface temperatures in a Mediterranean climate. Environmental variables such as irradiation and air temperature have been considered. A real-time monitoring system has been used, with a database of three years of measurements. Results show that on average, the control temperature is greater than the green wall temperature with maximum differences of 20 ºC in summer and 80 ºC in winter in the south wall surface. During the summer, the temperature reduction in the south facade occurs mainly in the central hours of the day, while in the west facade it occurs mainly in the afternoon. Being the summer the most relevant season for the use of green walls, this information is very valuable as it allows the designers to know at what time of day the facade provides a temperature reduction, depending on the orientation.

Keywords: Green walls, Green facades, Monitoring system, Exploratory data analysis.

1. Introduction

The impacts of urbanization and climate change are driving a transformation towards complex scenarios that threaten the sustainability of the planet [1]. The world population is constantly growing, using unrenewable natural resources in a continuous and unbalanced way. The consequences of climate change are becoming increasingly visible alongside this scenario: rising temperatures, floods, droughts, air pollution, noise, etc. These effects, in addition to harming life inside cities, diminish the development of new plant species, degrade habitats, alter the development of species adapted to a particular type of climate and reduce drinking water reserves, among others [2]. Currently cities are at the centre of political, social and environmental decision-making.

Mitigating and adapting cities to the effects of climate change means coping with the expected and widespread effects. It is estimated that more than half of the world population will live in cities by 2050, equivalent to 90% development of urban contexts [1]. In other words, urban growth will be approximately one million people per week. Nowadays, cities represent 3% of the earth's surface, and paradoxically are responsible for 80% of the energy consumption and about 75% of CO_2 emissions into the atmosphere. This is a reflection on the fact that population growth will not only be synonymous of urbanization but also of high consumption and pollution ratios [3, 4].

This scenario has been the starting point for global initiatives such as Agenda 2030 and the Sustainable Development Goals (SDGs) [5]. 193 member states of the United Nations unanimously adopted a route composed of 17 SDGs based on three main dimensions: society, environment, and economy. This new approach has changed how human development problems are addressed. It will require tackling challenges on a global scale and in an increasingly complex and interdependent world that requires significant resource management. To achieve these challenges in a stable and long-term scenario, transformations and incentives are needed to promote resilient technologies that stimulate current governance mechanisms.

Considering the challenges of climate change as opportunities for innovation, nature-based solutions can be part of new technologies aimed at preserving biodiversity and solving economic,

social and environmental problems. The nature-based solution term emerged in 2000 as the relationship between nature and people. It primarily focuses on the benefits that nature can bring to environmental and social challenges such as climate change. On the other hand, the European Commission defines them as “those that can turn nature into opportunities for social, economic, and environmental innovation” [6]. For example, through complex natural processes such as the absorption of carbon dioxide, the treatment and management of rainwater or the fixation of atmospheric particles, among others, succeed in reducing environmental risks and achieving human well-being. Nature-based solutions should be developed through four main objectives and seven actions to be developed in the field of research and innovation, highlighting the importance of their implementation to increase the resilience of urban environments.

The idea that nature brings benefits to city life and society as a whole has been developed in different contexts. All of them focusing on sustainability and the capacity to provide provisioning, regulation, and recreation services. It has also been contemplated and disseminated through environmental policies and initiatives of recent decades, shaping research programs that have incorporated this discourse aligning it with the SDGs, especially the SDG 11 “Make cities and human settlements inclusive, safe, resilient and sustainable”. According to this SDG, this paper focuses on investigating green walls as nature-based solutions to reduce temperatures in dense urban environments. More precisely, it focuses on analyzing the behavior of a vegetal facade in two orientations (south and west).

Greening the building envelope allows obtaining some benefits related to the improvement of building efficiency and its ecological and environmental performance. Green walls, as part of vertical greening solutions, are the result of the integration of vegetation on buildings aiming at improving air quality [7], related to the reduction of fine dust levels [8], increase of biodiversity [9], reduction of heat island effect in urban areas [10], and the reduction of energy consumptions for cooling and heating [11]. The benefits of these solutions can be synthesized as the influence of substrate and vegetation thickness, water content, air cavity between the various layers, and the materials used for their construction [12].

Within the classification of vegetal facades, there is a wide range of technical solutions characterized by vertical support structures that may be attached or not to the facade of a building. Depending on the type of the system, there are different configurations. They range from quite simple ones, such as those with vertical support to the more technologically and complex such as the modular ones. Nevertheless, the dimensional and material characteristics between the systems within the same classification are usually the same. A vegetal facade system is composed of fixed (or primary) and variable (or secondary) elements that are determined based on the complexity of the project. As primary components there are supporting elements, water absorption, retention elements, substrates, vegetation and irrigation and fertilisation systems. Second components create vapor barrier layers, insulating layers, vapor pressure diffusion layers and separation layers of different materials [13, 14, 15, 16, 17].

Modular facade systems emerge as an innovative solution for incorporating vegetation into building envelopes [18]. Their configuration and the pre-cultivation of plants allow the instantaneous coverage of large vertical surfaces, being an adaptable solution to any type of building. In this category, different solutions, that vary by composition, module dimensions, substrate type, number of plants per module and support material, can be developed in the form of trays, three-dimensional structures, containers or geotextile bags (see Figure 1).

Figure 1: Modular vegetal facade system before and after the insertion of plants

The trend towards construction with materials such as concrete, glass, and metals is one of the causes of the phenomenon of the urban heat island. This type of surface reflects the solar radiation incident to their immediate surroundings, generating a significant increase in temperatures [19]. It has implications for the energy balance of buildings, as well as problems related to public health [20]. Most of the solutions developed in the last decades include the implementation of high albedo materials [21], which guarantees the rebound of sunlight reflected on the surface to the radiation that affects it. This group of solutions includes green roofs, due to the ability of plants to absorb irradiation and use it in their natural biological processes [22]. The current market and most of the research have concentrated on solving the problem from horizontal surfaces [20, 23, 24, 25, 26]. However, few have stressed the importance of vertical surfaces in the comfort of the urban mesh.

The vegetation in walls can contribute to the improvement of the microclimate in cities both inside and outside buildings. It is a mitigation strategy due to its function as a natural regulator against the temperatures reached because of the climate change. In dense urban environments, vegetation can contribute to cooling the air and providing shade [27]. It can also be a passive energy efficiency strategy, as it acts as an isolating layer on building facades. These benefits have been extensively studied and linked to the ability of the foliar apparatus to reduce wind speed, the thermal inertia of the substrate, and the ability to regulate temperatures through moisture added to the air by evapotranspiration [27, 28, 29, 30, 31, 32].

Wong et al. [33] conducted a research to identify the influence of different vertical green systems on the urban microclimate. Results showed a reduction of up to 3.3 ºC at a distance of up to 15 cm due to the effect of evapotranspiration. Likewise Perini et al. [34], studied the behavior of three facades of different plants and their incidence on the air temperature. They demonstrate similar results for the three systems, which highlights the benefits of vegetation regardless of their constructive configuration. The results of Tabassom et al. [35], demonstrate the behavior of vertical green in humid and warm climates such as Malaysia, with reductions of up to 8 ºC in the air cavity after vegetation and a reduction of an air temperature of up to 4 ºC. Perez et al. [29] analyzed the effect of green walls in a Mediterranean climate. Results confirm the ability of green walls to generate shade on the walls of buildings, and the relevance of the microclimate created

in the cavity between the facade and the wall as well as within the building. It is important to emphasize that to study the behavior of green walls, variables, with the capacity of reducing temperature, must be considered. Different studies have shown the influence of the climate [36, 37], system design and components [38], the irrigation and fertilization system [39], and the type of plants and substrate [40, 17, 41], both in terms of performance and environmental sustainability [42].

The majority of the studies carried out compare conventional facade solutions with vegetable facade systems, being analyzed in the same geographical context and under the same orientation. Tendentially, they are the most beneficial in terms of solar exposure according to the latitude in which the research is carried out. Therefore, the objective of the present study is to analyze the effect of vegetation on the reduction of surface temperatures under different orientations (south and west) in a Mediterranean climate, from the study of environmental variables such as irradiation and air temperature. Since the objective is to measure the influence of the irradiation on the thermal behaviour of vegetation and the possible reduction of temperatures in different layers of the facade, the following questions have been asked:

- Is the temperature reduction effect of a green wall affected by its orientation?
- Is there an important difference between the surface temperatures of a green wall and a metal envelope exposed to the south and west?
- Is irradiation a determining value in the effects associated with green walls?

2. ITD building

The ItdUPM building at Universidad Politécnica de Madrid (UPM) was developed with the aim of creating the first building of almost zero energy consumption inside the campus. To comply with the thermal requirements of the new proposal, a retrofitting was made by adding materials such as glass wool to the existing walls for improving thermal transmittance. The building includes a drilled metal plate skin covering all the facades, leaving an air gap between the concrete wall and the mentioned skin of 20 cm. Additionally, some parts of the skin are covered by a green wall.

Figure 2: Headquarter of Innovation and Technology for Development Centre (itdUPM) – Madrid, Spain

The ItdUPM makes use of passive strategies to reduce the energy consumption as well as the indoor thermal comfort. The integration of a green wall in the south (11.25 m^2), east (6.25 m^2), and west (10 m^2) facade was part of these strategies (see Figure 2). The green wall installed is a modular system called BIOFIVER [12]. It is formed by two three-dimensional structures of polypropylene cells, separated by hydrophilic polyester fabric (see Table 1 for a detailed list of the components). Specifically, the dimension of each module is 50 cm x 50 cm x 10 cm. Additionally, the front structure is filled with organic substrate enriched for the cultivation of plants, that are selected based on their adaptation to the climate in which they are located. The plants selected for the itdUPM building are now shown in Table 1. They are pre-cultivated and inserted in gaps. The rear structure remains empty, generating a hollow space for air circulation (see Figure 3).

Table 1: Components of BIOFIVER system

Biofiver system	
External finishing layer	Polyester
Bearing structure	Polypropylene boxes, Hidrophilic layer, Polyester
Growing medium	Coconut fibre, turf, and hummus
Closing layer	Polyester
Hooking system	Aluminium
Vegetation layer	*Hedera h., Carex, Flagellifera, Carex Testacea, Carex Oshimensis, Crassula radicans "Small Red", Erigeron karvinskianus, Frankenia laevis, Helycrisum italicum, Heuchera americana, Lamium maculatum, Lampranthus aurantiacus, Lavandula dentata, Lavandula dentata, Lonicera n´ıtida, Myrtus communis, Polygonum capitatum, Rosmarinus, Santolina chamaecyparissus, Sedeveria, Sedum album, Sedum palmeri, Sedum lineare, Thymus vulgaris*

Moreover, the green wall has an exudation irrigation system that allows the entire surface to have the same amount of water at any point. This favours that the necessary irrigation for the green wall can be easy calculated. The number of plants installed per module is 16, i.e., 64 plants per m^2.

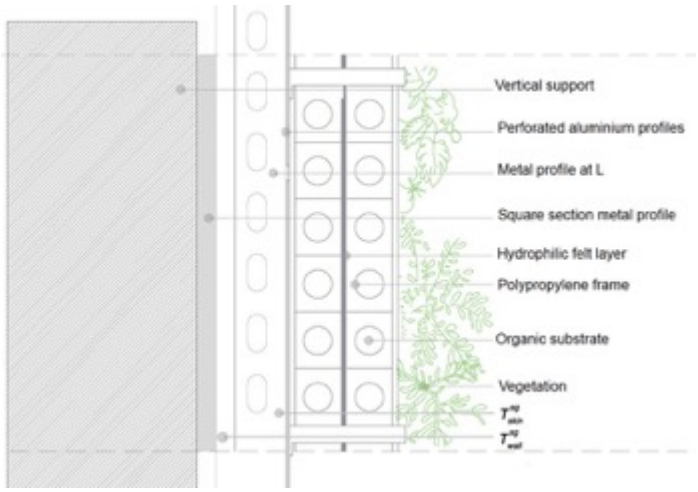

Figure 3: itdUPM green wall section

A real-time distributed monitoring system has been installed to analyze the behavior of the south and west facades. The monitoring system is based on an ad-hoc designed embedded system connected through an RS-485 serial bus to several distributed nodes. These nodes are directly connected to eight type-T thermocouples (0.1 ºC resolution), two pyranometers 3 (0.1

W/m^2 resolution) and one meteorological station 4. The nodes are running a real-time operating system which takes care of acquiring all measurements at specific time frames. Every 10 ms. each node obtains information from all the sensors at which it is connected. Every second the monitoring node performs the mean of the last 100 measurements and stores it internally to be acquired by the main controller through an RS-485 RTU-Modbus protocol. The main controller is based on an embedded Linux operating system. It is made of a microcontroller with a UPS system and an electronic carrier to connect to the nodes. Every minute, the main controller acquires all measurements stored on the nodes and accumulates them on an internal SD card. This information is stored together with the date and time. Moreover, every five minutes the main controller sends the data stored to the monitoring server. The monitoring server is in charge of synchronizing all data, performing all conversions from electrical to physical measurements and running periodic scripts which process the data and upload them to the monitoring database. A monitoring website has been created to allow researchers and the general public observe the behaviour of both facades in real time 5. All the information presented in this manuscript is extracted from that website and is accessible to the general public. The data obtained to the analysis performed in Section 3 is gathered from June 2016 until September 2019, although monitoring is still ongoing. The time series data set is currently composed by more than 2 million of samples with 1 minute sampling period.

3. Exploratory data analysis

In this section, a comparison between a control surface (the metal plate without the green wall) and the green wall is considered. Table 2 gathers the notation of the sensors under study (see Figure 4).

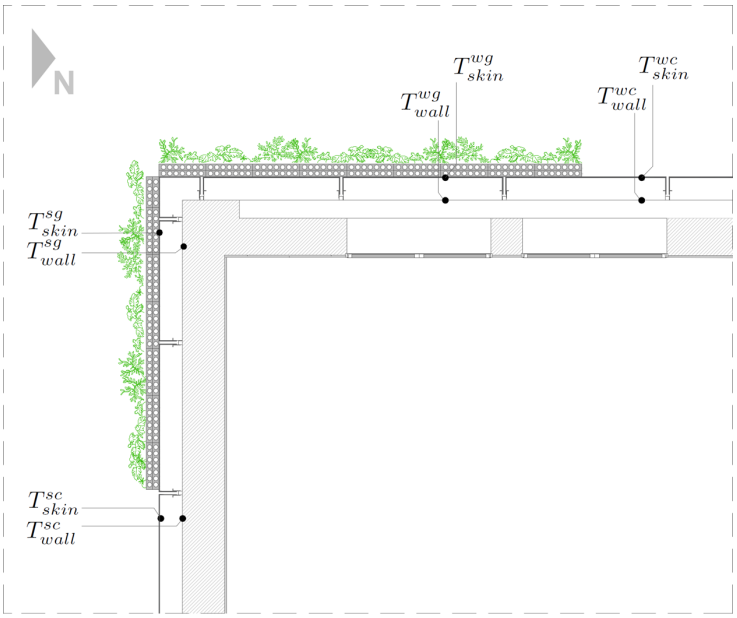

Figure 4: South-west corner of the itdUPM bulding where all variables measured are displayed (see Table 2).

Notice that subindex skin or wall represent that the sensor is located at the skin (metal plate with our without vegetation) or wall respectively. Superindex *s* and *w* denote south and west facades respectively. Moreover, superindex *c* denotes that the sensor is placed on the control surface, the metal plate without the green wall. On the contrary, superindex *g* indicates that the sensor is placed behind the green system.

Figure 5 depicts a heatmap representing a simplified correlation matrix between temperatures and environment variables. UV and V_{wind} share a noticeably weak and almost negligible correlation with the temperature features, concluding that their impact on the green facade behavior is not significant. On the contrary, there is an outstandingly strong correlation in the case of T_{ext} and H_{ext}. While the former variable shows a similar correlation with all temperatures, in the

case of the humidity, its impact is slightly less appreciable behind the green wall (temperatures with superindex *g*). Special attention is required in the first two columns of the matrix which collect the correlations with the irradiance in both facades. The first issue highlighted is the fact that, with exception of T^{sc}_{skin}, the south temperatures have a stronger correlation with the west façade irradiance compared to the south one. In the subsequent, some evidence supporting that the cause is a delay produced by the green wall in the temperature time series T^{sg}_{skin} with respect to T^{sc}_{skin} will be provided. Moreover, the mentioned delay causes a better curve fitting of T^{sg}_{skin} to I^{w} profile than to I^{s} (taking into consideration that the daily profile of I^{w} is also delayed with respect to I^{s}). This statement explains why the aforementioned correlations in the south areas with green wall are too weak when compared to I^{s}. Because of the strong dependence on temperature and Irradiance, these two variables have been selected for the behavior data analysis.

Table 2: Table of absolute variables notation

Absolute variables		
T^{sc}_{skin}	≜	South façade skin temperature, control surface.
T^{sc}_{wall}	≜	South façade wall temperature, control surface.
T^{sg}_{skin}	≜	South façade skin temperature, green wall.
T^{sg}_{wall}	≜	South façade wall temperature, green wall.
T^{wc}_{skin}	≜	West façade skin temperature, control surface.
T^{wc}_{wall}	≜	West façade wall temperature, control surface.
T^{wg}_{skin}	≜	West façade skin temperature, green wall.
T^{wg}_{wall}	≜	West façade wall temperature, green wall.
T_{ext}	≜	Exterior temperature
I^s	≜	South façade irradiance on the vertical plane.
I^w	≜	West façade irradiance on the vertical plane.
H_{ext}	≜	Exterior humidity
UV	≜	UV index on the horizontal plane.
v_{wind}	≜	Wind speed

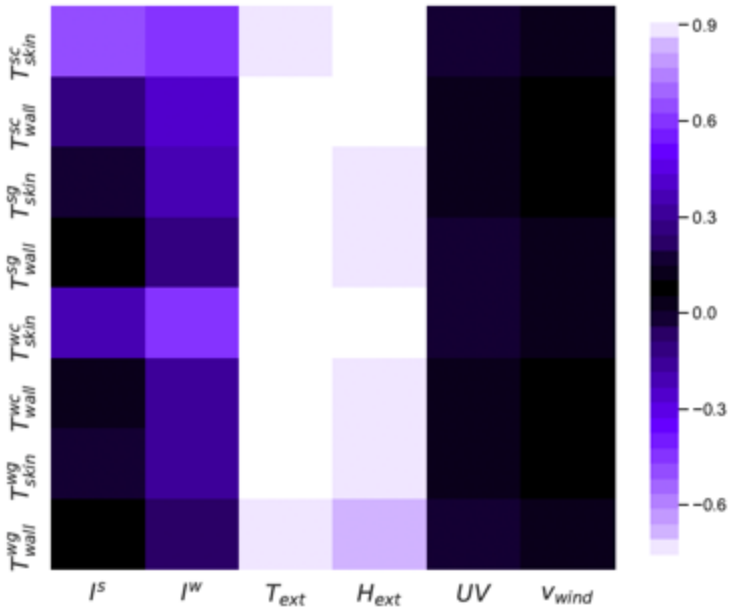

Figure 5: Simplified correlation matrix between temperatures and the remaining potentially relevant features. Black denotes a weak linear correlation between the variables and white represents an outstanding strong correlation. To increase its interpretability, the same colours were used for strong correlation and strong anticorrelation.

Figure 6 provides a better illustration of this phenomenon. The scatterplots relating control surface skin temperatures with irradiances in both south and west facades (Figure 6 a and Figure 6c) denote an existing linear relationship between the targeted variables. On the contrary, a different situation can be observed in the scatterplots where green facade skin temperatures and irradiances (Figure 6b and Figure 6d) are compared. In this scenario, the scatterplots show a

poor linear relationship between the variables in any of the studied facades. Although this observation could drive to the conclusion that the green wall is erasing the correlation between T^{sg}_{skin} versus I^{s} and T^{wg}_{skin} versus I^{w}, a deeper understanding of the wall behavior can be obtained by including the time factor in the analysis (see Figure 7).

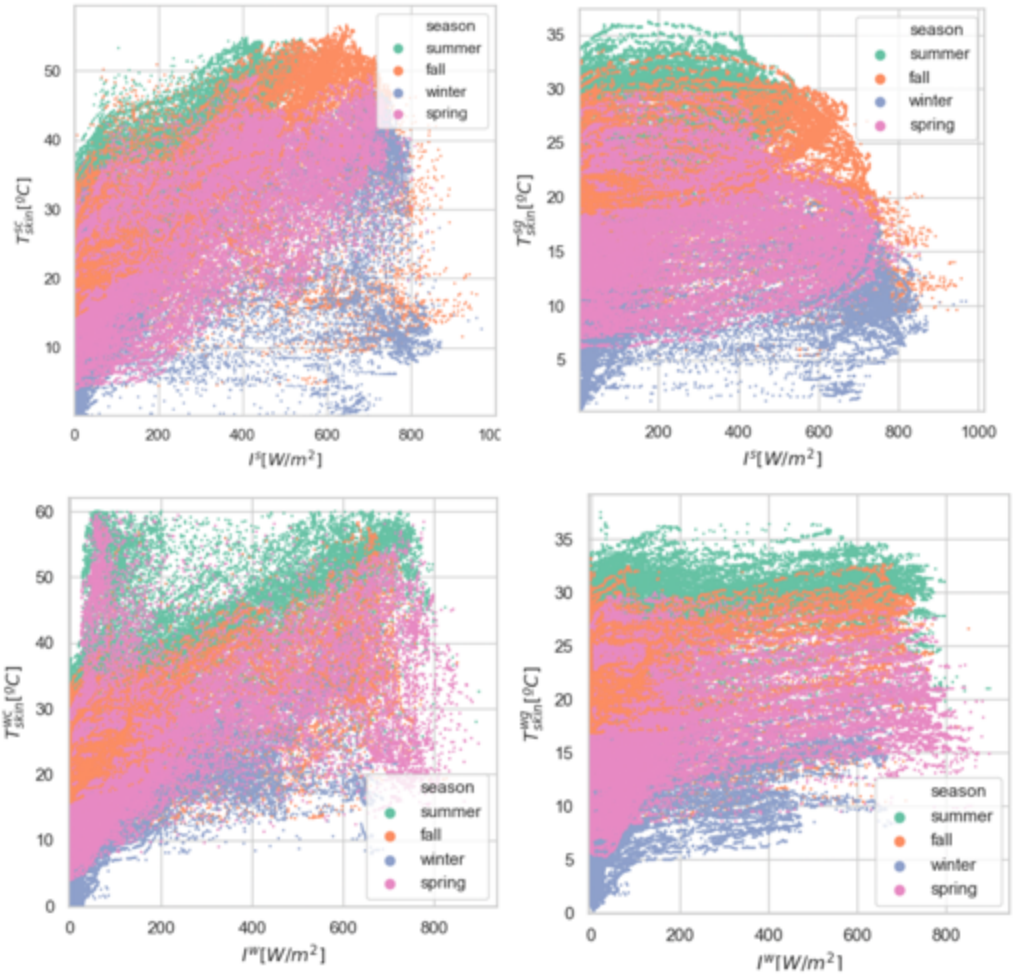

Figure 6: Scatterplots of (a) south control skin temperature (T^{sc}_{skin}) and south irradiance (I^{s}), (b) south green skin temperature (T^{sg}_{skin}) and south irradiance (I^{s}), (c) west control skin temperature (T^{wc}_{skin}) and west irradiance (I^{w}) and (d) west green skin temperature (T^{wg}_{skin}) and west irradiance (I^{w}) for each season of the year.

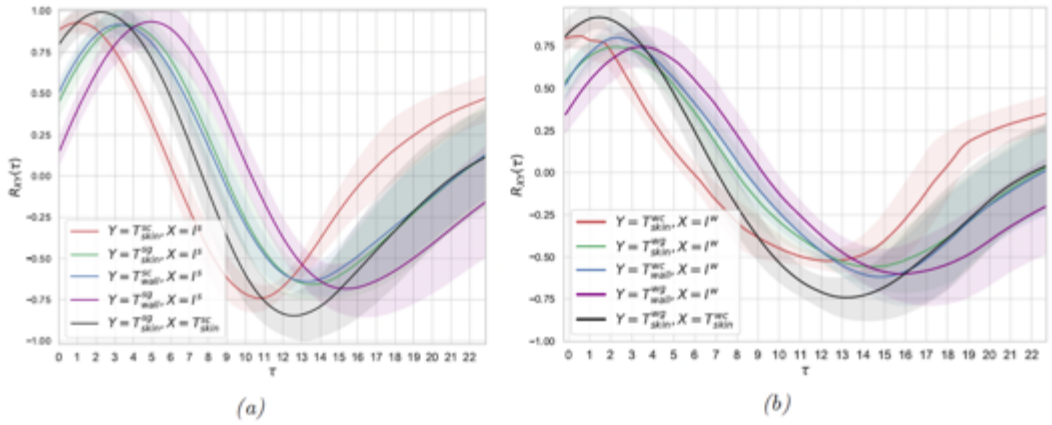

Figure 7: Cross correlation functions of the temperatures and irradiance in (a) south facade and (b) west facade in summer 2018. Additionally, the black curves show the cross-correlation function between control and green walls. The time series are partitioned into daily length segments. These segments are standardized and unbiased sample cross correlation is computed for each of them. In the curves, sample mean and sample standard deviation of each of the estimated cross correlations is depicted for each pair of variables.

Fig. 7 plots the cross correlation between each temperature in south and west facades and their corresponding irradiance (I^s or I^w) using data samples of the summer. The correlation analysed in Fig. 5 corresponds to the correlation for a zero lag or displacement (τ=0) in Fig.7. The illustrated graphs have been obtained by means of the unbiased sample cross correlation estimator as follows: the time series is splitted into a set of non-overlapping segments of length 1440 (so that each segment is a different day with 1 minute resolution of the time series). Subsequently, the unbiased sample cross correlation estimator between Y (k) and X(k), defined as in Equation (1), is applied to each segment. In this case, X (*k*) is either I^s or I^w depending on the facade and Y (*k*) is the temperature time series under assessment (see Fig. 7). It should be mentioned that, aiming to decrease the non-stationarity of the analysed processes, all the segments have been subject to a standarization process. Furthermore, the partitioning procedure and the selection of data belonging to the same season and year have also been applied in order to deal with the non-stationarity issue.

$$\hat{R}_{YX}(\tau) = \frac{1}{N-\tau} \sum_{k=0}^{N-\tau-1} Y[k+\tau]X[k], \quad \tau \in \{0, ..., 1439\}$$

Fig. 7 depicts the sample mean and sample standard deviations of the cross correlation estimates of all segments. The most relevant part of Figure 7 is the region of the function where the first cross correlation peaks are produced (values between 1 and 7 depending on the temperature sensor and the facade). This peak of correlation represents the delay between the temperatures and the irradiance. In the south area of the building, it can be highlighted that the peak of correlation between T^{sc}_{skin} and I^{s} is produced for a delay of 1 hour, while T^{sg}_{skin} exposes a maximum for 3.5 hours. Therefore, it is corroborated that a delay exists between the temperatures covered by the green wall and the irradiance at the corresponding orientation. Moreover, the black curve of Fig 7a display the direct cross correlation between T^{sc}_{skin} and T^{sg}_{skin}. In particular, the peak of cross correlation is approximately produced at a delay of 2.5 hours. This observation leads to the conclusion that the green wall is generating a delay of about 2.5 hours in the temperature of its skin surface. A similar scenario can be observed in the west facade, albeit the delays are less noticeable. This means that the green wall generates a positive effect on the outer layer of the building, providing a reduction in temperature and a delay in the maximum peak. Another remarkable observation is that the cross-correlation curves of T^{sg}_{skin} and T^{sc}_{wall} with I^{s} in south (Fig 7a) and T^{wg}_{skin} and T^{wc}_{wall} with I^{w} in west (Fig 7b) are extremely similar. Therefore, the delay produced by the green facade is comparable to the one caused by the air chamber between skin and wall surfaces.

Fig. 8 displays the daily profile of the temperature variables. In addition to the wall temperature measurements, the irradiance (black) and exterior temperature (green) are shown together. Focusing on the south facade, it can be observed that T^{sc}_{skin} is utterly high (for instance around 45 ºC in summer at 15:00). Furthermore, its thermal time constant is remarkably low [43], producing an almost simultaneous rise in temperature with the incident irradiance. Subsequently, the temperature T^{sc}_{wall} is substantially smoothed and suffers a delay of about 120 minutes (observing the time when the curves start to increase) and a decreased slope in the rising of the temperature in the morning, that can be interpreted as a low pass filter. Notice that the mentioned delay can be also observed in Fig 7a) between red and blue curves. Moreover, T^{sg}_{skin} (purple curve) is already smoothed with respect to T^{sc}_{skin} and its slope is even slower than T^{sc}_{wall}. Therefore, this fact suggests that the green wall is performing a similar low pass filtering as the

air chamber between the control surface and the wall of the building in the control area. The final temperature measurable in the area of the facade with green wall is T^{sg}_{wall} (pink curve), that is comparable to T^{sg}_{skin} but with lower temperatures in midday and larger values during the night, being a desirable behavior. Therefore, the green wall acts as a buffer of the external conditions, providing the building's skin with lower temperatures during the day when there is a greater need for cooling. At the same time, the green facade provides higher temperatures during the night, when the indoor temperatures tend to be lower due to the important thermal excursion that characterizes continental climates. As a consequence, the achieved daily profile of the temperature T^{sg}_{wall} is noticeably at, resulting in thermal stability in the outer skin of the building.

Looking at T^{sg}_{wall}, it can be observed that it has a similar daily pro le to T^{sg}_{skin} but with lower temperatures during the day and barely larger values during the night. This behaviour can be explained considering that the wall is less exposed to the external conditions than the skin. Therefore, during the daytime, the effect of the irradiation produces a higher temperature on the skin area, whereas during the nighttime the exterior temperature affects the skin temperature more than the wall temperature. Thus, the use of an air chamber behind the vegetal cover seems to amplify the effect of the vegetation, resulting in greater thermal stability for the wall behind the green facade.

Furthermore, it is worth of highlighting the behaviour of the wall temperature behind the green fa cade (T^{sg}_{wall}, pink curve) in comparison with the wall temperature in the control surface wall (T^{sc}_{wall}, red curve). Figure 8 shows that for all the seasons on both orientations, T^{sg}_{wall} is lower than T^{sc}_{wall}, being the differences highest in summer and fall (about 7 ºC max) and lower in winter (about 5 ºC max).

Table 3: Table of temperature differences notation

Temperature differences
$\Delta T^{s}_{skin} = T^{sc}_{skin} - T^{sg}_{skin}, \quad \Delta T^{w}_{skin} = T^{wc}_{skin} - T^{wg}_{skin}$
$\Delta T^{s}_{wall} = T^{sc}_{wall} - T^{sg}_{wall}, \quad \Delta T^{w}_{wall} = T^{wc}_{wall} - T^{wg}_{wall}$
Second order temperature differences
$\Delta^2 T^{sw}_{skin} = \Delta T^{s}_{skin} - \Delta T^{w}_{skin}$
$\Delta^2 T^{sw}_{wall} = \Delta T^{s}_{wall} - \Delta T^{w}_{wall}$

In addition to the absolute measurements, temperature differences (see Table 3) are calculated to compare how the green wall is working in comparison with the control surface at different orientations. Specifically, the difference between the skin and wall behaviours are compared both for the south (T^{s}_{skin} and T^{s}_{wall}) and west (T^{w}_{skin} and T^{w}_{wall}) orientations. These differences of temperature directly quantify how efficiently the green system is in terms of thermal protection compared to a control area in the same orientation. Fig. 9 depicts these variables for each season of the year. A remarkable fact is that during daytime there is a positive difference between south skin temperatures Ts skin (with maximum differences around 17 ºC depending on the season of the year), denoting that the sensor behind the green wall is measuring a lower temperature than the one on the control surface. Moreover, T^{s}_{wall} maintains this positive difference but strongly attenuated. Even with this attenuation, the peak of T^{s}_{wall} is between 5 ºC and 8 ºC depending on the season. This is an outstanding temperature reduction between the wall with and without green wall. On the contrary, results are less favourable during the night. During night-time, wall sensors measure on average very poor temperature differences (T^{s}_{wall}) that in most cases may not be noticeable. Winter, spring and fall seasons show values of ΔT^{s}_{wall} that are at most 1 ºC. In the case of summer season, the wall temperature differences are more important, measuring values between 2 ºC and 4 ºC. In regard to night-time thermal performance of the green wall, west orientation shows even worse results because of the reduced values in summer (maximum of 2 ºC in midnight) with respect to south measurements.

Therefore, the green wall allows reducing the incoming thermal loads during daytime in summer, fall and spring, performing as a very effective sun shading device. On the other hand, in winter and during night-time its effects are greatly reduced. This is a positive conclusion as the reduced thermal loads in the warm periods do not correspond to an increase in thermal loads in the cold periods. Another issue to be remarked is the fact that the temperature differences are highly dependent on the irradiance profile, as shown in Figure 9. This means that the green wall system reduces the wall temperature and thus the thermal load by conduction through the wall. In Figure 9, it is also observable that, with the exception of the summer season, the differences of temperature are larger in the south orientation. Besides, it can be noted that during the summer the temperature reduction in the south fa cade occurs mainly in the central hours of the day, while in the west facade it occurs mainly in the afternoon, corresponding in both cases with the radiation profile in the two orientations. Being the summer the most relevant season for the use of green walls, this information allows the designers to predict at what time of day the facade provides a temperature reduction, depending on the orientation. This is useful when selecting the facade where the green wall will be placed, and that will depend mainly on the hourly profile of the building.

Therefore, a direct comparison in terms of temperature difference between south and west facades is carried out. The objective is to deepen into the dependency of the green wall placement with the temperature. Fig. 10 shows the daily profile of the variables $\Delta^2T^{sw}_{skin}$ and $\Delta^2T^{sw}_{wall}$, representing the comparison between temperature differences in south and west facades (see Table 3). More precisely, a positive value indicates that the south green wall is performing more suitably due to a lower temperature in its green wall area. It is shown that the green wall located in the south surface is more efficient than the one facing to the west between 10:00 and 15:00. On the other hand, the green wall performs better in the west facade between 15:00 and 20:00. This difference is mainly caused by the irradiance pro le, whose peak is firstly produced in south and subsequently in west. This issue is also observable in Fig. 9, noticing that the peak of difference in each wall is produced at different instants of the day. One interesting issue to be pointed out is that, in winter and fall, $\Delta^2T^{sw}_{skin}$ is always positive. Being the autumn and winter seasons of the year in which in the city of Madrid normally do not have refrigeration charges, it

seems logical to conclude that during the cold seasons the south fa cade has better behaviour than the west. Moreover, if the pro le of $\Delta^2 T^{sw}_{wall}$ is observed, the west wall only behaves better in summer during the period of time between 17:00 and 20:30. This means that buildings that are mainly used in the afternoon or that have cooling loads that originate primarily in the west orientation, will be more favoured by the installation of a green wall on the west facade. For the rest of the buildings, it seems logical to conclude that a green wall in the south fa cades behaves better than a green system in the west ones, at least during the hot seasons.

Finally, the previous observations and conclusions taken from Figs. 8 and 9 are formalized by means of hypothesis testing. In order to define the tests, let $T_{sc;I\ wall}(k)$, $T_{sg;I\ wall}(k)$, $T_{wc;I\ wall}(k)$ and $T_{wg;I\ wall}(k)$ be the south control, south green, west control and west green wall temperature random variables for season of the year *i* and minute of the day. For instance, all the measurements of Tsg wall performed in summer at 14:00 form a sample of the random variable $T^{sg}_{wall}(840)$. With this notation, Hypotheses 2 and 3 are proposed as the null hypothesis to be assessed for season *i* and minute *k* of the day in south and west facades respectively μX is the population mean of the distribution *X*.

$$H_0^{i,k,south} : \mu_{T^{sc,i}_{wall}(k)} - \mu_{T^{sg,i}_{wall}(k)} = 0$$
$$H_0^{i,k,west} : \mu_{T^{wc,i}_{wall}(k)} - \mu_{T^{wg,i}_{wall}(k)} = 0$$

The starting point to validate or refuse the mentioned null hypotheses is to verify if the normality assumption was fulfilled for each sample. Therefore, Shapiro-Wilk test [44], which null hypothesis states that the underlying distribution of the sample is a normal random variable, is used. Owing to the fact that all the samples led to an extremely low p-value, the normality assumption of the data sample is rejected. Thus, a non-parametric hypothesis test is selected to decide on the validity of Equations 2 and 3. More precisely, Wilcoxon signed-rank test [45] is applied. With the aim of visualizing the results of all the tests in a compact way, a graph depicting the resulting log(*p*-value(*k*)) is presented in Fig. 11a for the south fa cade and in Fig. 11b for the west orientation. The black horizontal line shows the natural logarithm of the selected significance level

of the tests. Thereby, the null hypothesis is accepted for those instants of the day when log(*p*-value(*k*)) surpasses the horizontal line and rejected otherwise. Fig. 11a, shows that there is strong evidence to state that T^{sg}_{wall} is larger (see Fig. 9) than T^{sg}_{wall} during all the day in summer. The remaining seasons have just some periods of the day when $Ho^{i,k;south}$ is rejected (mainly between 11:00 and 21:00, corresponding to sun activity peak), highlighting the fact that fall is the season when the inequality of temperature means is less evident. On the contrary, the west fa cade tests results are less favourable. Even though summer tests are still rejected in almost all the instants of the day, the other seasons show a contrary scenario of p-values that provide strong evidence to reject the null hypotheses in shorter periods of time than in the south orientation.

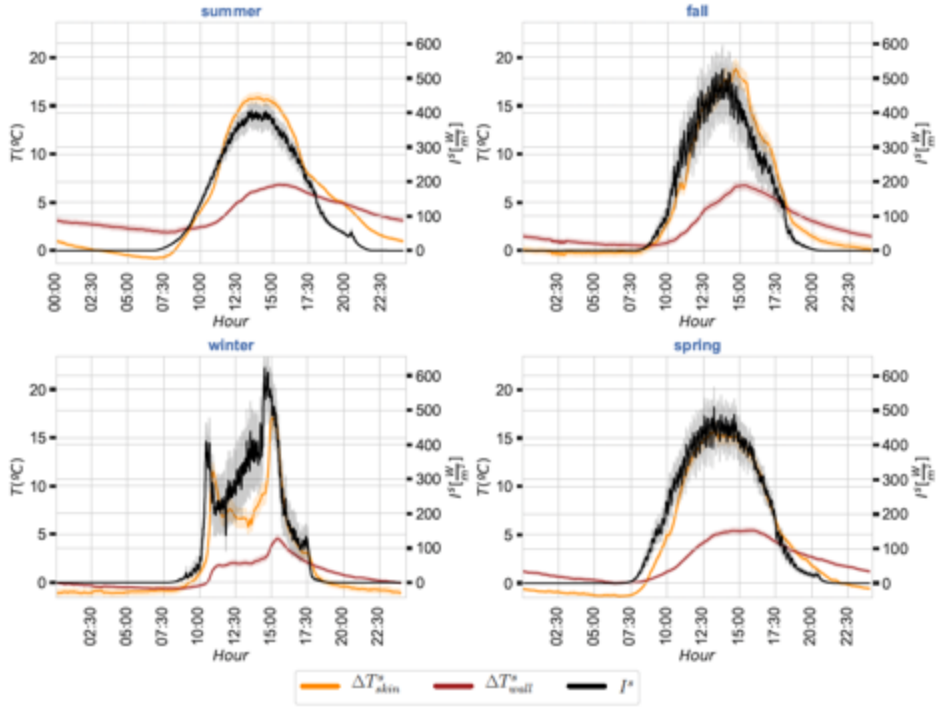

(a) South façade

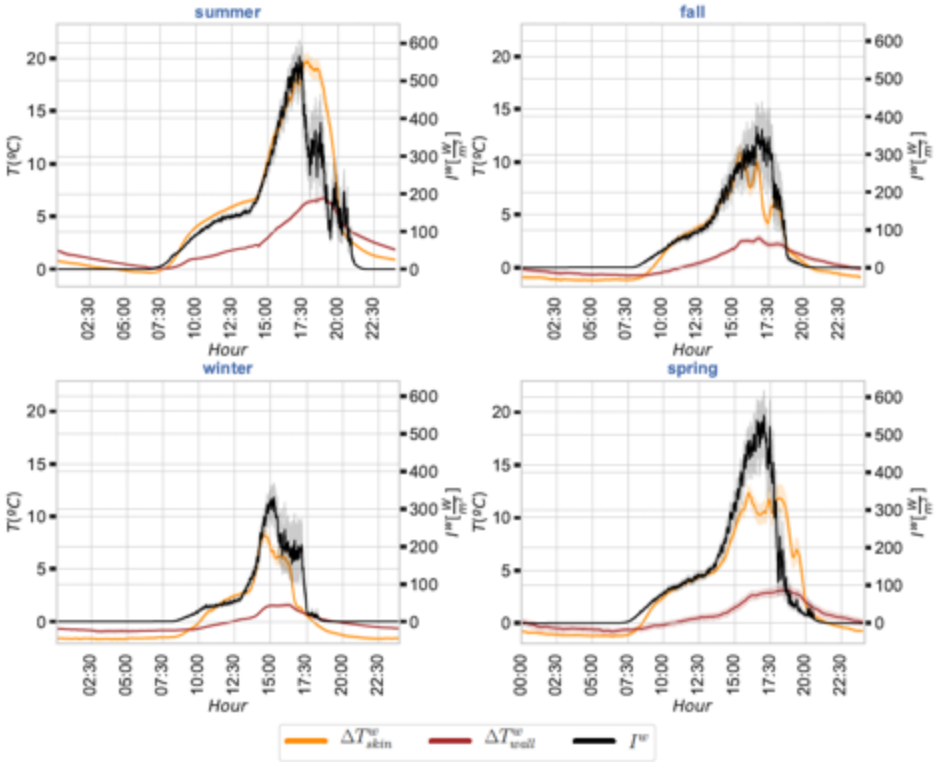

(b) West façade

Figure 9: Daily profile of temperature differences in south and west facades of the building. The daily median of the ΔT time series and its corresponding confidence interval with 95% of confidence level are represented.

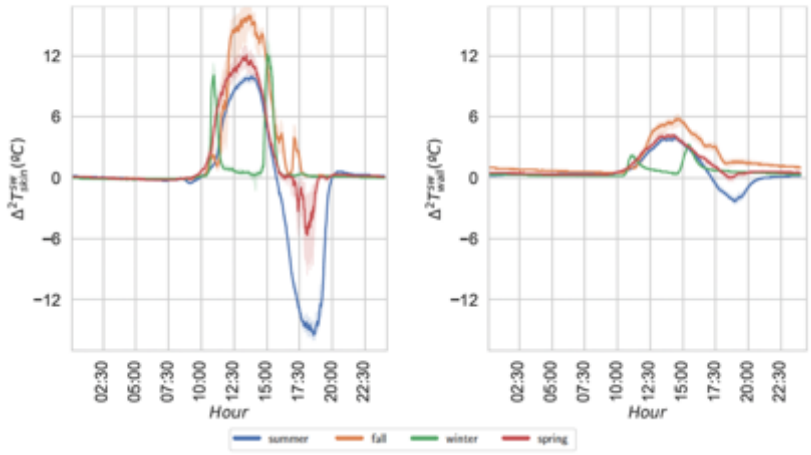

Figure 10: Comparison of south and west facades by means of second order temperature differences (see Table 3) in skin (left) and wall (right). It depicts the median estimation during the day for each season with its corresponding confidence interval with 95% of confidence level.

4. Conclusion

A retrofitted building located in Madrid was used to assess the impact of green wall systems on the building temperature in different orientations. The building is equipped with a monitoring system that gathers the temperature measurements with 1 minute time resolution in different points behind the green walls and control surfaces. Therefore, a total amount of 2 million samples was used to accomplish an exhaustive comparison between control and green wall in south and west orientations aiming to conclude if there is statistical difference on their measurements.

The statistical analysis led to the conclusion that, on average, the control temperature is greater than the green wall temperature with a maximum difference of around 20 ºC in summer and 8 ºC in winter in the south skin area and about 7 ºC in summer and in 2 ºC in winter in the south wall surface. Nonparametric hypotheses tests on the equality of means supported these observations. Although the results are positive during the day, difference of temperature in wall surface during the night period is not significant in any season (with maximum absolute temperature differences of 1 ºC) except summer (wall temperature differences ranging between 2 ºC and 4 ºC).

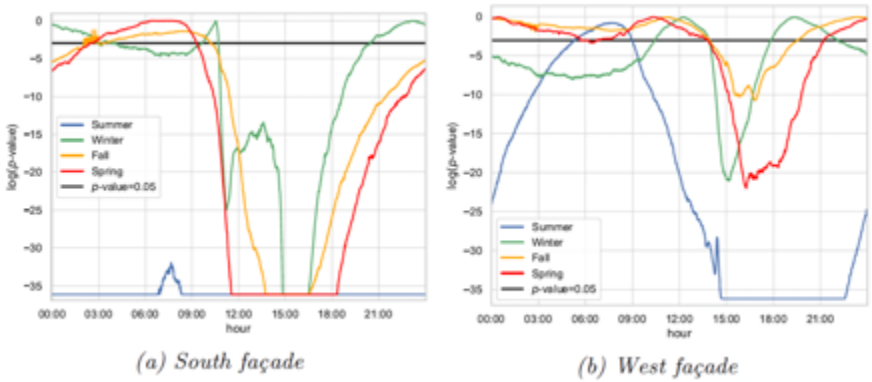

Figure 11: Natural logarithm of the p-values obtained from the non-parametric hypothesis tests to verify hypotheses (2) and (3) on each minute of the day and each season of the year for south facade in (a) and west facade in (b). Null hypotheses are rejected if the corresponding p-value lies below the black line (corresponding to the logarithm of the significance level log(α).)

The statistical analysis also revealed that the impact of the green wall on temperature reduction. Is more significant in the south facade than in the west facade. To assess it, the differences of temperature between control and green fa cades in south and west orientations were analysed. On average, south skin differences are noticeably higher during all day in fall and winter seasons (with maximum differences between south and west of about 16 ºC in fall and 12 ºC in winter). Similarly, summer and spring skin measurements also show superior temperature differences (about 16 ºC superior in summer and 6 ºC in spring) between 10:00 and 17:00. However, in the period of time between 17:00 and 20:30, west orientation provides more favourable results of about 16 ºC superior in summer and 6 ºC in spring.

The results obtained indicate that the green wall acts as a buffer of the external conditions, providing the building's skin with lower temperatures during the day when there is a greater need for cooling. At the same time, the vegetation layer provides higher temperatures during the night, when the indoor temperatures tend to be lower due to the important thermal excursion that characterizes continental climates. As a consequence, the daily pro le of the temperature in the external surface of the wall is almost at, resulting in thermal stability in the outer skin of the building. Furthermore, the use of an air chamber behind the vegetal cover seems to amplify the effect of the vegetation, resulting in greater thermal stability for the wall. The study also shows

that both for the south and the west facade, the reduced thermal loads in the warm periods do not correspond to an increase in thermal loads in the cold periods.

Focusing on the different behaviour of the two facades, it can be noted that during the summer the temperature reduction in the south fa cade occurs mainly in the central hours of the day, while in the west fa cade it occurs mainly in the afternoon. Being the summer the most relevant season for the use of green walls, this information is very valuable as it allows the designers to know at what time of day the fa cade provides a temperature reduction, depending on the orientation. This is useful when selecting the fa cade where the green wall will be placed, and that will depend mainly on the hourly use pro le of the building. The buildings that are mainly used in the afternoon or that have cooling loads that originate primarily in the west orientation, will be more favoured by the installation of a green wall on the west fa cade. For the rest of the buildings, it seems logical to conclude that a green wall in the south fa cade behaves better than a green wall in the west one, at least during the hot seasons. The results obtained also demonstrate that in the cold periods the green west wall has a better behaviour than the south one, as the shading power of the green wall does not affect the possible external thermal gains.

Acknowledgments

The authors are grateful to the Universidad Politécnica de Madrid and the Innovation and Technology for the Development Centre for providing the means and resources necessary for this research work. We also want to thank Vertiarte company for providing the technical information of the green wall system used in this research.

References

[1] UNITED NATIONS, Cities and climate change: Policy directions, https://unhabitat.org/sites/default/ les/download-manager- les/Cities[Online; accessed 20 December 2019] (2011).

[2] Dagmar Schröter, et al. (2005). *Ecosystem Service Supply and Vulnerability to Global Change in Europe*. https://doi.org/10.1126/science.1115233

[3] I. Andri c, M. Ko c, S. Al-Ghamdi, A review of climate change implications for built environment: Impacts, mitigation measures and associated challenges in developed and developing countries, Journal of Cleaner Production 211 (2019) 83{102.
[4] N. J. Paull, P. J. Irga, F. R. Torpy, Active green wall plant health tolerance to diesel smoke exposure, Environmental Pollution 240 (2018) 448 {456.
[5] UNITED NATIONS, Sustainable development goals, https://www.un.org/sustainabledevelopment/sustainabledevelopment-goals/, [Online; accessed 10 December 2019] (2015).
[6] European Commission, Nature-based solutions & re-naturing cities, https://ec.europa.eu/newsroom/horizon2020/document.cfm?doc id=10195, [Online; accessed 5 October 2019] (2015).
[7] J. Klingberg, M. Broberg, B. Strandberg, P. Thorsson, H. Pleijel, Infuence of urban vegetation on air pollution and noise exposure - a case study in gothenburg, sweden., Science of the Total Environment 599-600 (1) (2017) 1728{1739.
[8] K. Perini, M. Ottel e, S. Giulini, A. Magliocco, E. Roccotiello, Quanti cation of fine dust deposition on di erent plant species in a vertical greening system, Ecological Engineering 100 (1) (2017) 268{276.
[9] F. Mayrand, P. Clergeau, Green roofs and green walls for biodiversity conservation: A contribution to urban connectivity, Sustainability 10 (1) (2018) 985.
[10] M. Solera-Jimenez, Green walls: a sustainable approach to climate change, a case study of London, Architectural Science Review 61 (1-2) (2018) 48{57.
[11] S. Charoenkit, S. Yiemwattana, Living walls and their contribution to improved thermal comfort and carbon emission reduction: A review, Building and Environment 105 (2016) 82{94.
[12] K. Perini, M. Ottel e, E. M. Haas, R. Raiteri, O. M.4Ungers, Greening the building envelope, facade greening and living wall systems, Open Journal of Ecology 1 (2011) 1{8.
[13] M. Kohler, Green facades|a view back and some visions, Urban Ecosystems 11 (4) (2008) 423{436.
[14] G. Perez, J. Coma, I. Martorell, L. F. Cabeza, Vertical greenery systems (vgs) for energy saving in buildings: A review, Renewable and Sustainable Energy Reviews 39 (2014) 139{165.
[15] M. Manso, J. Castro-Gomes, Green wall systems: A review of their characteristics, Renewable and Sustainable Energy Reviews 41 (2015) 863{871.
[16] T. Sakhani, A. M. Abdullah, D. R. Ossen, M. Baharvand, A review of energy characteristic of vertical greenery systems, Renewable and Sustainable Energy Reviews 40 (2014) 450{462.
[17] V. Serra, L. Bianco, E. Candelari, R. Giordano, E. Montacchini, S. Tedesco, F. Larcher, A. Schiavi, A novel vertical greenery module system for building envelopes: The

results and outcomes of a multidisciplinary research project, Energy and Buildings 146 (2017) 333{352.
[18] F. Victorero, S. Vera, W. Bustamante, F. Tori, C. Bonilla, J. Giron as, V. Rojas, Experimental study of the thermal performance of living walls under semiarid climatic conditions, Energy Procedia 78 (2015) 3416{3421.
[19] B. Chun, J. M. Guldmann, Impact of greening on the urban heat island: Seasonal variations and mitigation strategies, Impact of greening on the urban heat island: Seasonal variations and mitigation strategies 71 (2018) 165{176.
[20] L. Kleerekoper, T. B. S. M. Van Esch, How to make a city climate-proof, addressing the urban heat island e ect, Resources, Conservation and Recycling 64 (2012) 30{38.
[21] Y. Xing, P. Jones, I. Donnison, Characterisation of nature-based solutions for the built environment, Sustainability 9 (1) (2017) 1{20
[22] N. Fernandez-Breg on, M. Urrestarazu, D. L. Valera, Effects of a vertical greenery system on selected thermal and sound mitigation parameters for indoor building walls, Journal of Food Agriculture and Environment 10 (3) (2012) 1025{1027.
[23] M. Taleghani, Outdoor thermal comfort by different heat mitigation strategies- a review, Renewable and Sustainable Energy Reviews 81 (2) (2018) 2011{2018.
[24] J. Kim, D. Gu, H. Y. Kim, Effects of urban heat island mitigation in various climate zones in the United States, Sustainable Cities and Society 41 (2018) 841{852.
[25] F. Olivieri, C. D. Perna], M. D'Orazio, L. Olivieri, J. Neila, Experimental measurements and numerical model for the summer performance assessment of extensive green roofs in a mediterranean coastal climate, Energy and Buildings 63 (2013) 1 {14.
[26] C. Bartesaghi Koc, P. Osmond, A. Peters, Evaluating the cooling effects of green infrastructure: A systematic review of methods, indicators and data sources, Solar Energy 166 (2018) 486{508.
[27] D. H. S. Duarte, P. Shinzato, C. dos Santos-Gusson, C. A. Alves, The impact of vegetation on urban microclimate to counterbalance built density in a subtropical changing climate, Urban Climate 14 (2015) 224{239.
[28] G. Perez, L. Rincon, A. Vila, J. M. Gonz alez, L. F. Cabeza, Behaviour of green facades in Mediterranean continental climate, Energy Conversion and Management 52 (4) (2011) 1861{1867.
[29] P. M. F. van de Wouw, E. J. M. Ros, H. J. H. Brouwers, Precipitation collection and evapo(transpi)ration of living wall systems: A comparative study between a panel system and a planter box system, Buildings and Environment 126 (2017) 221{237.
[30] M. I. Touceda, F. Olivieri, J. Neila, Energy e ciency of a pre-vegetated modular façade prototype, in: 27th International Conference on Passive and Low Energy Architecture, Librairie Wallonie-Bruxelles, Paris, France, 2011, pp. 733{738.
[31] C. Y. Jim, H. He, Estimating heat flux transmission of vertical greenery ecosystem, Ecological Engineering 37 (8) (2011) 1112{1122.

[32] N. H. Wong, A. Y. K. Tan, Y. Chen, K. Sekar, P. Y. Tan, D. Chan, K. Chiang, N. C. Wong, Thermal evaluation of vertical greenery systems for building walls, Building and Environment 45 (3) (2010) 663{672.
[33] M. Ottel e, K. Perini, Comparative experimental approach to investigate the thermal behaviour of vertical greened fa cades of buildings, Ecological Engineering 108 (A) (2017) 152{161.
[34] T. Sakhani, A. M. Abdullah, D. R. Ossen, M. Baharvand, Thermal impacts of vertical greenery systems, Environmental and Climate Technologies 14 (1) (2014) 5{11.
[35] F. Olivieri, D. Redondas, L. Olivieri, J. Neila, Experimental characterization and implementation of an integrated autoregressive model to predict the thermal performance of vegetal facades, Energy and Buildings 72 (2014) 309 {321.
[36] F. Olivieri, L. Olivieri, J. Neila, Experimental study of the thermal-energy performance of an insulated vegetal fa cade under summer conditions in a continental Mediterranean climate, Building and Environment 77 (2014) 61 {76.
[37] C. Jim, Greenwall classi cation and critical design-management assessments, Ecological Engineering 77 (2015) 348{362.
[38] S. Charoenkit, S. Yiemwattana, Living walls and their contribution to improved thermal comfort and carbon emission reduction: A review, Building and Environment 105 (2016) 82 { 94.
[39] A. M. Hunter, N. S. Williams, J. P. Rayner, L. Aye, D. Hes, S. J. Livesley, Quantifying the thermal performance of green fa cades: A critical review, Ecological Engineering 63 (2014) 102 { 113.
[40] H. Yin, F. Kong, A. Middel, I. Dronova, H. Xu, P. James, Cooling e ect of direct green facades during hot summer days: An observational study in nanjing, china using tir and 3dpc data, Building and Environment 116 (2017) 195 {206.
[41] V. Oquendo-Di Cosola, F. Olivieri, L. Ruiz-García, J. Bacenetti, An environmental life cycle assessment of living wall systems, Journal of Environmental Management 254 (2020) 109743.
[42] P. Tsilingiris, On the thermal time constant of structural walls, Applied Thermal Engineering 24 (5) (2004) 743 {757.
[43] S. S. Shapiro, M. B. Wilk, An analysis of variance test for normality (complete samples), Biometrika 52 (3/4) (1965) 591{611.
[44] F. Wilcoxon, Individual comparisons by ranking methods, Biometrics Bulletin 1 (6) (1945) 80{83.

Análisis del impacto de los sistemas modulares de jardinería vertical en la absorción acústica

La contaminación acústica en las ciudades es causa de numerosos problemas relacionados con la salud y el bienestar de las personas: problemas psicológicos, trastornos del sueño, problemas de concentración e incluso disminución de la productividad y el desarrollo cognitivo a edades tempranas (Magrini and Lisot, 2015). En la ciudad, la fuente principal de ruido es la actividad humana y, sobre todo, el tráfico rodado (Harris and Cohn, 1985).

En España, un estudio realizado en la ciudad de Madrid (Ruiz-Páez et al., 2023), estima que entre 2013 y 2018 los costes hospitalarios relacionados con enfermedades cardiovasculares y respiratorias asociadas a los picos de contaminación acústica y del aire alcanzan los 202 millones de euros anuales, a los que se le atribuyen 5.685 ingresos hospitalarios, cuyo coste ronda los 82 millones de euros. Por otro lado, un estudio realizado por la Agencia de Salud Pública de Barcelona (ASPB) (ASPB, 2020), constata que el ruido es el segundo factor ambiental que más impacta en la salud de la ciudadanía y, en concreto, estima que más de 210.000 barceloneses sufren problemas psicológicos debido al ruido, y más de 600.000 trastornos graves del sueño.

Contar con datos concretos es el primer paso hacia la toma de decisión y hacia el desarrollo de políticas públicas que rebajen la contaminación acústica en la ciudad. Dentro de las soluciones se encuentra la sustitución de pavimentos, la electrificación de coches y la introducción de barreras ante el ruido, entre las que se incluye el uso de vegetación y, en particular, las paredes vegetales (Azkorra et al., 2015b; Fernández-Bregón et al., 2012; Gabriel Pérez et al., 2016b).

A lo largo de los últimos años, el estudio del coeficiente de absorción acústica (α) de los jardines verticales ha evolucionado siguiendo dos vertientes según los métodos experimentales: estudios desarrollados en condiciones de ruido controladas (laboratorios, cámaras reverberantes, etc.), y los realizados en la ciudad bajo condiciones de ruido reales y no controladas. Las principales conclusiones apuntan a que el uso de vegetación en la ciudad puede reducir la contaminación acústica y mejorar la vida de las personas, principalmente por cuatro aspectos clave (Oquendo-Di Cosola et al., 2022):

- Este tipo de soluciones cuenta con una mayor capacidad de absorción a frecuencias medias y altas. Si tenemos en cuenta la frecuencia de la voz humana o del tráfico rodado, se corresponde con las frecuencias en las que un jardín vertical es más eficiente (más de 400 Hz). Esto lo hace una medida eficiente en espacios públicos.
- La absorción de ruido en los jardines verticales proviene fundamentalmente del sustrato. Es el componente responsable de absorber el 80% de la energía recibida a frecuencias superiores a 1000 Hz, y se comporta como cualquier otro material poroso.
- La densidad de la vegetación es la segunda variable más importante. Las diferencias entre los coeficientes de absorción acústica se sitúan entre 0.43 y 1.00, en función de la densidad de la vegetación. Este efecto se debe a las múltiples reflexiones entre las hojas de las plantas que minimizan eficazmente el ruido. En presencia de vegetación densa, el coeficiente de absorción puede aumentar en 0.2-0.3 (suponiendo unas mejoras de entre el 20 y el 50%), en particular en el espectro de frecuencias altas (por encima de 1000 Hz).

- Por último, la configuración del sistema en su conjunto es también una variable que influye en el coeficiente de absorción acústica. La impedancia de las juntas entre los módulos, la morfología de las partes que lo componen, y las características de la estructura de soporte pueden condicionar el comportamiento.

Estos resultados provienen de la investigación realizada en el marco de la revisión bibliográfica de esta tesis doctoral, que ha puesto en evidencia la necesidad de profundizar en determinados aspectos como: el comportamiento de estos sistemas en condiciones reales y el de algunas variables que pueden influir en la capacidad de absorción acústica del sustrato (espesor, saturación, exposición) y las plantas (densidad, forma, condición de la planta).

Para profundizar en dichos aspectos, se desarrolló la investigación recogida en el artículo científico: Valentina Oquendo-Di Cosola, María de los Ángeles Navacerrada, Francesca Olivieri, Luis Ruiz-García (enviado en abril de 2023). *Impact assessment of green walls on sound absorption*. Sustainable Cities and Society. Q1 (JCR). La investigación tiene dos objetivos: (i) estudiar en condiciones controladas la influencia de la estructura del módulo y de sus componentes (sustrato y vegetación) en el coeficiente de absorción acústica, teniendo en cuenta variables como la saturación del sustrato y la densidad y desarrollo de la vegetación; y (ii) verificar los resultados obtenidos en laboratorio en condiciones reales y no controladas de ciudad.

El sistema utilizado para el desarrollo de la investigación consiste en una estructura tridimensional de polietileno reciclado con un diseño celular. Esta estructura se rellena con sustrato y plantas pre-cultivadas. La última capa del módulo es de fieltro y cumple dos funciones, mantener la humedad del módulo y evitar el desprendimiento de la

vegetación. Cada unidad de cultivo modular se rellena con sustrato orgánico (fibra de coco, turba y humus) por lo que no requiere fertilizantes para el desarrollo de las plantas. El sistema de riego es automatizado y se regula según la estación del año, de media consume 8 l/m^2/día en días muy calurosos y hasta 2 l/m^2/día en días despejados o nublados.

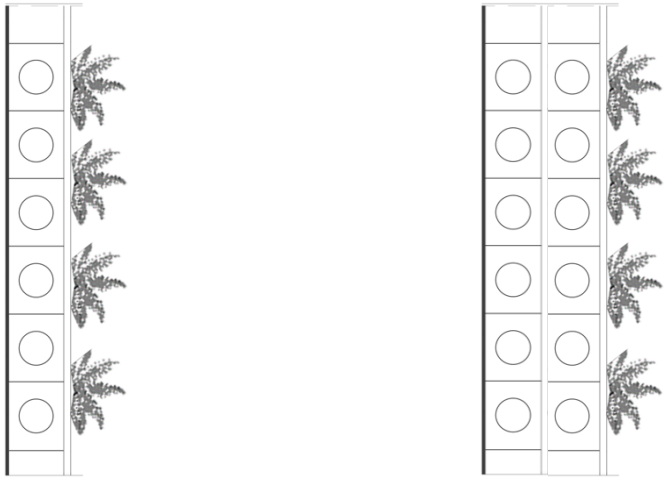

(a) (b)

Figura 28: Sección del sistema modular de jardinería vertical utilizado para el análisis de prestaciones acústicas: (a) sistema utilizado en pruebas de laboratorio; (b) sistema utilizado en pruebas *in-situ* instalado en el itdUPM

Todas las pruebas fueron realizadas con una pistola de impedancia "Microflown Technologies" que consta de un pequeño altavoz esférico de ⌀15 cm que sirve como fuente de sonido; una sonda de presión/velocidad de partículas con sensores de presión acústica y velocidad; y un soporte manual que permite al usuario manejar toda la estructura manteniendo simultáneamente una distancia constante de 27 cm entre la sonda y el altavoz.

El software Velo permite operar la pistola de impedancia en modo "*Scan&Paint*" para facilitar la recogida continua de datos y la rápida visualización de los campus acústicos superficiales. Las señales acústicas se adquieren moviendo manualmente la sonda sobre la superficie de medición mientras se graban imágenes con una cámara situada a cierta distancia. Para determinar la posición de la sonda, se utiliza un algoritmo de seguimiento que detecta la marca de color de la sonda a partir del vídeo.

- *Pruebas de absorción acústica en laboratorio:*

Para el desarrollo de pruebas de absorción acústica en laboratorio se realizaron mediciones en módulos con distintas características. Para evaluar la influencia del sustrato y la densidad de vegetación se utilizaron tres módulos: (i) módulo con sustrato y *Hedera helix* seca; (ii) módulo con sustrato y *Hedera hélix*; (iii) módulo con sustrato y césped.

Mientras que para la evaluación de los componentes y la morfología del módulo se realizaron mediciones sobre cuatro módulos: (i) módulo con sustrato sin capa de fieltro; (ii) módulo con sustrato y capa de fieltro; y (iii) módulo con sustrato y capa de fieltro con cortes previos a la inserción de la planta. La capa de fieltro se ha considerado una variable relevante al estar compuesto por un material poroso que puede influir en la capacidad de absorción del módulo.

Figura 29: Módulos de jardinería vertical utilizados para las pruebas de absorción acústica en laboratorio

Para llevar a cabo las mediciones se realizó la toma de datos a partir de la técnica "*Scan&Paint*", la cual a través de un barrido manual sobre la superficie permite calcular el valor de coeficiente de absorción del módulo.

Figura 30: Técnicas utilizadas para la toma de datos en laboratorio

Los resultados más relevantes de estas pruebas se clasifican en dos categorías de acuerdo con su impacto sobre la absorción acústica del módulo de jardinería vertical:

a. Impacto de la estructura del módulo y sus componentes

En general, y a pesar de las distintas configuraciones testadas, el módulo demuestra un comportamiento estándar en todo el espectro de frecuencias utilizado. Los resultados muestran un coeficiente de absorción que varía entre 0.1 y 0.55 (hasta 250 Hz), entre 0.65 y 0.8. (250-2000 Hz), y cercano a 1.00 para altas frecuencias (por encima de 2000 Hz). Sin embargo, destacan los siguientes aspectos de cada una de las configuraciones:

- *El módulo con sustrato* muestra un coeficiente de absorción medio de 0.70 a bajas frecuencias, 0.86 a medias frecuencias, y 0.95 a altas frecuencias. Se puede afirmar que una vez rellenado el módulo con el sustrato, el comportamiento del módulo en cuanto a absorción es el de un material poroso.

- *El módulo con sustrato y capa de fieltro* demuestra una capacidad de absorción elevada, de entre 0.91 y 0.98 a frecuencias medias y altas, mientras que la media es de 0.62 para frecuencias bajas. Estos resultados demuestran la influencia del fieltro, sobre todo a medias y altas frecuencias.

- *El módulo con sustrato y capa de fieltro con cortes previos a la inserción de las plantas* muestra un ligero aumento del coeficiente de absorción en comparación con el módulo con solo sustrato (0.14-0.6), especialmente a bajas frecuencias. Sin embargo, se observan picos de absorción debidos a los cortes en el fieltro que generan cavidades que se comportan como resonadores de Helmholtz.

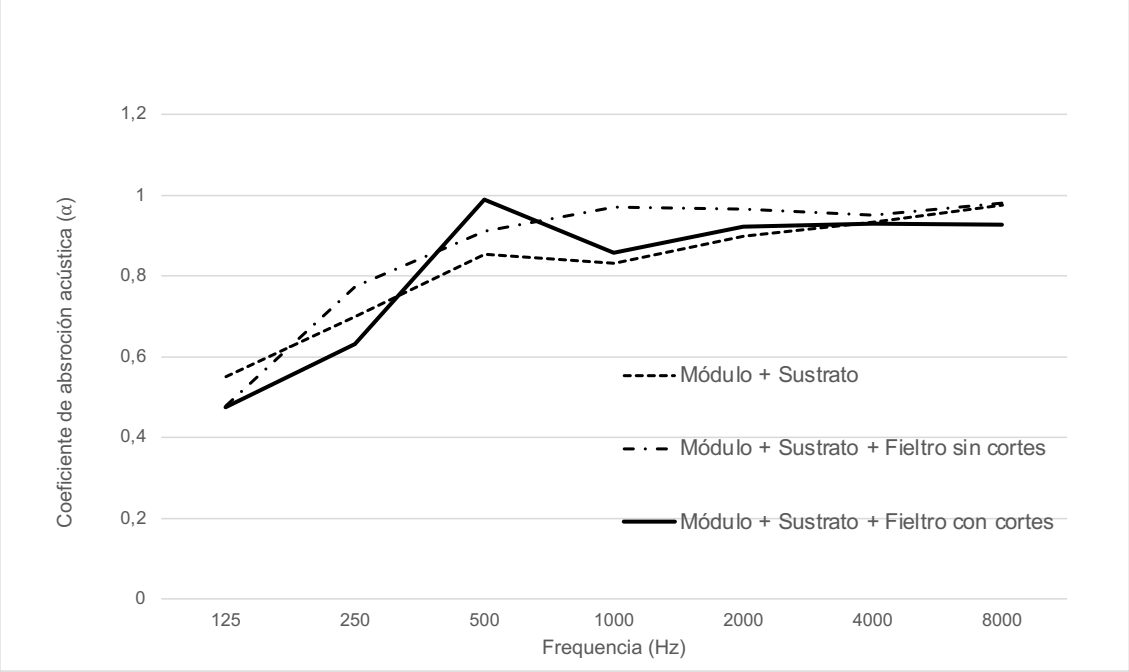

Figura 31: Curvas de absorción acústica obtenidas en pruebas de laboratorio a partir del análisis de las prestaciones acústicas de los componentes del módulo

Frecuencia (Hz)	Módulo + Sustrato	Módulo + Sustrato + Fieltro sin cortes	Módulo + Sustrato + Fieltro con cortes
125	0,55	0,48	0,47
250	0,70	0,77	0,63
500	0,85	0,91	0,99
1000	0,83	0,97	0,86
2000	0,90	0,96	0,92
4000	0,93	0,95	0,93
8000	0,98	0,98	0,93

Tabla 17: Coeficientes de absorción acústica obtenidos en pruebas de laboratorio a partir del análisis de las prestaciones acústicas de los componentes del módulo

b. Impacto de la vegetación y su desarrollo

Una vez obtenidos los coeficientes de absorción acústica del módulo a partir de sus distintas configuraciones, se continuó con el análisis de la influencia de la vegetación en el coeficiente de absorción. Para el desarrollo de estas pruebas se utilizaron dos especies, *Hedera hélix* y césped. Esta selección permitió comparar los resultados de dos especies distintas en densidad y morfología. Además, la *Hedera hélix* es una de las especies más utilizada en módulos de jardinería vertical para evaluar tanto la

capacidad de reducción de temperaturas como la de fijación de partículas en suspensión, mientras que para el rendimiento acústico no se encontraron estudios.

A partir del análisis de datos se destacaron los siguientes resultados:

- *El módulo con Hedera hélix* comparado con el módulo con sustrato y capa de fieltro con cortes previos a la inserción de la planta, demuestra una mejora del 14% debido a la capa de vegetación. Además, el pico observado a 500 Hz debido a las cavidades de los cortes desaparece porque se rellenan con la vegetación.

- *El módulo con Hedera hélix seca* posee un coeficiente de absorción medio de 0.91 para frecuencias bajas, y de 1.00 para frecuencias medias y altas. Esto demuestra que la capacidad de absorción del módulo va más allá de la salud y el desarrollo de la planta. Sin embargo, si comparamos los resultados con el módulo de *Hedera hélix* viva y desarrollada, el coeficiente de absorción aumenta 0.3 a 1000 Hz, lo que demuestra que la densidad de la vegetación es una variable que puede afectar la absorción acústica.

- *El módulo de césped* muestra un comportamiento totalmente distinto. La capacidad de absorción disminuye con respecto a los módulos con *Hedera hélix* seca y natural en un 15% a bajas frecuencias y en un 39% a medias frecuencias. Lo que lleva a la conclusión de que este tipo de vegetación, pese a ser tupida, no cuenta con una capacidad de absorción acústica tan relevante como la *Hedera hélix*.

Estos resultados sugieren dos hipótesis que justifican el elevado rendimiento de la especie *Hedera hélix* y su utilidad para la absorción acústica: (i) se debe al desarrollo de la propia planta, que en su crecimiento forma cavidades que dejan al descubierto el sustrato, de manera que el resultado que se obtiene es la combinación del efecto de la planta y del sustrato; (ii) la propia planta, debido a su morfología, dispersa las ondas sonoras de manera que el sensor del instrumento de medición capta menos energía y por ende, el coeficiente de absorción es mayor.

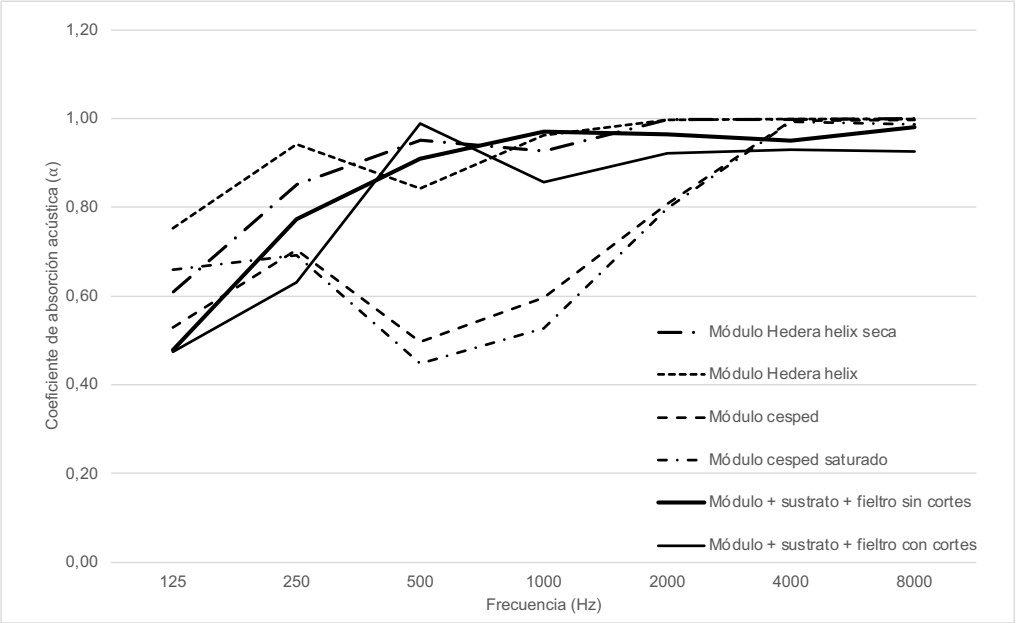

Figura 32: Coeficientes de absorción obtenidos en pruebas de laboratorio a partir del análisis de las prestaciones acústicas del módulo con plantas

Frecuencia (Hz)	Módulo *Hedera helix* seca	Módulo *Hedera helix*	Módulo cesped	Módulo cesped saturado	Módulo + sustrato + fieltro sin cortes	Módulo + sustrato + fieltro con cortes
125	0,61	0,75	0,53	0,66	0,48	0,47
250	0,85	0,94	0,70	0,69	0,77	0,63
500	0,95	0,84	0,50	0,45	0,91	0,99
1000	0,93	0,96	0,60	0,53	0,97	0,86
2000	1,00	1,00	0,81	0,80	0,96	0,92
4000	1,00	1,00	0,99	0,99	0,95	0,93
8000	1,00	1,00	1,00	0,99	0,98	0,93

Tabla 18: Coeficientes de absorción acústica obtenidos en pruebas de laboratorio a partir del análisis de las prestaciones acústicas del módulo con plantas

- *Pruebas de absorción acústica in-situ:*

Para evaluar la absorción bajo condiciones no controladas, se realizaron mediciones en el Centro de Innovación en Tecnología para el Desarrollo Humano (itdUPM) de la Universidad Politécnica de Madrid. Las medidas se tomaron en los jardines verticales instalados en las fachadas sur y oeste, los cuales están construidos a partir de los mismos módulos utilizados para las mediciones en laboratorio con la única diferencia de que estos constan de dos estructuras de polipropileno reciclado en lugar de uno. Esto se debe principalmente a la necesidad de contar con una estructura adicional para su enganche a la piel metálica.

Para evaluar la influencia de las especies vegetales en el coeficiente de absorción de la fachada, se testaron diez especies distintas, repitiendo en algunos casos las mediciones con la misma especie para evaluar la influencia de la densidad. Las especies son precultivadas e insertadas en los huecos de la estructura delantera del módulo, mientras que la estructura trasera permanece vacía generando una cámara de aire que previene humedades. Cada módulo cuenta con 16 plantas, dando lugar a una densidad de 64 plantas/m^2.

Figura 33: Técnica “Scan&Paint” utilizada para la toma de datos in-situ

Los resultados de las mediciones se han clasificado según el coeficiente de absorción obtenido (bajo, medio y alto) con respecto al coeficiente de absorción en laboratorio para el módulo con sustrato y capa de fieltro con cortes (estado previo a la introducción de la vegetación).

a. Aumento bajo del coeficiente de absorción acústica en relación con el módulo sin vegetación

Dentro de esta categoría se encuentran cuatro especies: *Heuchera americana* "dale's strain", *Sedum acre*, *Gazania rigens*, y *Heuchera americana* "palace purple". Todas son distintas, desde la forma de sus hojas hasta la densidad y el desarrollo de la planta. Sin embargo, demostraron un comportamiento similar en cuanto a la capacidad de absorción de ruido, aumentando el coeficiente de absorción proporcionalmente a la frecuencia.

La comparación detallada de la absorción con respecto a los resultados obtenidos en el módulo sin vegetación para distintos niveles de frecuencia, muestra que a bajas frecuencias no se produce una mejora significativa de la absorción al introducir la planta. Sin embargo, a frecuencias medias y altas sí se produce un aumento del 4-8% y del 6-8%, respectivamente.

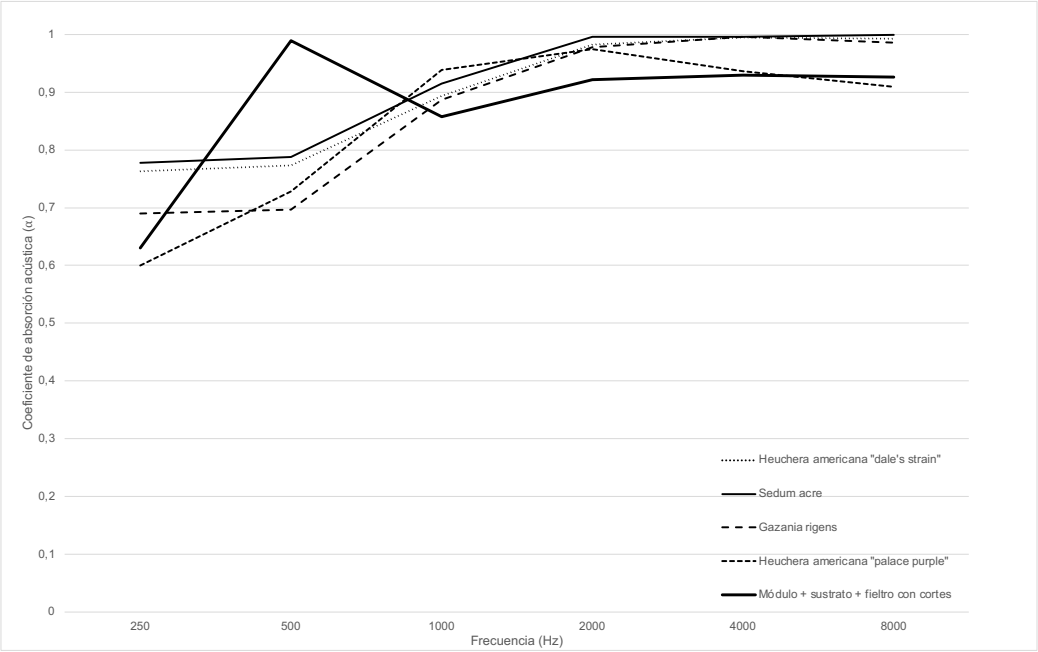

Figura 34: Curvas de absorción acústica obtenidas en pruebas in-situ sobre especies con aumento bajo del coeficiente de absorción en relación con el módulo sin vegetación

Frecuencia (Hz)	*Heuchera americana "dale's strain"*	*Sedum acre*	*Gazania rigens*	*Heuchera americana "palace purple"*
250	0,76	0,78	0,69	0,60
500	0,77	0,79	0,70	0,73
1000	0,89	0,91	0,89	0,94
2000	0,98	1,00	0,98	0,97
4000	0,99	1,00	1,00	0,94
8000	0,99	1,00	0,99	0,91

Tabla 19: Coeficientes de absorción acústica obtenidos en pruebas in-situ sobre especies con aumento bajo del coeficiente de absorción en relación con el módulo sin vegetación

b. Aumento medio de la absorción acústica en relación con el módulo sin vegetación

Bajo esta categoría se encuentran los resultados de tres especies: *Delosperma coopera, Lonicera nítida* "magrun", *Sedum album* "coral carpet". Las tres especies cuentan con características muy distintas, pero poseen una capacidad de

absorción muy similar. El coeficiente de absorción medio es de 0.85 a frecuencias bajas y medias y de 1.00 a altas frecuencias. A diferencia de las especies analizadas en el apartado anterior, estas se caracterizan por un coeficiente de entre 0.80 y 1.00.

Estos resultados conducen a reafirmar que el aumento de la densidad de vegetación, especialmente las especies con tallos gruesos o que crean superficies tupidas, proporciona un aumento en la absorción. Aunque las especies son muy distintas, su efecto no está condicionado por la forma sino por la densidad.

Si se comparan estos resultados con el módulo sin vegetación, el aumento del coeficiente de absorción es evidente para todas las especies y en todo el espectro de frecuencias. Esta mejora se traduce en un aumento de la absorción del 4-5% a bajas frecuencias, del 10-11% a medias frecuencias, y del 8% a altas frecuencias.

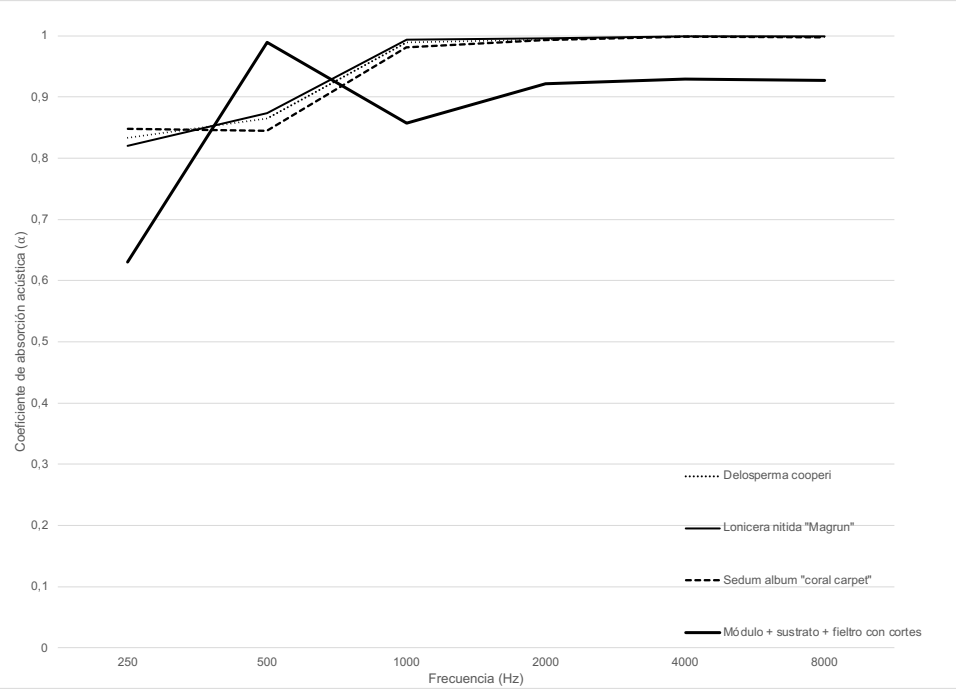

Figura 35: Curvas de absorción acústica obtenidas en pruebas in-situ sobre especies con aumento medio del coeficiente de absorción en relación con el módulo sin vegetación

Frecuencia (Hz)	*Delosperma cooperi*	*Lonicera nitida* "Magrun"	*Sedum album* "coral carpet"
250	0,83	0,82	0,85
500	0,87	0,87	0,84
1000	0,99	0,99	0,98
2000	0,99	1,00	0,99
4000	1,00	1,00	1,00
8000	1,00	1,00	1,00

Tabla 20: Coeficientes de absorción acústica obtenidos en pruebas in-situ sobre especies con aumento medio del coeficiente de absorción en relación con el módulo sin vegetación

c. Aumento alto de la absorción acústica en relación con el módulo sin vegetación

En esta categoría se encuentran tres especies: *Sedum album* "coral carpet", *Thymus communis,* and *Carex oshimensis.* Como en los casos anteriores, se trata

de especies muy distintas morfológicamente, pero con un comportamiento similar y, en este caso, elevados coeficientes de absorción acústica en todo el espectro de frecuencias.

En estas muestras, la vegetación forma una capa uniforme sobre el módulo, aumentando su espesor y, por tanto, su coeficiente de absorción. Estas afirmaciones se comprueban comparando los resultados obtenidos en el módulo sin vegetación, a partir de los cuales se demuestra un aumento significativo del coeficiente de absorción acústica tras la introducción de la vegetación. A bajas frecuencias se produce una mejora entre el 12-20%, a medias frecuencias de 11-12%, y a altas frecuencias la mejora es del 8% en todos los casos.

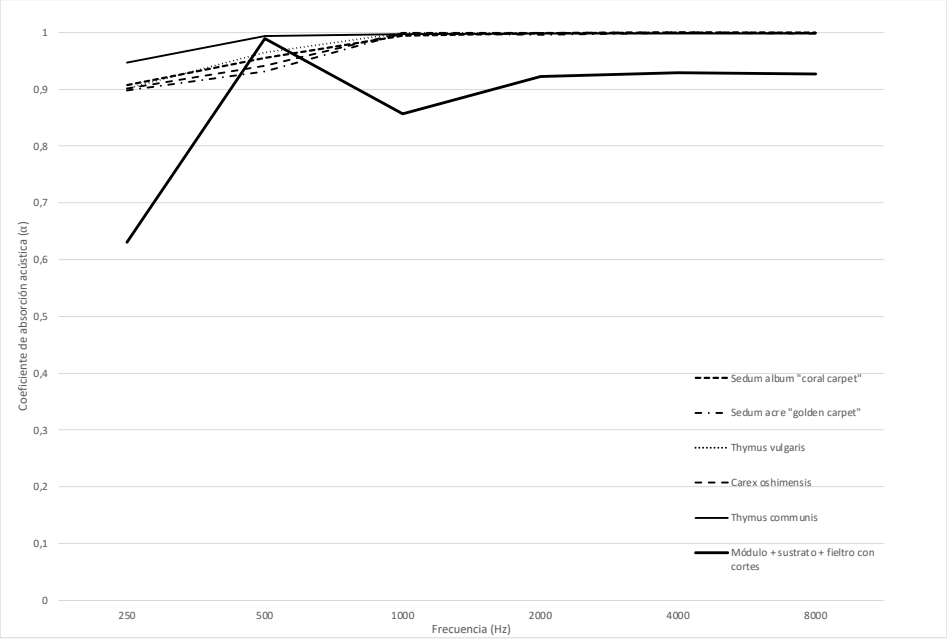

Figura 36: Curvas de absorción acústica obtenidas en pruebas in-situ sobre especies con aumento alto del coeficiente de absorción en relación con el módulo sin vegetación

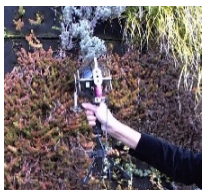
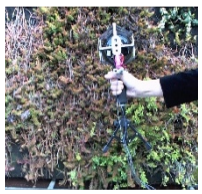


Frecuencia (Hz)	*Sedum album* "coral carpet"	*Sedum acre* "golden carpet"	*Thymus vulgaris*	*Carex Oshimensis*	*Thymus communis*
250	0,91	0,90	0,90	0,90	0,95
500	0,96	0,93	0,96	0,94	0,99
1000	0,99	1,00	1,00	1,00	1,00
2000	1,00	1,00	1,00	1,00	1,00
4000	1,00	1,00	1,00	1,00	1,00
8000	1,00	1,00	1,00	1,00	1,00

Tabla 21: Coeficientes de absorción acústica obtenidos en pruebas in-situ sobre especies con aumento alto del coeficiente de absorción en relación con el módulo sin vegetación

En términos generales, se encontraron mejoras en la absorción acústica entre el módulo sin vegetación y los módulos evaluados con diferentes especies. En concreto, un aumento del 4-8% para las especies con bajo aumento de la absorción, del 4-10% para las especies con aumento medio de la absorción y del 8-20% para las especies con aumento alto de la absorción. Esto confirma otras investigaciones según las cuales el 80% de la absorción procede del sustrato y el 10% de la vegetación (D'Alessandro et al., 2015; Davis et al., 2017).

Los resultados obtenidos a partir de esta investigación demuestran que las prestaciones acústicas de un módulo de jardinería vertical están condicionadas tanto por el diseño del módulo como por la presencia del sustrato y la vegetación. Esta consideración pone de manifiesto los aspectos a tener en cuenta para mejorar su diseño, y por consecuencia, contribuir a su difusión como elementos constructivos y barreras acústicas eficientes y sostenibles. Además, se confirma el potencial de la vegetación como herramienta de absorción acústica en las ciudades.

Artículo 7

Impact assessment of green walls on sound absorption

Valentina Oquendo-Di Cosola, María de los Ángeles Navacerrada, Francesca Olivieri, Luis Ruiz-García.

Applied Acoustics Journal

(Enviado abril 2023)

Q1 (JCR)

Impact assessment of green walls on sound absorption

Authors: Valentina Oquendo-Di Cosola.[1*], María Ángeles Navacerrada[2], Luis Ruiz-García[3], Francesca Olivieri[1]

[1]: Departamento de Construcción y Tecnología Arquitectónicas, Escuela Técnica Superior de Arquitectura, Universidad Politécnica de Madrid, Av. Juan de Herrera 4, 28040, Madrid, Spain.
[2]: Departamento de Estructuras y Física de la Edificación, Escuela Técnica Superior de Arquitectura, Universidad Politécnica de Madrid, Av. Juan de Herrera 4, 28040, Madrid, Spain.
[3]: Departamento de Ingeniería Agroforestal, Escuela Técnica Superior de Ingeniería Agronómica, Alimentaria y de Biosistemas, Universidad Politécnica de Madrid, Av. Juan de Herrera 4, 28040, Madrid, Spain.

Abstract:

This research involves the study of the sound absorption coefficient (α) of a green wall module in laboratory conditions and on a green wall made of ten different vegetal species. An impedance gun is used for measurements using the *Scan&Paint* method to facilitate the continuous collection and the rapid visualisation of the sound absorption coefficient through software. All system components, both the vegetation and the substrate, as well as the supporting structure and the hydrophilic felt layer, were analysed for their sound absorption coefficient. Results show a stronger absorption at high to middle frequencies due to the absorbing effect of the substrate, while a smaller absorption is observed at low frequencies. The structure and felt layer of the system showed high absorption coefficients, which are modified as soon as substrate and vegetation are introduced. In addition, it is noted that the sound absorption coefficient of the module increase by 4-20% if vegetation is added. Furthermore, as the density of the vegetation increases, the sound absorption coefficient increases.

Keywords: Green wall; Urban comfort; Urban noise; Noise reduction; Sound absorption coefficient.

1. Introduction

Noise pollution in cities is a common cause of discomfort and psychological problems related to speech interference, sleep disturbances, impaired concentration, and even reduced productivity and learning ability in children (Lacasta et al., 2018). Sources of noise associated with pollution in cities are related to human activities and, above all, to road traffic. Rapid urban growth has led to overcrowding in cities, leaving apart the intrinsic link between environmental noise and urban planning (Van Renterghem et al., 2020).

The achievement of noise mitigation depends on the distance between the source and the receiver and the barriers that prevent the propagation of sound waves (Yilmaz et al., 2023). The noise perception is subjective, and the theory encompasses it in the soundscape, a concept studied to address noise problems in urban areas (Aletta et al., 2016). Previous research has defined the acoustic comfort properties of public space in cities. These properties comprise physical, social, and psychological aspects. Combined, these aspects determine acoustic comfort as the range of sounds perceptible in space, at a given time, that are conditioned by the way humans respond to particular stimuli. (Guan et al., 2020; Liu et al., 2014; Yin et al., 2022).

The implementation of vegetation in cities includes different solutions that contribute to the naturalisation of urban surfaces and thus improve human well-being. Green walls provide many ecosystem services: increase biodiversity, improve water cycle management, energy savings in buildings, reduce the heat island effect (Xiao et al., 2018), capture suspended particles and improve air quality (Kandelan et al., 2022), and mitigation of noise (Van Renterghem et al., 2020), all of which are crucial to adapting and mitigate climate change in cities (Kabisch et al., 2016; Teotónio et al., 2021).

The sound absorption coefficient (α) produced by green walls has been studied with different approaches. It can be divided into two groups according to the experimental methods: those developed under controlled conditions and those carried out outdoors or under uncontrolled conditions. These studies have shown that the use of urban vegetation to reduce noise can have positive impacts on human health (Imran et al., 2019; Jamei et al., 2016; Ling and Chiang, 2018; Tong et al., 2016), mainly due to four key aspects (Oquendo-Di Cosola et al., 2022):

- Green walls offer higher performance at mid to high frequencies. If we consider the human voice's frequency, it perfectly corresponds to the frequency at which the green wall is most efficient (over 400 Hz), so it could be used as a sustainable design tool in public spaces (Azkorra et al., 2015b).
- In a green wall, the substrate absorbs 80% of the energy received at frequencies above 1000 Hz. It behaves like any other porous material as its sound reduction is proportional to the noise frequency - the higher the frequency, the greater the absorption (N H Wong et al., 2010).
- For vegetation, density is the most relevant variable. Differences between sound absorption coefficients in the literature are on average between 0.43 and 1.00, depending on the density of the vegetation. The absorption coefficient can increase by α= 0.2 and 0.3 due to the presence of plants with a relatively high leave area density, particularly in the medium and high-frequency range (above 1000 Hz). This effect seems mainly due to multiple reflections between plant leaves that effectively minimise noise, where the acoustic wavelength becomes comparable or smaller than the characteristic leaf dimension. The leaf vibration and multiple scattering contribute to the energy dissipation in the incident sound wave (Romanova et al., 2019).
- The configuration of the system can influence the sound absorption coefficient, mainly due to the thickness and composition of the substrate, the layers of vegetation, the impedance of the seal joints between the modules, and the insulation of the supporting structure (Sierra-Pérez et al., 2016).

Most of the studies conducted to date have been carried out under controlled conditions using methods such as reverberation chambers or impedance tubes in laboratories (Asdrubali et al., 2014; Attal et al., 2016; Horoshenkov et al., 2013; Nyuk Hien Wong et al., 2010b). However, more research is needed to investigate the performance of these solutions under full-scale, uncontrolled conditions. In particular, the analysis of the absorption coefficient of the construction materials of the modules and their influence on the coefficient of the system has yet to be further analysed. Furthermore, although the influence of vegetation has been extensively studied, studies

have yet to be identified that consider a wide variety of species from which specific conclusions can be drawn on their influence on noise absorption.

This research has two objectives. The first is to study a green wall module; the influence of the following aspects on the sound absorption coefficient will be analysed: (i) the structure of the module and the acoustic performance of its components (including the substrate); (ii) the vegetation and its development (density). The second verify that the results obtained in the laboratory are replicated under natural conditions by analysing the effect of the type and density of vegetation. The study is carried out using the PU probe, a method that has not been used in the development of this type of study until now.

2. Materials and Methods

2.1 Green wall modules

Experiments have been carried out on a green wall module, mainly used for façades and green roofs. It comprises a three-dimensional structure of recycled polyethene with a cellular design. This structure is filled with substrate and plants. The final layer of the module is made of felt and performs two functions, maintaining the module's humidity and preventing the detachment of vegetation. Each modular cultivation unit is filled with an organic and sustainable substrate: coconut fibre, turf, and humus. The details of the system components can be found in (Table 1 and Figure 2).

It is an organic system that has a reduced water consumption (this system consumes around 8 l/m^2 per day on sweltering days and up to 2 l/m^2 in other conditions); little or no dependence on fertilisers as the substrate is organic and is based on natural processes to obtain the nutrients necessary for plant development; and reduced maintenance requirements as it is developed from natural substrates that maintain a balance in the nutrition and growth of the plants, so pruning is limited (once or twice a year).

Table 1:Description of the components and features of the system

System components and characteristics	Description
Polyethylene module	50 cm x 50 cm x 5 cm
Weight without plants	2 kg / module
Weight at half saturation	3,40 kg / module
Weight at total saturation	5,60 kg / module
Number of plants	12 per module
External finishing layer	Polyester
Bearing structure	Polypropylene boxes
Hydrophilic layer	Polyester
Growing medium	Coconut fibre, turf, and humus
Hooking system	Hooking brackets in aluminium and galvanised steel

Laboratory sound absorption measurements were performed on the described green wall module to assess the performance of the substrate, the vegetation, and the system components regarding the sound absorption coefficient. To study the influence of substrate and vegetation density, three modules were used: (a) module with substrate and dried *Hedera helix*; (b) module with substrate and regular *Hedera helix*; (c) module with substrate and grass (Figure 37).

To evaluate the impact that the components and morphology of the module itself could have on the sound absorption results, a set of measurements was taken in modules with the following characteristics: (a) module with substrate without felt layer; (b) module with substrate and felt layer without cuts made to insert plants; (d) module with substrate and felt layer with cuts made to insert plants (Figure 37).

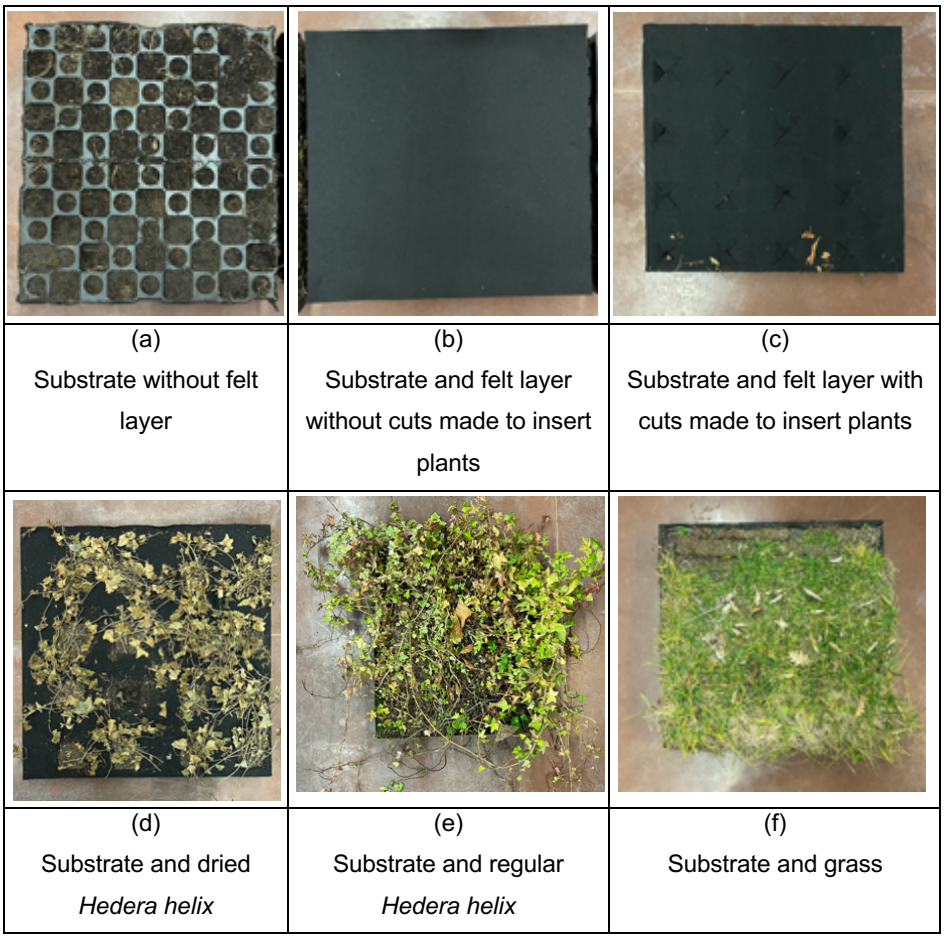

(a) Substrate without felt layer	(b) Substrate and felt layer without cuts made to insert plants	(c) Substrate and felt layer with cuts made to insert plants
(d) Substrate and dried *Hedera helix*	(e) Substrate and regular *Hedera helix*	(f) Substrate and grass

Figure 37: Modules used during laboratory measurements to assess the impact of the morphology and components of the system (a-c) and to assess the impact of vegetation density and substrate saturation (d-f)

2.2 Green wall façade

In-situ measurements were made at the Innovation and Technology for Development Centre (itdUPM), the first retrofitted building of the Technical University of Madrid located in Madrid, Spain. The building includes a drilled metal plate skin covering all façades, leaving an air gap between the concrete wall and the mentioned skin of 20 cm. Furthermore, green walls on the south façade (11.25 m^2) and the west façade (10 m^2) cover some parts of the skin.

The experimental set-up consists of two façades, one covered by a green wall and a bare wall. The walls present the following layers from the inside out: vertical support, square section metal profile, air gap, metal profile in L, perforated aluminium profiles, polypropylene structure, hydrophilic felt layer, polypropylene structure with organic substrate and vegetation (see details in Figure 2).

The modules used for façade construction are the same as those used in laboratory tests. The only difference is that it consists of two recycled polyproline structures instead of one (see Table 1 for a detailed list of components). It is mainly to be able to adapt it to its installation on the metal façade.

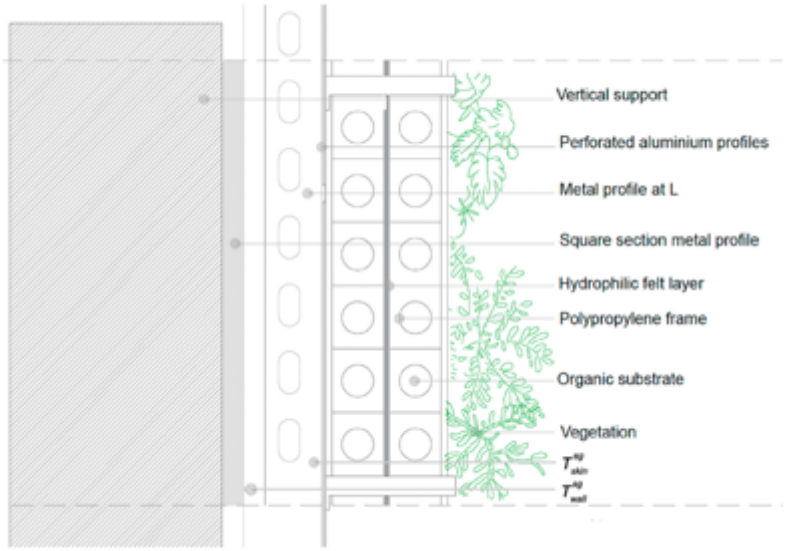

Scale 1.100

Figure 38: Modular vertical gardening system installed in the itdUPM building.

To evaluate the influence of plant species on the sound absorption coefficient of the green façade, ten of the species planted on the façade were tested to analyse their acoustic absorption coefficient (see Figure 39). The front structure is filled with an organic substrate enriched for cultivating plants selected based on their adaptation to the climate in which they are located (the substrate used in the green wall was the same tested in laboratory). They are pre-cultivated and inserted into gaps. The rear structure remains empty, generating a hollow space for air circulation. The green wall has an exudation irrigation system that allows the entire surface to have the same amount of water at any point. It favours that the necessary irrigation for the green wall can be easily calculated. The number of plants installed per module is 16, i.e., 64 plants/m^2.

		
Heuchera americana “dale’s strain”	*Sedum acre “golden carpet”*	*Sedum album* “coral carpet”
		
Thymus communis	*Lonicera nitida* “maigrun”	*Heuchera americana* “palace purple”
		
Carex oshimensis	*Delosperma cooperi*	*Gazania rigens*
		
Thymus vulgaris		

Figure 39: Plant species tested on the green wall.

2.3 Sound intensity PU probe

A Microflown Technologies impedance gun was used for both laboratory and *in-situ* measurements of the sound absorption coefficient α (de Bree et al., 2007; E. Tijs, 2013, 2008; H. E. de Bree, E. Tijs, 2006; H. E. de Bree, M. Nosko, E. Tijs, 2008). The impedance gun consists of a small ⌀15-cm spherical loudspeaker that serves as a sound source, a pressure/particle-velocity (PU) comprising sound pressure and particle velocity sensors, and a hand-held bracket that allows the user to handle the impedance gun while simultaneously maintaining a constant distance of 27 cm (

Figure 40) (E. Tijs, 2013). The loudspeaker was chosen for the hand-held set-up because such a sound source is small, broadband, and easily powered. Vibrations through the set-up frame, which can affect measurements, were reduced using multiple springs and elastic bands.

Complementary acoustic properties describe any single point in a sound field: a sound pressure scalar and a particle velocity vector. In each direction and a single-frequency sound field, the specific acoustic impedance *Z* in a medium is a complex ratio of sound pressure *p* to particle velocity u_{dir} in the specified direction at the same point:

$$Z = \frac{p}{u_{dir}}$$

Because the PU probe is slight, sound pressure and acoustic particle velocity can be measured at a single point near the sample surface (de Bree et al., 2007; E. Tijs, 2008; H. E. de Bree, E. Tijs, 2006). When a known sound source is used, the sound field can be described by a model, and the absorption the sample's surface can be calculated from the measured impedance. It assumes that the material under test is exposed to a plane wave of normal incidence, and the specific impedance from the material is related to the reflection coefficient R by:

$$Z = \frac{1 + R}{1 - R}$$

Moreover, the absorption coefficient α can directly be calculated from the reflection coefficient (Kinsler L. E., Frey A. F., n.d.).

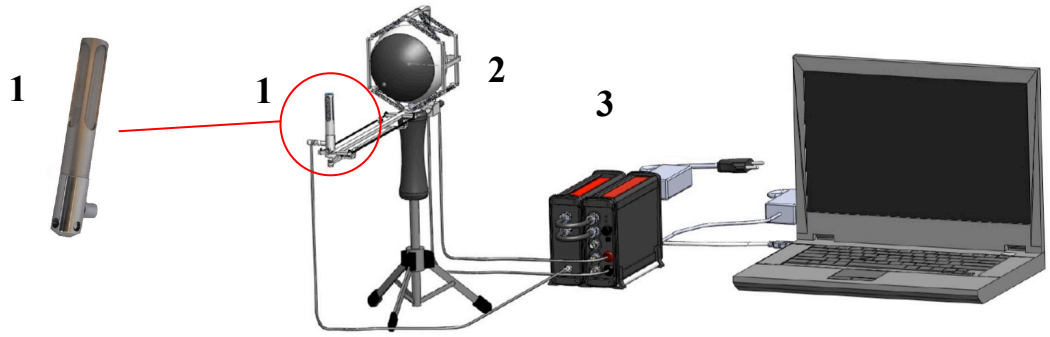

Figure 40: Measurement system assembly. Impedance gun consists of (1) PU (pressure–particle velocity) probe (enlarged photo is also shown) and (2) ⌀15-cm loud-speaker mounted on structure enabling both components to be handled together and to maintain a fixed 27 cm separation distance between them. The impedance gun is connected through (3) signal conditioner to the computer that collects signals and performs the necessary calculations.

These calculations were performed using the Velo software from the same company. The hand-held device was connected by Microflown MFSC-2 signal conditioner to a laptop computer [(3) in Figure 4], which collected the measured signals and performed the required calculations. Many models are described in the sound field above due to a source to obtain the absorption properties. The plane wave, mirror source, and Q-term models were implemented in the software, and these three models can be applied for the calculation of the material impedance. The atmospheric parameters, pressure, and temperature would be considered applying the calculation model to obtain absorption values. They should only be changed if the measurement environment changes dramatically from the standard values.

Before conducting the measurements, the impedance gun was calibrated (E. Tijs, 2013; Siano et al., 2016) by pointing the impedance gun to the best free field conditions possible, to the ceiling or another surface far from the measurement position. The frequency measurement range was established between 300 and 10.000 Hz. The user must set the measurement range and frequency step at which the results are displayed (e.g., octave bands, third-octave bands, or narrow frequency). A spherical loudspeaker, its broadband radiation efficiency is higher than

typical omnidirectional sound sources. Furthermore, the PU probe should remain perpendicular to the surface throughout the scan (E. Tijs, 2013, 2008; H. E. de Bree, M. Nosko, E. Tijs, 2008).

The Velo software allows the impedance gun to be operated in Scan&Paint mode to facilitate the continuous collection of pressure and particle velocity data and the rapid visualisation of surface sound fields (Comesaña et al., 2013; E. Tijs, H. E. de Bree, 2010; Fernandez Comesaña et al., 2016). Acoustic signals are acquired by manually moving the PU probe over the material measurement surface while recording surface images with a webcam at a certain distance. An automatic tracking algorithm that detects the probe colour marking was used to determine the probe position from the video. The camera must be perpendicular to the measurement area to prevent camera-projection-induced graphical errors. The sound absorption coefficient was calculated for each position shortly after each measurement point was acquired. The measurement area was discretised into numerous grid sections with an additional associated time dimension to divide the original signal and assign each segment a position on the measurement area. A single grid cell can contain multiple sections associated with the original signal if the probe crosses the same area several times. A discrete mesh can then be linearly interpolated to compute the acoustic variation colour representation across the sound field. The results can be combined with a background image of the measured data to obtain a visual representation.

On the other hand, the mathematical models proposed in Velo software are not equivalent and may be used for different situations. Previous studies have shown that not all models were equally sensitive to the influence of factors such as the distance from the surface probe and the measurement environment. Therefore, the plane-wave model was used to calculate the sound absorption coefficient because the model exhibits near-insensitivity to environmental changes and can measure surfaces at any distance. However, shorter distances are recommended (Pedrero et al., 2020).

The measurement procedure for the in-situ test consisted of performing a free-field calibration. Once calibration was performed, the loudspeaker and probe were placed perpendicular to the module at approximately 1 cm. Each measurement lasted 20 seconds, was repeated thrice at the same point in the sample and was averaged. The sound absorption coefficient was measured in third-octave bands at various positions in front of the façade and the green wall module.

2.4 *Measurements of sound absorption coefficient*

To carry out laboratory measurements, the first step was to establish efficient and repeatable measurement conditions since measurement of the absorption at specific points of the module and sweep over the surface of the modules was performed manually. The method used was Scan&Paint, previously described in the materials and methods section. This method allows the calculation of the value of the absorption coefficient at a point in an area of the scanning zone or the whole scanning zone. To generate the absorption curves, the average value resulting from the central area of the sample (an area of 20 cm x 20 cm to avoid errors that the instrument often throws up when it encounters the edges of the sample) was calculated.

Figure 41: Sound absorption measurements in laboratory and in-situ green wall.

3. Results and Discussion

The analysis of results is presented in two sections, one on the results of the laboratory measurements and the other on the *in-situ* measurements.

3.1 Measurement of the sound absorption in laboratory

a. The structure of the module and the acoustic performance of its components

This series of data collection aimed to characterize the module and quantify the absorption coefficient of the module with substrate before studying the effect of vegetation (Attal et al., 2016; Attal, de l'Epine, Dauchez, & Dubus, 2021) . The absorption coefficient was measured using the impedance gun at different stages of the module assembly prior to the introduction of vegetation. As mentioned in the material section, the sound absorption coefficient measurements were carried out in three different modules. Measurements were taken varying the characteristics of the felt (with and without cuts made before inserting the plants) as it was considered that it could have a significant effect since it is composed of a porous material.

The curves of the sound absorption coefficient measured as a function of frequency are shown, and the values are given in Figure 42. Despite the different configurations tested, the module has a similar absorption coefficient across the frequency spectrum.

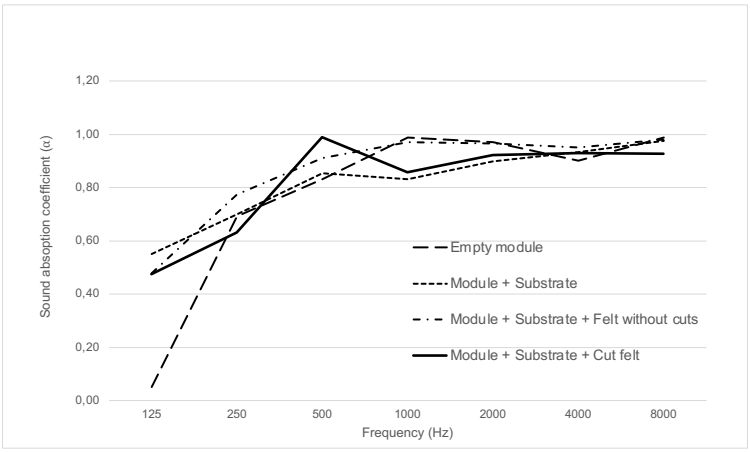

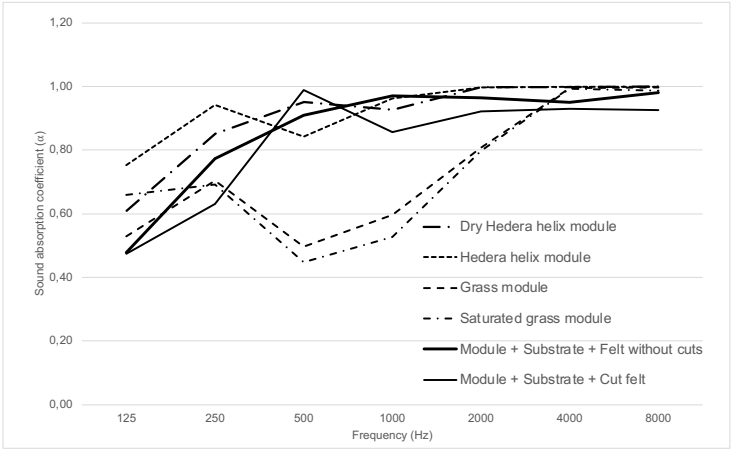

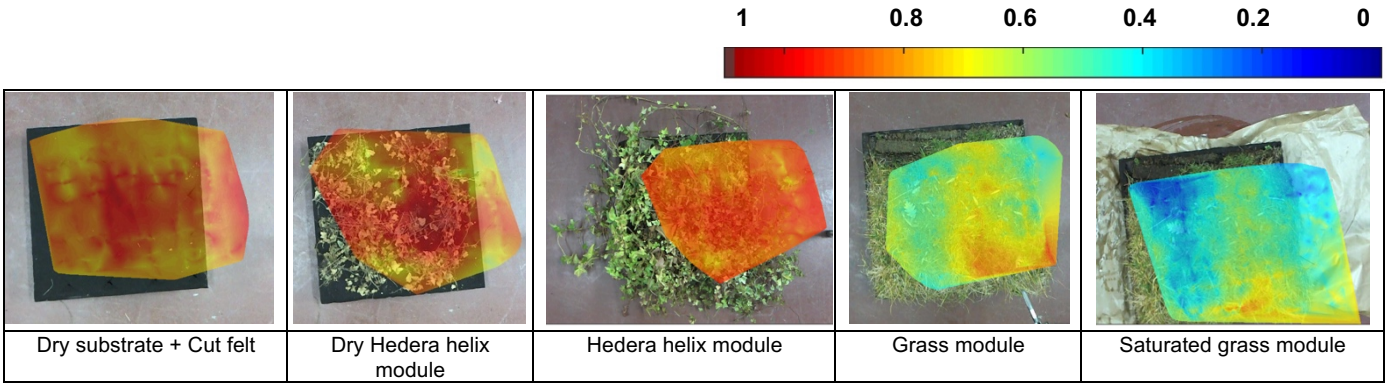

(c)

Figure 42: (a) Absorption curves of the modules analysed to study the influence of the system components; (b) Absorption curves of the modules analysed to study the influence of vegetation density and conditions; (c) Results of the Scan&Paint method showing a colour map with the sound absorption coefficient recorded at different points of the sample at a frequency of 1000 Hz.

The **substrate-only** module has an average absorption coefficient of 0.70 at low frequencies (125 – 500 Hz), 0.86 at medium frequencies (1000 – 2000 Hz), and 0.95 at high frequencies (4000 – 8000 Hz). The averages were calculated using the coefficient resulted for each level of frequencies. It can be said that once the module is filled with the substrate, the behaviour of the sound absorption coefficient is that of a porous material of a certain thickness. These results agree with those obtained in 2010 and 2016 by Wong et al. and G. Pérez et al., in which the sound absorption capacity increases in the intermediate frequency, reaching a peak around 800 Hz, due to the absorption effect of the substrate (G Pérez et al., 2016; Nyuk Hien Wong et al., 2010b).

The results vary slightly when the final felt layer is added. For **the module with uncut felt,** it has high absorption coefficients (0.91 - 0.98) at medium and high frequencies, while the average is lower (0.62) for low frequencies (125 - 250 Hz). On the other hand, the **module with felt with cut-outs** shows a slight increase in the absorption coefficient compared to the module with substrate only (0.14 - 0.6), especially at low frequencies (125 - 500 Hz). However, there are some absorption peaks (1.00) at medium frequencies, which are due to cuts in the felt that generate cavities (as can be seen in Figure 11) that behave like Helmholtz resonators, which, given their geometry, resulting in an absorption peak in the sound absorption coefficient curve at around 500 Hz that is superimposed on the absorption curve of the substrate.

These results demonstrate that the acoustic performance of a green module can be conditioned by both the module's design and the presence of the substrate, which in this case, is incorporated into the façade and ensures greater absorption. Therefore, a thick organic substrate (5 cm) achieves better sound performance in this case. As the substrates' composition and thickness improve, the system's acoustic performance will improve. This consideration highlights the system's efficiency and the substrate's impact as relevant aspects that can be considered in future studies to improve the design of green wall modules and ensure the dissemination of these building elements as suitable noise absorbers in urban settings.

b. The vegetation and its development

Once the module was characterized, and the sound absorption coefficients of the module with different configurations and substrates were obtained, we continued to study the influence of vegetation on absorption. Three different modules were used for data collection (Figure 5) a substrate module and dry *Hedera helix*; a substrate module and *Hedera helix* under natural conditions; and a grass module, in which measurements were also taken at full saturation of the substrate to assess whether the amount of moisture in the module would have an impact on the results.

The selection of species fulfils two objectives: Hedera helix is one of the species most studied in vertical green modules to evaluate its capacity for thermal regulation and fixation of atmospheric particles (Cameron, Taylor, & Emmett, 2015; Hoelscher, Nehls, Jänicke, & Wessolek, 2016). However, until now there have been no studies that have evaluated its acoustic behaviour. Similarly, the choice of the same species (dry and live) allowed us to evaluate the influence of other variables, such as vegetation density, on noise absorption. This variable also contributed to the choice of a grass module, as it is one of the species with the highest density. This selection allowed us to compare the density results between two different species and study the effect of plant morphology on noise absorption.

Figure 42 shows the different absorption curves and coefficients obtained during the tests. The sound absorption coefficient values of the curves shown are the average values obtained by the Scan&Paint method in the central region of the module. Higher absorption capacity is shown at medium and higher frequencies. In this case, unlike the previous data analysis, the behaviour varies according to the type and development of the plant species, using two different types of plants and different stages of development for the same plant.

Compared to the **module with the only substrate**, the **Hedera helix module** show an improvement of 14% due to the vegetation layer. In addition, the observed 500 Hz peak disappears because the introduction of vegetation fills the cavities created by cutting the felt. It confirms the results obtained by (D'Alessandro et al., 2015), in which it is stated that 80% of the energy absorbed by this type of solution is due to the substrate, while vegetation can improve this absorption by 10-20%. Other studies also confirm that the substrate performs better at low and medium frequencies, while the vegetation performs better at high frequencies (Nyuk Hien Wong et al., 2010b). From these results, it should be noted that the presence of the substrate is fundamental because it is what gives rise to the absorption; however, when the dense plant is included, the absorption of the whole improves, especially in the range of 125 - 500 Hz in relation to that obtained with the substrate.

Specifically, the **module with dried *Hedera helix*** has an average absorption coefficient of 0.91 for low frequencies and 1.00 for medium and high frequencies. It shows the absorption capacity of the substrate, and that the module can perfectly absorb the energy even when

the plant is not developed. In these results, it is essential to consider the influence of felt, which as a porous material, also influences the results. As seen in previous analyses, the module without substrate and felt had absorption coefficients of 0.91 to 0.98 at medium and high frequencies.

Similarly, the ***Hedera helix* module** shows improvements at high frequencies compared to the dry plant, with an increase in absorption of 0.3 at 1000 Hz. It is consistent with the results of (Gabriel Pérez et al., 2016b) who state that the impact of vegetation on sound absorption is observed at high frequencies. According to these findings, increasing the leaf mass in vertical garden modules can be considered an aspect to optimise their noise absorption capacity, either by increasing the thickness or using dense plant species. It is one of the main aspects relevant over time when using vegetation as an acoustic absorber in cities (Bullen and Fricke, 1982; Lacasta et al., 2016; Van Renterghem et al., 2012). Furthermore, more recent studies confirm that the higher the vegetation cover, the greater the noise absorption, with an improvement in the absorption coefficient between 0.2 and 0.3 (Oquendo-Di Cosola et al., 2022).

In the case of the **grass module,** the results are entirely different. The absorption capacity decreases compared to the **module with dry *Hedera helix* and natural *Hedera helix*** by 15% at low frequencies and 39% at medium frequencies, while at high frequencies, it is equal to the other modules. In general, this type of vegetation does not have an absorptive capacity at low and medium frequencies (average of 0.62 across the frequency spectrum). At the same time, it reaches its maximum absorption at very high frequencies.

In the case of ***Hedera helix* modules**, two hypotheses could be suggested to justify the increased absorption (1) due to the development of the plant itself, cavities or hollows are formed that exposes the substrate so that the combination of plant and substrate is being measured, and this increases its absorption capacity; (2) the plant itself, due to its morphology, scatters sound waves in all directions in space, so that the impedance gun sensor picks up less reflected energy in the direction of measurement. These two hypotheses

were made because, in measurement with the impedance gun, it is impossible to distinguish whether the increase in absorption is due to one effect or the other.

Figure 42 shows the results obtained with the Scan&Paint method at a frequency of 1000 Hz, which confirms the results discussed throughout this section.

3.2 Measurement of the sound absorption coefficient in-situ

For the absorption coefficient measurement on the green wall installed in the itdUPM, measurements were taken on ten different species. The results of the measurements have been classified according to the increase in the absorption coefficient they represent compared to that obtained in the laboratory test. The absorption coefficient measured in the module with the substrate and the cut felt measured in the laboratory were taken as a reference.

Table 2: Description of plant species associated with each measure.

Measure	Vegetal specie
1	*Heuchera americana "*dale's strain*"*
2	*Delosperma cooperi*
3	*Sedum acre "*golden carpet*" (1)*
4	*Sedum album "*coral carpet*" (1)*
5	*Sedum acre "*golden carpet*" (2)*
6	*Thymus vulgaris*
7	*Carex oshimensis*
8	*Thymus communis*
9	*Lonicera nitida "*maigrun*"*
10	*Gazania rigens*
11	*Sedum album "c*oral carpet*" (2)*
12	*Heuchera americana "*palace purple*"*

a. Low absorption increase

Four species are among the modules tested in this section: *Heuchera americana* "dale's strain" (measure 1), *Sedum acre "golden carpet"* (measure 3), *Gazania rigens* (measure 10), and *Heuchera americana* "palace purple" (measure 12). All species differ, from leaf shape to plant density and development. This species does not represent major variations with respect to the results of the module without vegetation. Figure 7a shows the absorption coefficient curves calculated as the average of all measured points for these species.

Measurement 1 - *Heuchera Americana* "dale's strain" (a species with lobed, almost round, red leaves) shows good absorption capacity at high frequencies with an average of 0.99, while at medium and low frequencies, 0.93 and 0.76, respectively. These absorption coefficients are affected not only by the plant itself but also by the exposure of the felt, which, as the plant is not fully developed, influences the results (Figure 7b).

Measurement 3 – Sedum acre "golden carpet", shows the best absorption, with an average of 0.78 at low frequencies, 0.95 at medium frequencies, and 1.00 at high frequencies. These two measurements have similar behaviour; they are above the same absorption coefficients, although measurement 3 improves by approximately 10% compared to measurement 1. It is mainly due to the development of the plant and the coverage it provides to the module. Although the increase in the absorption coefficient (in relation to the module without vegetation) is proportional to the increase in the noise frequency, the results show that species with more foliage achieve higher absorption coefficients at higher frequencies. In contrast, the irregular plant surface scatters the noise at lower frequencies.

On the other hand, measures 10 and 12 show another trend. In the case of **measurement 10 – *Gazania rigens*** (a shrublike succulent plant that densely covers surfaces, with elongated leaves reaching 2.5 cm), it shows absorption coefficients that start from an average of 0.69 for low frequencies and 0.93 for medium frequencies, while its absorption capacity is evidenced at high frequencies, with an average of 0.99. **Measure 12 - *Heuchera Americana* "palace purple"** (perennial herbaceous plant with showy foliage of 30 to 40 cm) is the specie

with the best sound absorption at medium frequencies with an average of 0.95, while its capacity decreases at low frequencies with an average of 0.60.

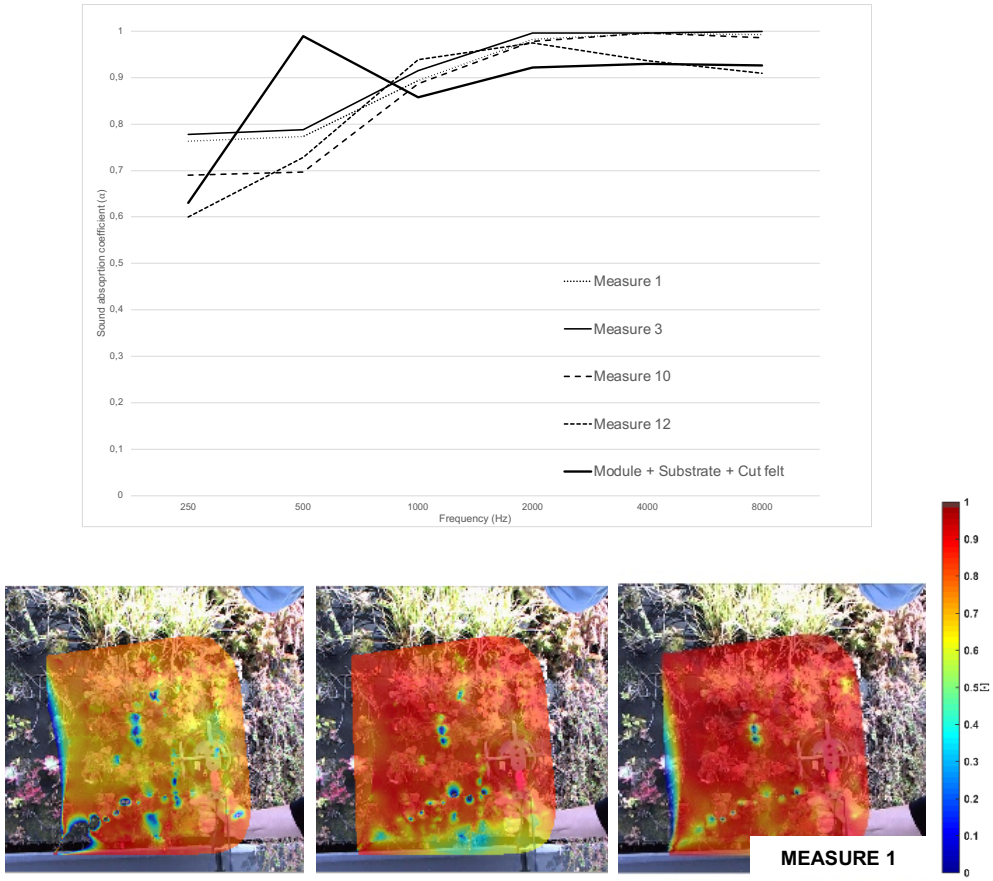

Figure 43: (a) Absorption curves for modules with low-density vegetation; (b) Results of the Scan&Paint method in measurement 1 at 500, 1000 and 2000 Hz.

Therefore, it can be stated that in green modules with low-density vegetation, either due to the development of the plant or the morphology of the plant itself, the highest absorption capacity occurs at high frequencies, while they produce almost no effect at low and medium frequencies.

When these results are compared with those obtained in the module with substrate and cut felt (the state prior to the introduction of the plants), it is evident that at low frequencies, there is no significant improvement in sound absorption when the plant is introduced. However, at medium frequencies and high frequencies, there is an increase in the sound absorption coefficient between 4-7% and 6-8%, respectively. The results are explained in

Table 3, which shows the differences between the sound absorption coefficient obtained in the measurements corresponding to the different plant species and the absorption coefficient obtained in the felt module and without vegetation. These results are expressed as absolute values and as a percentage. The same analysis has been performed for the medium and high absorption increases.

Table 3*:* Evaluation of the sound absorption performance of different plant species at low, medium, and high frequencies.

Measures	∆ Sound Absorption Coefficient			Absorption increase %		
	Low	Med	High	Low	Med	High
M1	-0.05	0.04	0.06	-6%	4%	6%
M3	-0.03	0.06	0.07	-4%	7%	8%
M10	-0.12	0.04	0.06	-15%	4%	6%
M12	-0.21	0.06	-0.01	-26%	7%	-1%

b. Medium absorption increase

Three species were evaluated for medium absorption: *Delosperma cooperi, Lonicera nitida* "Magrun", and *Sedum album* "coral carpet". All three species have very different characteristics but similar absorption capacities: a sound absorption coefficient with an average of 0.85 between 250 - 1000 Hz and a high absorption coefficient at high frequencies (1.00 between 4000 - 8000 Hz). Unlike the species analysed in the previous section, these are characterized by an absorption coefficient of 0.80 up to a maximum of 1.00 (Figure 8).

Specifically, **measure 2 – *Delosperma cooperi*** (a medium-sized climbing shrub, with a pendulous habit and persistent foliage, with a length between 2.5 and 4m) has an average absorption coefficient of 0.85 at low frequencies and 0.99 and 1.00 at medium frequencies and high frequencies respectively —similar behaviour to the other two measurements.

Measure 9 - *Lonicera nitida* "maigrun" (dense, evergreen, rustic shrub, reaching a maximum height of 80-100 cm), shows an average absorption coefficient of 0.84 at low

frequencies and 0.99 and 1.00 at medium and high frequencies, while **measure 11 - *Sedum album* "coral carpet"** (rhizomatous, evergreen, spreading, bushy plant with a height of 5-8 cm) has an average absorption coefficient of 0.84 at low frequencies and 0.98 and 1.00 at medium and high frequencies.

From the results, it is possible to reaffirm that the increase in vegetation density (especially those with dense stems or those that create dense surfaces) is proportional to the increase in the absorption coefficient. Although the three species are very different, their absorption capacities are again not conditioned by the plant type but by their biomass. However, this absorption will be particularly noticeable at high frequencies since the absorption coefficient increases proportionally and progressively at higher frequencies. This proportional and progressive increase across the frequency spectrum can also be seen in the colour maps at frequencies of 500, 1000 and 2000 Hz (Figure 44).

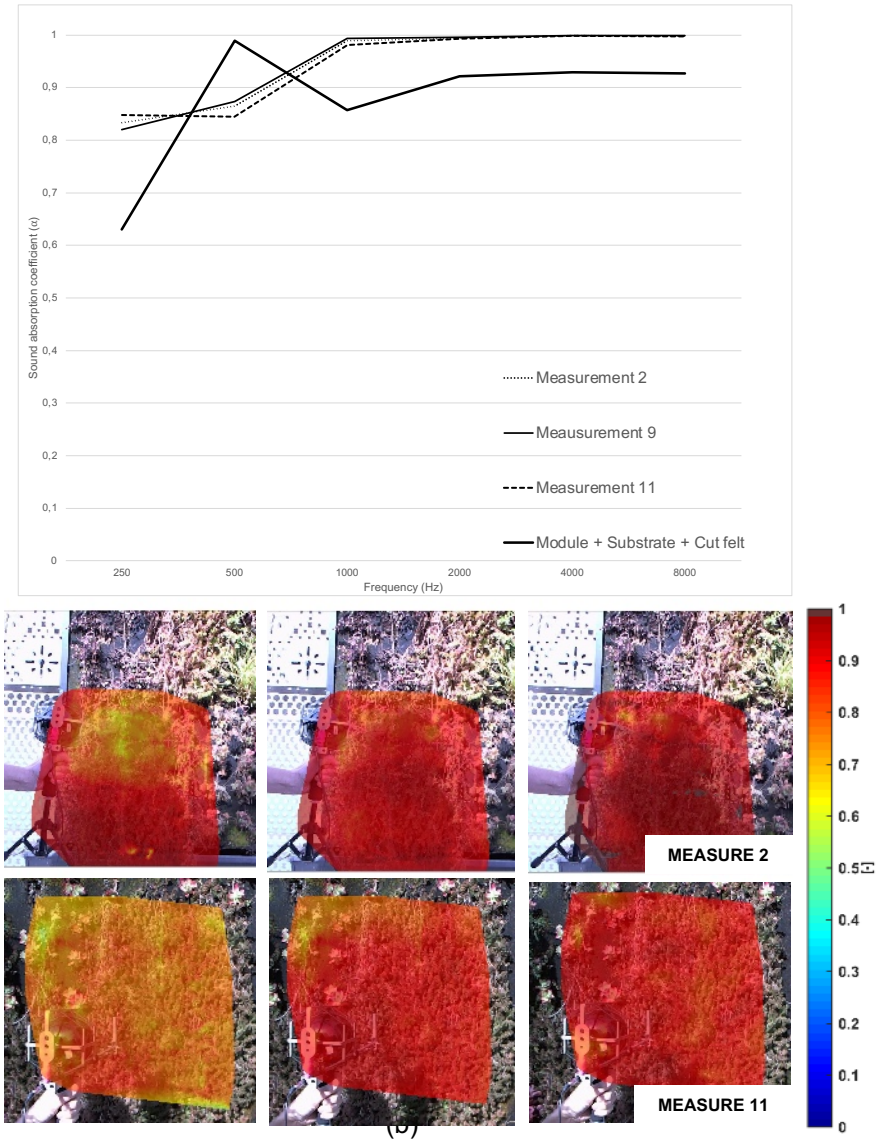

Figure 44: (a) Absorption curves for modules with medium-density vegetation; (b) Results of the Scan&Paint method on measurements 2 and 11 at 500, 1000 and 2000 Hz.

Compared to the results obtained in the module without plants, the results show an increase in the sound absorption coefficient after the introduction of vegetation in all cases and across the whole frequency spectrum. This improvement results in 4% (0.03) - 5% (0.04) at low frequencies, 10% (0.09) - 11% (0.10) at medium frequencies, and 8% (0.07) at high frequencies (

Table 4).

Table 4*:* Evaluation of the sound absorption performance of different plant species at low, medium, and high frequencies.

Measures	Δ Sound Absorption Coefficient			Absorption increase %		
	Low	Med	High	Low	Med	High
M2	0.04	0.10	0.07	5%	11%	8%
M9	0.03	0.10	0.07	4%	11%	8%
M11	0.03	0.09	0.07	4%	10%	8%

c. High absorption increase

Five species were tested for high absorption: *Sedum album* "coral carpet", *Thymus communis*, *Sedum acre* “golden carpet”, *Thymus vulgaris*, and *Carex oshimensis*. As in the previous cases, these are very different species but with similar behaviour and high absorption coefficients throughout the frequency spectrum (Figure 9).

In the case of **measurement 4 - *Sedum album* "coral carpet"**, two measurements were made. One has been classified as medium density due to the plant's development and obtained an average absorption coefficient of 0.84 at low frequencies and 1.00 at medium and high frequencies. In contrast, this second measure is classified as high density, with an average absorption coefficient of 0.93 at low frequencies and 0.99 and 1.00 at medium and high frequencies. It shows that the results go beyond the type of plant and depend mainly on the density of the plant.

For **measurement 5 – *Sedum acre “golden carpet”*** (succulent, perennial, evergreen plant with short, dense leaves, not exceeding 15 cm in height), **measurement 6 – *Thymus vulgaris*** (shrub with woody stems at the base and herbaceous stems at the top, with abundant leaves of minute size, between 5 and 8 mm in length), and **measurement 7 - *Carex oshimensis*** (herbaceous

perennial plant with thin, narrow leaves forming rounded, compact clumps up to 25-30 cm in diameter), the behaviour is practically the same; the changes are imperceptible. Both have an average absorption coefficient of 0.92 at low frequencies and 1.00 at medium and high frequencies.

The species that stands out in this data analysis section is tested under **measure 8 – *Thymus communis*** (aromatic, perennial plant with a robust habit that reaches a height of 30 – 45 cm). It has an average absorption coefficient of 0.97 at low frequencies and 1.00 at medium and high frequencies. In these cases, the vegetation forms a uniform layer over the module, increasing its thickness and, therefore, its absorption coefficient at all frequencies. Since the vegetation structure is a porous layer, the result is equal to the contribution of the substrate and the vegetation. The morphology of the plant does not appear to play a defining role in the change in the absorption coefficient. However, at low frequencies, the increase in the absorption coefficient in measurement 8 stands out above the rest; this could be due to the morphology of the plant, which, being leafy, generates a large and thick layer that absorbs the noise.

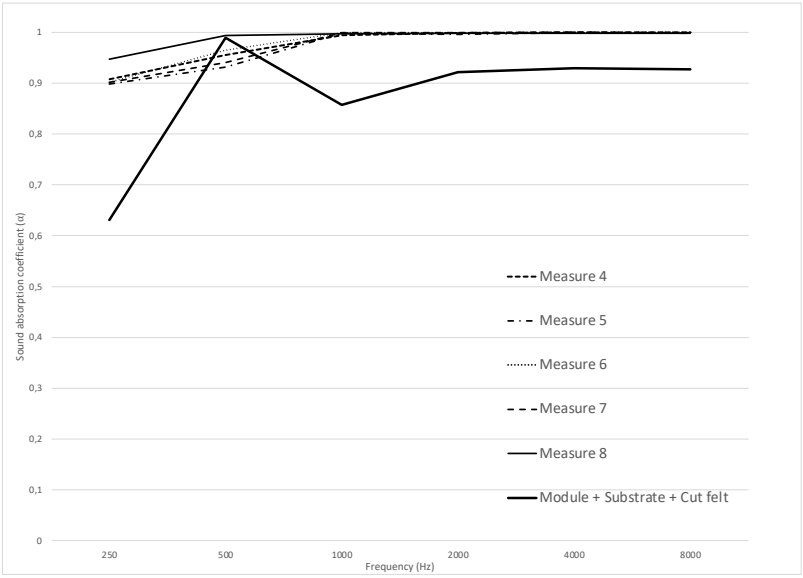

Figure 45: Absorption curves for modules with high density vegetation.

These statements are verified by comparing the results obtained with those of the module without vegetation, from which a significant increase in the sound absorption coefficient is demonstrated after the introduction of vegetation. At low frequencies, there is an improvement between 12-20%; at medium frequencies of 11-12%, and at high frequencies, the improvement is 8% in all cases (

Table 5).

Table 5*:* Evaluation of the sound absorption performance of different plant species at low, medium, and high frequencies.

Measures	∆ Sound Absorption Coefficient			Absorption increase %		
	Low	Med	High	Low	Med	High
M4	0.12	0.10	0.07	15%	11%	8%
M5	0.11	0.11	0.07	14%	12%	8%
M6	0.16	0.11	0.07	20%	12%	8%
M7	0.10	0.11	0.07	12%	12%	8%
M8	0.12	0.11	0.07	15%	12%	8%

Table 6 summarizes the study's findings of the sound absorption coefficient in modules installed on the façade of the itdUPM. These are classified according to the level of absorption (low, medium, high) and show the sound absorption coefficient for each specie, the average absorption coefficient at low, medium, and high frequencies, and the NRC (Noise Reduction Coefficient), which was calculated with the average of the coefficients obtained at 250, 500, 1000 and 2000 Hz.

Table 6*:* Summary of sound absorption coefficients according to the tested plant species

Plant Specie	Sound absorption coefficient						Average sound absorption coefficient			Noise Reduction Coefficient (NRC)
	250 Hz	500 Hz	1000 Hz	2000 Hz	4000 Hz	8000 Hz	Low (250 – 500 Hz)	Medium (1000 – 2000 Hz)	High (2000 – 4000 Hz)	
Low absorption increase										
Heuchera americana "dale's strain"	0.76	0.77	0.89	0.98	0.99	0.99	0.76	0.93	0.99	0.85
Sedum acre "golden carpet" *(1)*	0.78	0.79	0.91	1.00	1.00	1.00	0.78	0.95	1.00	0.87
Gazania rigens	0.69	0.70	0.89	0.98	1.00	0.99	0.69	0.93	0.99	0.81
Heuchera americana "palace purple"	0.60	0.73	0.94	0.97	0.94	0.91	0.60	0.95	0.92	0.81
Medium absorption increase										
Delosperma cooperi	0.83	0.87	0.99	0.99	1.00	1.00	0.85	0.99	1.00	0.92
Lonicera nitida "maigrun"	0.82	0.87	0.99	1.00	1.00	1.00	0.84	0.99	1.00	0.92
Sedum album "coral carpet" (1)	0.85	0.84	0.98	0.99	1.00	1.00	0.84	0.98	1.00	0.91
High absorption increase										
Sedum album "coral carpet" (2)	0.91	0.96	0.99	1.00	1.00	1.00	0.93	0.99	1.00	0.96
Carex oshimensis	0.90	0.94	1.00	1.00	1.00	1.00	0.92	1.00	1.00	0.96
Thymus communis	0.95	0.99	1.00	1.00	1.00	1.00	0.97	1.00	1.00	0.98
Sedum acre "golden carpet" *(2)*	0.90	0.93	1.00	1.00	1.00	1.00	0.91	1.00	1.00	0.96
Thymus vulgaris	0.90	0.96	1.00	1.00	1.00	1.00	0.93	1.00	1.00	0.96

4. Conclusions

In this paper, the sound absorption capacity of a green wall module was evaluated by analysing the sound absorption coefficient of its main components. It is important to note that, as far as the authors have been able to research, this study is the first of its kind to be carried out with an impedance gun, which, compared to the usual methods, allows for the evaluation of the absorption coefficient in situ.

As green walls are relatively new systems that are expected to spread soon, it is essential to study the behaviour of their components in-depth and innovate the methods used to obtain data on their properties in the laboratory and verify them under natural operating conditions to be able to offer results that guarantee the dissemination and use of this type of solution in the city.

The tests were carried out using a novel instrument for this field of research (PU probe), and the conclusions are as follows.

- The substrate is the component that has the most significant impact on the sound absorption of the module. An absorption coefficient of 0.70 was observed at low frequencies (250-500 Hz), which progressively increased with increasing noise frequency. As the substrates' composition and thickness improve, the system's acoustic performance will improve. These considerations would ensure the dissemination of these building elements as sound noise absorbers in urban contexts.
- The felt placed on the substrate has a sound absorption capacity that can contribute slightly to an increase in the sound absorption coefficient. During the laboratory measurements, sound absorption coefficients of 0.91 and 0.98 were observed over the entire frequency spectrum.
- Vegetation generally has effective absorption properties at high frequencies (2000-4000 Hz), verified in laboratory and *in-situ* tests. However, this sound absorption capacity is proportional to the density of the vegetation, which influences the ability to block noise propagation.
- Improvements in sound absorption were found between the module without vegetation and the modules evaluated with different species. Specifically, a 4-8% improvement was found for species with low absorption enhancement, 4-10% for species with medium absorption enhancement, and 8-20% for species with high absorption enhancement. It confirms other research that 80% of the uptake comes from the substrate and 10-20% from the vegetation.

- Not all dense species have high absorption coefficients, and the tests demonstrated this on modules with grass, which, being a very compact sample, does not allow noise absorption (the absorption coefficient does not increase).
- The water content is relevant to the acoustic performance of a green wall. On average, a fully saturated module (8 l/m^2) has a sound absorption coefficient of 43% lower than a module at medium saturation (4 l/m^2). These findings are significant facts for the optimisation of irrigation systems usually used to maintain this type of solution installed in buildings, and proper irrigation programming, adapted to the site's weather conditions, will guarantee good acoustic performance.

The results obtained in this study demonstrate that the sound absorption coefficients are equal to or better than those of some common building materials. When comparing these results with those of previous studies, there were some small differences in the absorption coefficients found, probably due to differences in the construction system and plant species tested in each case. However, despite these differences, the potential of vegetation as a sound absorption tool in cities is confirmed.

This research analysed the sound absorption coefficient of a green wall module with an organic substrate. As the acoustic performance of these technological solutions is a field yet to be explored, future studies should consider aspects such as the influence of substrate saturation levels, the compaction and composition of the substrate, different types of hydrophilic layers, or even the different support systems on the sound absorption coefficient.

References

Aletta, F., Kang, J., Astolfi, A., & Fuda, S. (2016). Differences in soundscape appreciation of walking sounds from different footpath materials in urban parks. *Sustainable Cities and Society*, *27*, 367–376. https://doi.org/10.1016/j.scs.2016.03.002

Asdrubali, F., D'Alessandro, F., Mencarelli, N., & Horoshenkov, K. V. (2014). Sound absorption properties of tropical plants for indoor applications. *21st International Congress on Sound and Vibration 2014, ICSV 2014*, *4*(July), 3249–3256.

Attal, E., Côté, N., Haw, G., Pot, G., Vasseur, C., Shimizu, T., … Dubus, B. (2016). Experimental characterization of foliage and substrate samples by the three-microphone

two-load method. *Inter-Noise 2016*, (11), 6602–6609.

Attal, E., de l'Epine, Y. B., Dauchez, N., & Dubus, B. (2021). Experimental investigation of the effect of moisture on the acoustic properties of lightweight substrates used in green envelopes. *Applied Acoustics*, *180*, 108108. https://doi.org/10.1016/j.apacoust.2021.108108

Azkorra, Z., Pérez, G., Coma, J., Cabeza, L. F., Bures, S., Álvaro, J. E., … Urrestarazu, M. (2015). Evaluation of green walls as a passive acoustic insulation system for buildings. *Applied Acoustics*, *89*, 46–56. https://doi.org/10.1016/j.apacoust.2014.09.010

Boer, L. C. (Eelco) den, & Schroten, A. (Arno). (2007). Traffic noise reduction in Europe Health effects , social costs and, (August), 1–64.

Bullen, R., & Fricke, F. (1982). Sound propagation through vegetation. *Journal of Sound and Vibration*, *80*(1), 11–23. https://doi.org/10.1016/0022-460X(82)90387-X

Cameron, R. W. F., Taylor, J., & Emmett, M. (2015). A Hedera green façade - Energy performance and saving under different maritime-temperate, winter weather conditions. *Building and Environment*, *92*, 111–121. https://doi.org/10.1016/j.buildenv.2015.04.011

Comesaña, D. F., Steltenpool, S., Carrillo Pousa, G., de Bree, H.-E., & Holland, K. R. (2013). Scan and Paint: Theory and Practice of a Sound Field Visualization Method. *ISRN Mechanical Engineering*, *2013*, 241958. https://doi.org/10.1155/2013/241958

D'Alessandro, F., Asdrubali, F., & Mencarelli, N. (2015). Experimental evaluation and modelling of the sound absorption properties of plants for indoor acoustic applications. *Building and Environment*, *94*, 913–923. https://doi.org/10.1016/j.buildenv.2015.06.004

de Bree, H.-E., Tijs, E., & Basten, T. (2007). An Ultra Miniature Measurement Tool to Measure the Reflection Coefficient of Acoustic Damping Materials in Situ. In *SAE 2007 Noise and Vibration Conference and Exhibition*. SAE International. https://doi.org/https://doi.org/10.4271/2007-01-2212

Ding, L., Van Renterghem, T., Botteldooren, D., Horoshenkov, K., & Khan, A. (2013). Sound absorption of porous substrates covered by foliage: Experimental results and numerical predictions. *The Journal of the Acoustical Society of America*, *134*(6), 4599–4609. https://doi.org/10.1121/1.4824830

E. Tijs, H. E. de Bree, S. S. (2010). Scan and Paint: a novel sound visualization technique. In *Proc. 39th Int. Congr. Noise Control Eng. 2010 (Inter-noise 2010: noise and sustainability)*. Lisbon, Portugal. https://doi.org/9781617823961

E. Tijs. (2013). *Study and development of an in situ acoustic absorption measurement method*. University of Twente.

E. Tijs, H. E. de B. (2008). Recent developments free field PU impedance technique. In *SAPEM 2008, Symp. Acoust. Poro-elastic Mater.* Bradford,, UK.

Fernandez Comesaña, D., Holland, K. R., & Fernandez-Grande, E. (2016). Spatial resolution limits for the localization of noise sources using direct sound mapping. *Journal of Sound and Vibration*, *375*, 53–62. https://doi.org/https://doi.org/10.1016/j.jsv.2016.04.010

Guan, H., Hu, S., Liu, G., & Zhang, L. (2020). The combined effects of temperature and noise

on the comfort perceptions of young people with a normal Body Mass Index. *Sustainable Cities and Society*, *54*(11), 101993. https://doi.org/10.1016/j.scs.2019.101993

H. E. de Bree, E. Tijs, T. G. H. B. (2006). Two complementary Microflown based methods to determine the reflection coefficient in situ. In *ISMA Int. Conf. Noise Vib. Eng., Heverlee.* Belgium.

H. E. de Bree, M. Nosko, E. Tijs. (2008). A handheld device to measure the acoustic absorption in situ. In *Proc. SNVH 2008, 5th Int. Styrian Noise Vib. Harshness Conf.* Graz, Austria.

Hoelscher, M. T., Nehls, T., Jänicke, B., & Wessolek, G. (2016). Quantifying cooling effects of facade greening: Shading, transpiration and insulation. *Energy and Buildings*, *114*, 283–290. https://doi.org/10.1016/j.enbuild.2015.06.047

Horoshenkov, K. V. . B. H. K. A., Khan, A., & Benkreira, H. (2013). Acoustic properties of low growing plants. *The Journal of the Acoustical Society of America*, *133*(5), 2554–2565. https://doi.org/10.1121/1.4798671

Imran, H. M., Kala, J., Ng, A. W. M., & Muthukumaran, S. (2019). Effectiveness of vegetated patches as Green Infrastructure in mitigating Urban Heat Island effects during a heatwave event in the city of Melbourne. *Weather and Climate Extremes*, *25*(June). https://doi.org/10.1016/j.wace.2019.100217

Jamei, E., Rajagopalan, P., Seyedmahmoudian, M., & Jamei, Y. (2016). Review on the impact of urban geometry and pedestrian level greening on outdoor thermal comfort. *Renewable and Sustainable Energy Reviews*, *54*, 1002–1017. https://doi.org/10.1016/j.rser.2015.10.104

Kabisch, N., Frantzeskaki, N., Pauleit, S., Naumann, S., Davis, M., Artmann, M., … Bonn, A. (2016). Nature-based solutions to climate change mitigation and adaptation in urban areas : Perspectives on indicators , knowledge ... urban areas : perspectives on indicators , knowledge gaps , barriers , and. *Ecology and Society*, *21*(June). https://doi.org/10.5751/ES-08373-210239

Kandelan, S. N., Yeganeh, M., Peyman, S., Panchabikesan, K., & Eicker, U. (2022). Environmental study on greenery planning scenarios to improve the air quality in urban canyons. *Sustainable Cities and Society*, *83*(May), 103993. https://doi.org/10.1016/j.scs.2022.103993

Kinsler L. E., Frey A. F., A. B. C. and J. V. S. (n.d.). Fundamentals of acoustics. *John Wiley and Sons Inc. New York, United States of América.*, *4º Edición*.

Lacasta, A. M., Penaranda, A., Cantalapiedra, I. R., Auguet, C., Bures, S., & Urrestarazu, M. (2016). Acoustic evaluation of modular greenery noise barriers. *Urban Forestry and Urban Greening*, *20*, 172–179. https://doi.org/10.1016/j.ufug.2016.08.010

Lacasta, Ana M., Peñaranda, A., & Cantalapiedra, I. R. (2018). Green streets for noise reduction. *Nature Based Strategies for Urban and Building Sustainability*, 181–190. https://doi.org/10.1016/B978-0-12-812150-4.00017-3

Ling, T. Y., & Chiang, Y. C. (2018). Well-being, health and urban coherence-advancing vertical greening approach toward resilience: A design practice consideration. *Journal of Cleaner*

Production, *182*, 187–197. https://doi.org/10.1016/j.jclepro.2017.12.207

Liu, J., Kang, J., Behm, H., & Luo, T. (2014). Effects of landscape on soundscape perception: Soundwalks in city parks. *Landscape and Urban Planning*, *123*, 30–40. https://doi.org/10.1016/j.landurbplan.2013.12.003

Oquendo-Di Cosola, V., Olivieri, F., & Ruiz-García, L. (2022). A systematic review of the impact of green walls on urban comfort: temperature reduction and noise attenuation. *Renewable and Sustainable Energy Reviews*, *162*(April), 112463. https://doi.org/10.1016/j.rser.2022.112463

Pedrero, A., Navacerrada, M. Á., de la Prida, D., Iglesias, L., & Díaz-Chyla, A. (2020). On the accuracy of the sound absorption measurement with an impedance gun. *Applied Acoustics*, *158*, 107039. https://doi.org/https://doi.org/10.1016/j.apacoust.2019.107039

Pérez, G, Coma, J., Barreneche, C., De Gracia, A., Urrestarazu, M., Burés, S., & Cabeza, L. F. (2016). Acoustic insulation capacity of Vertical Greenery Systems for buildings. *Applied Acoustics*, *110*, 218–226. https://doi.org/10.1016/j.apacoust.2016.03.040

Przybysz, A., Sæbø, A., Hanslin, H. M., & Gawroński, S. W. (2014). Accumulation of particulate matter and trace elements on vegetation as affected by pollution level, rainfall and the passage of time. *Science of the Total Environment*, *481*(1), 360–369. https://doi.org/10.1016/j.scitotenv.2014.02.072

Romanova, A., Horoshenkov, K. V., & Hurrell, A. (2019). An application of a parametric transducer to measure acoustic absorption of a living green wall. *Applied Acoustics*, *145*, 89–97. https://doi.org/10.1016/j.apacoust.2018.09.020

Siano, D., Viscardi, M., & Panza, M. A. (2016). Automotive Materials: An Experimental Investigation of an Engine Bay Acoustic Performances. *Energy Procedia*, *101*, 598–605. https://doi.org/https://doi.org/10.1016/j.egypro.2016.11.076

Sierra-Pérez, J., Boschmonart-Rives, J., & Gabarrell, X. (2016). Environmental assessment of façade-building systems and thermal insulation materials for different climatic conditions. *Journal of Cleaner Production*, *113*(2016), 102–113. https://doi.org/10.1016/j.jclepro.2015.11.090

Teotónio, I., Silva, C. M., & Cruz, C. O. (2021). Economics of green roofs and green walls: A literature review. *Sustainable Cities and Society*, *69*(February). https://doi.org/10.1016/j.scs.2021.102781

Tong, Z., Baldauf, R. W., Isakov, V., Deshmukh, P., & Max Zhang, K. (2016). Roadside vegetation barrier designs to mitigate near-road air pollution impacts. *Science of the Total Environment*, *541*, 920–927. https://doi.org/10.1016/j.scitotenv.2015.09.067

Van Renterghem, T., Botteldooren, D., & Verheyen, K. (2012). Road traffic noise shielding by vegetation belts of limited depth. *Journal of Sound and Vibration*, *331*(10), 2404–2425. https://doi.org/https://doi.org/10.1016/j.jsv.2012.01.006

Van Renterghem, Timothy, Dekoninck, L., & Botteldooren, D. (2020). Multi-stage sound planning methodology for urban redevelopment. *Sustainable Cities and Society*, *62*(June), 102362. https://doi.org/10.1016/j.scs.2020.102362

Weerakkody, U., Dover, J. W., Mitchell, P., & Reiling, K. (2018). The impact of rainfall in remobilising particulate matter accumulated on leaves of four evergreen species grown on a green screen and a living wall. *Urban Forestry and Urban Greening*, *35*(July), 21–31. https://doi.org/10.1016/j.ufug.2018.07.018

Wong, N H, Kwang Tan, A. Y., Tan, P. Y., Chiang, K., & Wong, N. C. (2010). Acoustics evaluation of vertical greenery systems for building walls. *Building and Environment*, *45*(2), 411–420. https://doi.org/10.1016/j.buildenv.2009.06.017

Xiao, X. D., Dong, L., Yan, H., Yang, N., & Xiong, Y. (2018). The influence of the spatial characteristics of urban green space on the urban heat island effect in Suzhou Industrial Park. *Sustainable Cities and Society*, *40*(April 2017), 428–439. https://doi.org/10.1016/j.scs.2018.04.002

Yilmaz, N. G., Lee, P. J., Imran, M., & Jeong, J. H. (2023). Role of sounds in perception of enclosure in urban street canyons. *Sustainable Cities and Society*, *90*(January), 104394. https://doi.org/10.1016/j.scs.2023.104394

Yin, Y., Zhang, D., Zhen, M., Jing, W., Luo, W., & Feng, W. (2022). Combined effects of the thermal-acoustic environment on subjective evaluations in outdoor public spaces. *Sustainable Cities and Society*, *77*(8), 103522. https://doi.org/10.1016/j.scs.2021.103522

PARTE IV. CONCLUSIONES Y FUTURAS LÍNEAS DE INVESTIGACIÓN

Este último apartado se divide en dos partes. Un primer capítulo en el que se recogen las principales conclusiones obtenidas en esta tesis doctoral, destacando especialmente las relativas a las fases del estudio experimental y a las estrategias de optimización del módulo de jardinería vegetal seleccionado. Y un segundo y último capítulo en el que se plantean las líneas de trabajo que esta investigación deja abiertas y los posibles desarrollos futuros de las mismas.

10. Conclusiones

11. Futuras líneas de investigación

Conclusiones

Esta tesis doctoral ha confirmado la hipótesis y cumplido con el objetivo general de desarrollar una metodología que permitiera evaluar las prestaciones medioambientales de un sistema de jardinería vertical a través de datos experimentales. Se ha comprobado que, a través de su aplicación, se pueden determinar los aspectos relevantes para incrementar el impacto de estas soluciones en la mejora del confort en contextos urbanos densos.

La propuesta metodológica ha posibilitado, por un lado, el análisis del impacto medioambiental que puede tener una solución basada en la naturaleza en todo su ciclo de vida. Por otro lado, el desarrollo del análisis experimental sobre las condiciones medioambientales en el entorno inmediato del módulo evaluado ha contribuido a identificar las variables que influyen en la reducción de temperaturas y absorción de ruido de estas. Esta investigación contribuye con un procedimiento de análisis experimental que puede ser replicado en otros contextos urbanos.

En el desarrollo de la investigación se ha cumplido con los cinco objetivos específicos de esta tesis doctoral que, a su vez, se corresponden con las fases metodológicas planteadas:

Primer objetivo: "*Estudiar el estado del arte de la tecnología y su aplicación en entornos urbanos densos*". La evaluación sistemática de los estudios previos concluye que el efecto regulador térmico se debe principalmente al proceso de fotosíntesis y evapotranspiración de las hojas de las plantas, mostrando reducciones de hasta 2,7 ºC en comparación con la temperatura del aire, debido principalmente a la absorción de la radiación solar y la transferencia de calor por convección. Asimismo, el efecto de la combinación de la sombra y la evapotranspiración de las plantas reduce la temperatura del aire entre 1 y 3 ºC, aunque esto puede variar en función del clima y la composición

del sustrato. La mayoría de los resultados obtenidos son atribuibles a la presencia del sustrato y su inercia térmica. El tipo de especie, el índice foliar, la superficie cubierta y el espesor de la planta influyen significativamente en el rendimiento de los sistemas de jardinería vertical, siendo mayor el impacto de reducción de temperatura a mayor cobertura.

En cuanto al efecto de los jardines verticales en la absorción acústica, la evaluación sistemática de los estudios previos concluye que los sistemas de jardinería vertical cuentan con una mayor capacidad de absorción a frecuencias medias y altas, lo que los convierte en una solución eficaz para el control de ruido ambiental en espacios públicos. También se concluye que la absorción del ruido proviene fundamentalmente del sustrato, el cual absorbe el 80% de la energía recibida a frecuencias superiores a 1000 Hz. Estas características lo convierten en un material tan útil como cualquier otro material poroso utilizado para el aislamiento en la construcción (como lana de roca o fibra de coco), siendo el espesor una variable relevante para garantizar las prestaciones acústicas del sistema.

Asimismo, la densidad de la masa vegetal es también un condicionante para el aumento de la absorción de ruido, siendo de hasta un 20% adicional con respecto a la capacidad de absorción del sustrato. Por último, se determinó que la configuración del módulo es una variable que influye directamente en la capacidad de absorción acústica, no sólo por el espesor y composición del sustrato o la densidad de la vegetación, sino también por la impedancia de las juntas entre los módulos y el aislamiento de la estructura de soporte.

Segundo objetivo: "*Identificar el sistema modular de jardinería vertical más adecuado para el estudio*". El ACV demostró el impacto de los materiales y sustancias utilizadas para la fabricación y mantenimiento de los módulos, que, en ambos casos, representan

más del 80% del impacto ambiental en la mayoría de las categorías analizadas. El sistema modular en fieltro cuenta con una estructura de soporte en aluminio que supone el 40% del impacto total y requiere del uso de fertilizantes durante la fase de mantenimiento del sistema contribuyendo al 50% del impacto en la mayoría de categorías analizadas. El sistema modular en plástico arrojó mejores resultados durante las tres fases analizadas, principalmente por la cantidad y tipo de materiales empleados para su fabricación y el uso de sustrato orgánico no dependiente de fertilizantes para su mantenimiento. Los impactos identificados en este sistema podrían reducirse aún más sustituyendo materiales como el poliéster de los geotextiles y el aluminio de los anclajes por textiles y aluminio reciclado.

El estudio pone en evidencia el potencial de establecer un proceso de diseño de la construcción, producción y puesta en funcionamiento integral y alineada con la sostenibilidad. Además, se ha puesto de manifiesto que, a través de la incorporación de metodologías como el ACV en todo el proceso de toma de decisión, desde la elección de los materiales hasta los métodos de montaje y de mantenimiento, puede mejorar el rendimiento medioambiental de este tipo de sistemas y en última instancia, el balance energético y de emisiones del edificio en el que sean instalados.

Tercer objetivo: "*Cuantificar e identificar las variables que influyen sobre la reducción de temperaturas*". A través del análisis estadístico y la interpretación de los datos de la monitorización del comportamiento del módulo de jardinería vertical en condiciones reales, se ha comprobado que existe una correlación positiva entre la temperatura del aire registrada por los sensores frente al jardín vertical y la temperatura del aire ambiente, especialmente durante el verano. También se ha demostrado que no existen correlaciones significativas entre la humedad relativa y las temperaturas

registradas por los sensores durante el invierno. Sin embargo, sí existen correlaciones negativas durante el verano, lo que evidencia el efecto de la irradiación sobre el jardín vertical, que aumenta la temperatura del aire y reduce la humedad relativa, especialmente durante las horas de luz. Por otra parte, no existe una fuerte correlación entre la irradiancia y la temperatura del aire registrada por los sensores, descartando la irradiancia como una variable que condiciona el comportamiento de la fachada y la reducción de las temperaturas adyacentes.

A través del análisis de la varianza (ANOVA) se demostró que el jardín vertical reduce la temperatura de forma estadísticamente significativa, con mayor significancia en la fachada sur, demostrando también la influencia en la humedad relativa con significancia estadística en todas las estaciones y en ambas orientaciones. En particular, la reducción de temperaturas es de 0,63 ºC en verano y 0,54 ºC en invierno. En todos los casos el p valor es inferior a 0,0001, lo que significa que la diferencia estadística es significativa con una confianza superior al 99.9%. En el caso de la fachada oeste, se detectó un aumento de la temperatura de 0,56 ºC.

Así, se concluye que el sistema evaluado puede mejorar el microclima urbano a nivel peatonal en un clima mediterráneo fundamentalmente durante el verano. Sin embargo, no se puede concluir que la distancia influya significativamente en la reducción de temperaturas, ya que la diferencia máxima encontrada para la temperatura y la humedad relativa no es significativamente relevante.

Cuarto objetivo: "*Cuantificar e identificar las variables que influyen sobre la absorción de ruido*". Se concluye que el sustrato es el componente que más incide en la absorción acústica del módulo de jardinería vertical, con una influencia del 80% de la

absorción total. Se observó un coeficiente de absorción de α= 0,70 a bajas frecuencias (250-500 Hz), que aumentó progresivamente al aumentar la frecuencia del ruido, lo cual demuestra que estos elementos de construcción pueden actuar como absorbentes efectivos de ruido en contextos urbanos.

También se concluye que el fieltro utilizado para garantizar la humedad del sustrato y evitar desprendimientos tiene una capacidad de absorción acústica que puede contribuir a un aumento del coeficiente de absorción. Durante las mediciones de laboratorio, se observaron coeficientes de absorción de ruido de α=0,91 y α=0,98 en todo el espectro de frecuencias.

Finalmente, se demostró que la capacidad de absorción del ruido es proporcional a la densidad de la vegetación, encontrando mejoras en la absorción acústica entre el módulo sin vegetación y los módulos evaluados con diferentes especies. Específicamente, se encontró una mejora del 4 al 8% para las especies *Heuchera americana* "dale's strain", *Sedum acre "*golden carpet*"*, *Gazania rigens*, y *Heuchera americana* "palace purple", del 4 al 10% para las especies *Delosperma cooperi, Lonicera nitida* "magrun", and *Sedum album* "coral carpet", y del 8 al 20% para las especies *Sedum album* "coral carpet", *Thymus communis*, *Sedum acre* "golden carpet", *Thymus vulgaris* y *Carex oshimensis*. Además, se ha demostrado que el contenido de agua es relevante para el rendimiento acústico del jardín vertical puesto que, de media, un módulo totalmente saturado (8 l/m^2) tiene un coeficiente de absorción acústica un 43% inferior al de un módulo en saturación media (4 l/m^2).

Estos hallazgos son significativos para la optimización de los sistemas de riego, de forma que, una correcta programación del riego, adaptada a las condiciones climáticas del lugar, garantizará un buen comportamiento acústico. Como conclusión general, se demuestra

que los coeficientes de absorción acústica son iguales o mejores que los de algunos materiales de construcción comunes.

Quinto objetivo: "*definir las líneas de optimización de un módulo de jardinería vertical para la mejora del confort higrotérmico y el confort acústico en contextos urbanos densos".* Las líneas de optimización que se definen son:

- **Uso de sustratos orgánicos compuestos de materiales como fibra de coco, turba y humus.** Los sistemas hidropónicos requieren unas sustancias para su mantenimiento que generan un 50% del impacto ambiental del sistema. Especialmente en las categorías "agotamiento de los recursos hídricos", "ecotoxicidad del agua dulce", "uso de la tierra", y "cambio climático", en las que constituyen un impacto del 99,17% del total, debido a la necesidad de fertilizaciones químicas 10 veces al año.
- **Capa de sustrato con espesor igual o superior a 5 cm.** El espesor del sustrato es una variable que condiciona las prestaciones acústicas del sistema. Esta capacidad de absorción se verá incrementada según el tipo de especies vegetales plantadas, y disminuida según el nivel de saturación. Los resultados le atribuyen una absorción de entre 80-90% de la energía recibida tanto en pruebas de laboratorio como en condiciones reales.
- **Uso de *Sedum album* "coral carpet", *Thymus communis*, *Sedum acre* "golden carpet", *Thymus vulgaris* y *Carex oshimensis* en clima mediterráneo.** Cuanto mayor sea la cobertura, mayor será el impacto. Esto influye también en la capacidad de absorción acústica, en concreto, un aumento de entre el 4-20% del coeficiente de absorción según el tipo de planta. En concreto, las especies

propuestas, son capaces de aumentar el coeficiente de absorción entre un 8 y un 20% con respecto a un módulo sin vegetación, según la frecuencia.

- **Uso de textiles no tejidos en la estratigrafía del sistema a efectos fonoabsorbentes.** Se ha demostrado un comportamiento estándar en todo el espectro de frecuencias utilizado que varía con la incorporación de la capa de fieltro. El módulo con sustrato y capa de fieltro arrojó coeficientes de absorción de entre 0,91 y 0,98 a frecuencias medias y altas, lo que demuestra la influencia en la absorción del ruido. La incorporación de capas de textil no tejido, además contribuyen a evitar los desprendimientos y a mantener la humedad en el sistema.
- **Garantizar un riego del sistema de 4 l/m^2 en clima mediterráneo.** Existe relación entre la saturación del sustrato y su capacidad de absorción acústica, la cual depende en gran medida de la interacción entre el agua y las partículas del sustrato a microescala, y tiende a reducirse por la impedancia acústica del sustrato o la menor velocidad del sonido debido a la porosidad de este. Se demostró que un módulo totalmente saturado (8 l/m^2), posee un coeficiente de absorción acústica un 43% inferior al de un módulo con una saturación media (4 l/m^2).
- **Garantizar la orientación sur del sistema en clima mediterráneo.** Se ha demostrado que la orientación es un factor influyente en la magnitud de la reducción de temperaturas de los jardines verticales. En particular, la reducción de temperatura es notablemente mayor en la fachada orientada a sur en un clima mediterráneo, siendo de 0,63 ºC en verano y de 0,54 ºC en invierno con respecto a la temperatura del aire.

Estos resultados demuestran que la jardinería vertical tiene un impacto positivo en el confort en entornos urbanos densos. Además, frente a las grandes barreras regulatorias y financieras a las que se enfrentan este tipo de soluciones, esta tesis espera ser un aporte para el desarrollo de instrumentos de evaluación de los beneficios de las envolventes

vegetales que apoyen la toma de decisión y, por tanto, a mejorar el confort higrotérmico y acústico en contextos urbanos densos.

Futuras líneas de investigación

El desarrollo de esta tesis doctoral ha permitido identificar algunas áreas de interés sobre las que se podría profundizar en futuros trabajos de investigación. A continuación, se recogen las líneas propuestas siguiendo los aspectos contemplados en el desarrollo de esta tesis doctoral.

En primer lugar, se propone dar continuidad a la evaluación de la capacidad de reducción de temperaturas producida por un jardín vertical en entornos urbanos densos. Es necesario profundizar en variables como la velocidad del viento, su influencia en el rendimiento de la fachada y sobre otras variables, para caracterizar con mayor precisión el comportamiento de la vegetación y el sustrato. Durante la revisión bibliográfica de esta tesis doctoral, no se encontraron estudios que evaluaran la influencia de la velocidad del viento. Partir del análisis estadístico y la base de datos sistematizada para clima mediterráneo que se ha desarrollado en esta tesis doctoral, contribuiría a facilitar el desarrollo del trabajo de investigación.

Otra línea de interés está relacionada con el estudio de la absorción acústica de este tipo de soluciones en contextos urbanos densos, dado que el rendimiento acústico de la envolvente vegetal en el edificio es un campo en desarrollo. Esta tesis doctoral ha analizado el coeficiente de absorción acústica de un módulo de jardinería vertical con sustrato orgánico, sin embargo, son muchos los sistemas comercializados que responden a otras características y sobre los que convendría estudiar su rendimiento. Además, se

recomienda profundizar en aspectos como la influencia de la distancia de la fuente emisora de ruido, los niveles de saturación del sustrato, la compactación o composición del sustrato, los diferentes materiales utilizados como capa hidrófila (fieltros de distintas composiciones), e incluso los distintos sistemas de juntas y soportes del módulo.

Los resultados de esta tesis doctoral también pueden ser la base para estudios en otros campos de investigación. El confort urbano comprende una serie de factores entre los que se encuentra la calidad del aire, en la que la vegetación puede tener un impacto importante. En estudios anteriores se asocia la presencia de la vegetación en la ciudad con la reducción de partículas finas en suspensión ($PM_{2.5}$ y PM_{10}) y gases contaminantes (NO_X, CO_X, COV_X, O_3), lo que ocurre fundamentalmente debido a la captura y absorción de partículas en suspensión por parte de las hojas de las plantas, y la filtración mediante un proceso en el que las raíces y los microorganismos que habitan en el sustrato absorben los gases contaminantes.

Son escasos los estudios que profundizan en este ámbito, a la vez que, cada clima y tipo de sistema arrojará resultados distintos. En este tipo de estudios factores como la densidad de la especie, el tipo de clima, la macro y micro-morfología de las hojas, la porosidad, el índice de área foliar, entre otros, condicionan la capacidad de absorción y fijación de este tipo de soluciones, por lo que el campo de investigación es vasto y ofrece múltiples líneas de investigación.

Finalmente, cabe señalar que en la discusión se ha mencionado la importancia de medir en condiciones reales de ciudad. Aunque los estudios experimentales realizados en la tesis doctoral parten de datos en condiciones reales y no en prototipos, convendría analizar el

comportamiento de este tipo de soluciones en espacios con otras configuraciones urbanas: espacios congestionados de la ciudad donde se perciban altas temperaturas y haya una exposición a fuentes de ruido extremas (vías principales o autopistas), para evaluar si el comportamiento se replica o incluso incrementa.

ANEXO A: COLECCIÓN COMPLETA DE PUBLICACIONES Y OTROS TRABAJOS DE INVESTIGACIÓN

Artículos en revistas indexadas

Exploring the possibilities for deliberately cultivating more effective ecologies of intermediation
Miguel Soberón; Teresa Sánchez-Chaparro; Adrian Smith; Jaime Moreno-Serna; ***Valentina Oquendo-Di Cosola****; Carlos Mataix*
Enviromental Innovation and Societal Transitions
2022
DOI: 10.1016/j.eist.2022.06.003

Proyectos de investigación competitivos

Proyecto: Bluebloqs Circular Water System
Programa: Climate KIC Demonstrator
Entidad financiadora: Instituto Europeo de Innovación y Tecnología (EIT)
Duración: enero 2019 - enero 2021
IP: Francesca Olivieri
Grant agreement: EH1903020348

Proyecto: MUAC Modules for Urban Air Cleaning
Programa: Climate KIC Pathfinder
Entidad financiadora: Instituto Europeo de Innovación y Tecnología (EIT)
Duración: julio 2018 - diciembre 2018
IP: Francesca Olivieri
Grant agreement: EH1803020290

Proyecto: Lugo+Biodinámico: Planificación de un barrio multi-ecológico como modelo de resiliencia urbana
Programa: LIFE
Entidad financiadora: Comisión Europea
Duración: 2016 - 2020
IP: Luis Ruiz García
Grant agreement: E160017380

Proyecto: Powertree
Programa: Retos Colaboración 2017
Entidad financiadora: Ministerio de Ciencia, Innovación y Universidades
Duración: 2018 - 2020
IP: Lorenzo Olivieri
Grant agreement: RTC1803020133

Proyecto: Madrid Deep Demonstration Healthy and Clean Cities
Programa: Climate KIC Demonstrator
Entidad financiadora: Instituto Europeo de Innovación y Tecnología (EIT)
Duración: 2018 - 2021
IP: Carlos Mataix
Grant agreement: EH210017320

Proyecto: Accelerating cities' transition to net zero emissions by 2030 (NetZeroCities)
Programa: European Union's Horizon 2020
Entidad financiadora: Comisión Europea
Duración: 2021 – actualidad
IP: Julio Lumbreras
Grant agreement: 101036519

Reportes e informes para instituciones públicas

La Agenda 2030 en el diseño de proyectos estratégicos industriales
Raquel Fernández; Miguel Soberón; Simona Perfetti; Andrea Amaya Beltrán; Valentina Oquendo-Di Cosola; Lucía Vázquez; Irene Ezquerra.
Estrategia de Desarrollo Sostenible 2030
Ministerio de Derechos Sociales y Agenda 2030
2022
Disponible aquí:
https://www.mdsocialesa2030.gob.es/agenda2030/documentos/sintesisfinal.pdf

Accelerating Urban Climate Neutrality Through National Multi-Stakeholder Platforms: The Case of Spain
Valentina Oquendo-Di Cosola; Julio Lumbreras; Jaime Moreno-Serna.
"Next Generation EU" Cities. Local Communities in a post-pandemic future
ISPI – Istituto per gli Studi di Politica Internazionale
2021
DOI: 10.14672/55266123

Los retos de las ciudades ante la pandemia: El Día Después. Una incubadora de proyectos transformadores.
Valentina Oquendo-Di Cosola; Julio Lumbreras; Jaime Moreno-Serna.
Los objetivos de desarrollo sostenible en 100 ciudades españolas - ¿Cómo está avanzando la Agenda 2030 a nivel local? Una mirada práctica.
REDS – Red Española para el Desarrollo Sostenible
2020
ISBN: 978-84-09-25763-8

Comunicaciones en congresos

Accelerating urban climate neutrality through national multistakeholder platforms: the case of Spain
Internacional (Valencia)
Julio Lumbreras; Valentina Oquendo-Di Cosola; Carolyn Daher; Jordi Peris-Blanes
18th International Conference of Urban Health. October 2022.
Enviado

High tenacity thermoformable recycled rubber material: recycling as added value in construction
Internacional (A Coruña)
Jorge Adán Sánchez-Reséndiz; Valentina Oquendo-Di Cosola; Francesca Olivieri; Lorenzo Olivieri.
Planning Post Carbon Cities: 35th PLEA Conference on Passive and Low Energy Architecture, A Coruña, 1st-3rd September 2020: Proceedings
ISBN: 978-84-9749-794-7

Retrofitting actions to convert a building into net zero energy: the case study of the itdUPM headquarters
Internacional (A Coruña)
Lorenzo Olivieri; Carmen Fuertes-Arguello; Valentina Oquendo-Di Cosola; Francesca Olivieri; Jorge Adán Sánchez-Reséndiz.
Planning Post Carbon Cities: 35th PLEA Conference on Passive and Low Energy Architecture, A Coruña, 1st-3rd September 2020: Proceedings
ISBN: 978-84-9749-794-7

Incubando políticas públicas locales desde una perspectiva multiactor: la Comunidad de Ciudades de "El Día Después"
Nacional (Madrid)
Jaime Moreno-Serna; Julio Lumbreras; Teresa Sánchez-Chaparro; Leda Stott; Fernando Fernández-Monge; Miguel Soberón; Cristina Monge; Valentina Oquendo-Di Cosola
III Congreso Internacional del Instituto Complutense de Ciencia de la Administración sobre Gobierno y Políticas Públicas en el marco de los Objetivos de Desarrollo Sostenible. 2019.

Supporting Innovations to Incorporate the SDGs at Universities through MOOCs
Internacional (Madrid)
Miguel Soberón; Teresa Sánchez-Chaparro; Valentina Oquendo-Di Cosola; Francesca Olivieri; Irene Ezquerra.
14th International Conference on Industrial Engineering and Industrial Management.
ISBN: 978-3-030-95966-1

Nature Based Solutions for Cities Resilience: opportunities for action in Madrid
Internacional (Soria)
Valentina Oquendo-Di Cosola; Jorge Adán Sánchez-Reséndiz; Lorenzo Olivieri; Francesca Olivieri.
Smart Cities Soria. Second Ibero-American Congress, ICSC-CITIES 2019
ISBN: 978-3-030-38888-1

Patentes solicitadas

Sistema de cultivo modular para agricultura urbana
Luis Ruiz García, Valentina Oquendo-Di Cosola
Universidad Politécnica de Madrid
Nacional

Otras publicaciones no indexadas

University-City Partnerships: reinforcing convening capacities to accelerate sustainable urban transformations
Julio Lumbreras; Jaime Moreno-Serna; Guillermo Palau; Jordi Peris; Valentina Oquendo-Di Cosola; Teresa Sánchez-Chaparro; Carlos Mataix.
The Bloomsbury Handbook of Sustainability in Higher Education: An Agenda for Transformational Change. Bloomsbury Institute.
ISBN: 9781350244344
2023

El verde de las ciudades: salud para las personas y el planeta
Julio Lumbreras; Valentina Oquendo-Di Cosola
Equipamientos y servicios municipales n.39
ISSN: 1131-6381
2023

Misión Europea de Ciudades hacia la neutralidad climática: una oportunidad para la transición energética en España
Julio Lumbreras; Valentina Oquendo-Di Cosola; Nayla Saniour; Jaime Moreno-Serna; Martín Sanz; Tomás Conde; Luis López-Cózar.
Papeles de Economía Española
ISSN: 0210-9107
2022

Nuestra misión para 2030: ciudades más saludables, sostenibles y prósperas
Julio Lumbreras; Valentina Oquendo-Di Cosola
Equipamientos y servicios municipales n.38
ISSN: 1131-6381
2021

Si decimos que son el futuro ¿por qué no compramos más coches eléctricos?
Jorge Adán Sánchez-Reséndiz; Francesca Olivieri; Lorenzo Olivieri; Valentina Oquendo-Di Cosola.
The Conversation
Enlace
2020

La UPM quiere ser un espacio neutro en carbono para 2040
Irene Ezquerra; Miguel Soberón; Simona Perfetti; Valentina Oquendo-Di Cosola
Revista Ciudad Sostenible n.38
2019

Living Wall Systems: technological and environmental optimization strategies
Valentina Oquendo-Di Cosola; Francesca Olivieri.
Editorial Agrícola Española
Multifunctional Green Urban Infrastructures
ISBN: 9788417884000
2019

Proyecto LIFE Lugo+Biodinamico: Asi se diseña un barrio multi-ecológico como modelo de resiliencia urbana.
Candela de la Sota; Valentina Oquendo-Di Cosola; Luis Ruiz-García.
Revista Ciudad Sostenible n.34
2018

Invernaderos en azoteas: una alternativa de futuro para la producción de alimentos
Valentina Oquendo-Di Cosola; Lucía Muñóz Martí; Luis Ruiz-García.
Editorial Agrícola Española
Agricultura Urbana en Altura
ISBN: 9788492928828
2017

BIBLIOGRAFÍA

En este apartado se incluye únicamente la bibliografía utilizada para la elaboración de la memoria de esta tesis doctoral, queda excluida la bibliografía de los artículos pertenecientes al compendio.

(ISO), I.O. for S., n.d. Environmental Management e Life Cycle Assessment e Requirements and Guidelines. ISO 14044.

(ISO), I.O. for S., n.d. Environmental Management e Life Cycle Assessment e Principles and Framework. ISO 14040.

Abdo, P., Huynh, B.P., 2021. An experimental investigation of green wall bio-filter towards air temperature and humidity variation. J. Build. Eng. 39. https://doi.org/10.1016/j.jobe.2021.102244

Abhijith, K. V., Kumar, P., Gallagher, J., McNabola, A., Baldauf, R., Pilla, F., Broderick, B., Di Sabatino, S., Pulvirenti, B., 2017. Air pollution abatement performances of green infrastructure in open road and built-up street canyon environments – A review. Atmos. Environ. 162, 71–86. https://doi.org/10.1016/j.atmosenv.2017.05.014

Afshari, A., 2017. A new model of urban cooling demand and heat island—application to vertical greenery systems (VGS). Energy Build. 157, 204–217. https://doi.org/10.1016/j.enbuild.2017.01.008

Alcázar, S., 2015. Efectos de las cubiertas ajardinadas sobre el microclima urbano en verano. (Tesis Dr. Univ. Politécnica Madrid).

Aletta, F., Kang, J., Astolfi, A., Fuda, S., 2016. Differences in soundscape appreciation of walking sounds from different footpath materials in urban parks. Sustain. Cities Soc. 27, 367–376. https://doi.org/10.1016/j.scs.2016.03.002

Altan, H., John, N., Yoshimi, J., Ilyas, T., Galadari, M., n.d. Comparative life cycle analysis of green wall systems in the uk.

Amani-Beni, M., Chen, Y., Vasileva, M., Zhang, B., Xie, G. di, 2022. Quantitative-spatial relationships between air and surface temperature, a proxy for microclimate studies in fine-scale intra-urban areas? Sustain. Cities Soc. 77, 103584. https://doi.org/10.1016/j.scs.2021.103584

Andric, I., Kamal, A., Al-Ghamdi, S.G., 2020. Efficiency of green roofs and green walls as climate change mitigation measures in extremely hot and dry climate: Case study of Qatar. Energy Reports 6, 2476–2489. https://doi.org/10.1016/j.egyr.2020.09.006

Asdrubali, F., D'Alessandro, F., Mencarelli, N., Horoshenkov, K. V., 2014. Sound absorption properties of tropical plants for indoor applications. 21st Int. Congr. Sound Vib. 2014, ICSV 2014 4, 3249–3256.

Asif, M., Muneer, T., Kelley, R., 2007. Life cycle assessment: A case study of a dwelling home in Scotland. Build. Environ. 42, 1391–1394. https://doi.org/https://doi.org/10.1016/j.buildenv.2005.11.023

ASPB, 2020. Soroll ambiental i salut a la ciutat de Barcelona 2021.

Atlanta: American Society of Heating, Refrigerating, and Air-conditioning Engineers. Inc., U., 2004. Standard 55-2004, thermal environmental conditions for human occupancy,.

Atmaca, I., Kaynakli, O., Yigit, A., 2007. Effects of radiant temperature on thermal comfort. Build. Environ. 42, 3210–3220. https://doi.org/10.1016/j.buildenv.2006.08.009

Attal, E., Côté, N., Haw, G., Pot, G., Vasseur, C., Shimizu, T., Granger, C., Croënne, C., Dubus, B., 2016. Experimental characterization of foliage and substrate

samples by the three-microphone two-load method. Inter-Noise 2016 6602–6609.

Attal, E., de l'Epine, Y.B., Dauchez, N., Dubus, B., 2021a. Experimental investigation of the effect of moisture on the acoustic properties of lightweight substrates used in green envelopes. Appl. Acoust. 180, 108108. https://doi.org/10.1016/j.apacoust.2021.108108

Attal, E., Dubus, B., Leblois, T., Cretin, B., 2021b. An optimal dimensioning method of a green wall structure for noise pollution reduction. Build. Environ. 187. https://doi.org/10.1016/j.buildenv.2020.107362

Australian Bureau of Statistics, A.G., 2011. Environmental Issues: Energy use and Conservation. https://doi.org/4602.0.55.001

Azkorra, Z., Pérez, G., Coma, J., Cabeza, L.F., Bures, S., Álvaro, J.E., Erkoreka, A., Urrestarazu, M., 2015a. Evaluation of green walls as a passive acoustic insulation system for buildings. Appl. Acoust. 89, 46–56. https://doi.org/10.1016/j.apacoust.2014.09.010

Bartesaghi Koc, C., Osmond, P., Peters, A., 2018. Evaluating the cooling effects of green infrastructure: A systematic review of methods, indicators and data sources. Sol. Energy 166, 486–508. https://doi.org/10.1016/j.solener.2018.03.008

Besir, A.B., Cuce, E., 2018. Green roofs and facades: A comprehensive review. Renew. Sustain. Energy Rev. 82, 915–939. https://doi.org/10.1016/j.rser.2017.09.106

Bianco, L., Serra, V., Larcher, F., Perino, M., 2017. Thermal behaviour assessment of a novel vertical greenery module system: first results of a long-term monitoring campaign in an outdoor test cell. Energy Effic. 10, 625–638. https://doi.org/10.1007/s12053-016-9473-4

Bit, E., 2010. La vegetazione per le chiusure verticali. Università degli Studi di Ferrara.

Boeri, A., Gaspari, J., Gianfrate, V., Longo, D., 2017. Accelerating Urban transition: An

approach to greening the built environment. WIT Trans. Ecol. Environ. 223, 3–14. https://doi.org/10.2495/SC170011

Brambilla, G., Gallo, V., Asdrubali, F., D'Alessandro, F., 2013. The perceived quality of soundscape in three urban parks in Rome. J. Acoust. Soc. Am. 134, 832–839. https://doi.org/10.1121/1.4807811

Broun, R., Menzies, G.F., 2011. Life cycle energy and environmental analysis of partition wall systems in the UK. Procedia Eng. 21, 864–873. https://doi.org/10.1016/j.proeng.2011.11.2088

Brown, A.L., Kang, J., Gjestland, T., 2011. Towards standardization in soundscape preference assessment. Appl. Acoust. 72, 387–392. https://doi.org/10.1016/j.apacoust.2011.01.001

Bullen, R., Fricke, F., 1982. Sound propagation through vegetation. J. Sound Vib. 80, 11–23. https://doi.org/10.1016/0022-460X(82)90387-X

Cameron, R.W.F., Taylor, J., Emmett, M., 2015. A Hedera green façade - Energy performance and saving under different maritime-temperate, winter weather conditions. Build. Environ. 92, 111–121. https://doi.org/10.1016/j.buildenv.2015.04.011

Cameron, R.W.F., Taylor, J.E., Emmett, M.R., 2014. What's "cool" in the world of green façades? How plant choice influences the cooling properties of green walls. Build. Environ. 73, 198–207. https://doi.org/10.1016/j.buildenv.2013.12.005

Castaldo, V.L., Pisello, A.L., Piselli, C., Fabiani, C., Cotana, F., Santamouris, M., 2018. How outdoor microclimate mitigation affects building thermal-energy performance: A new design-stage method for energy saving in residential near-zero energy settlements in Italy. Renew. Energy 127, 920–935. https://doi.org/10.1016/j.renene.2018.04.090

Castiglia Feitosa, R., Wilkinson, S.J., 2020. Small-scale experiments of seasonal heat stress attenuation through a combination of green roof and green walls. J. Clean. Prod. 250. https://doi.org/10.1016/j.jclepro.2019.119443

Castiglia Feitosa, R., Wilkinson, S.J., 2018. Attenuating heat stress through green roof and green wall retrofit. Build. Environ. 140, 11–22. https://doi.org/10.1016/j.buildenv.2018.05.034

César Díaz Sanchidrían, 2002. Apuntes de acústica en la edificación y el urbanismo (II). Madrid.

Chan, S.Y., Chau, C.K., Leung, T.M., 2017. On the study of thermal comfort and perceptions of environmental features in urban parks: A structural equation modeling approach. Build. Environ. 122, 171–183. https://doi.org/10.1016/j.buildenv.2017.06.014

Charoenkit, S., Yiemwattana, S., 2017. Role of specific plant characteristics on thermal and carbon sequestration properties of living walls in tropical climate. Build. Environ. 115, 67–79. https://doi.org/10.1016/j.buildenv.2017.01.017

Charoenkit, S., Yiemwattana, S., 2016a. Living walls and their contribution to improved thermal comfort and carbon emission reduction: A review. Build. Environ. 105, 82–94. https://doi.org/10.1016/j.buildenv.2016.05.031

Charoenkit, S., Yiemwattana, S., Rachapradit, N., 2020. Plant characteristics and the potential for living walls to reduce temperatures and sequester carbon. Energy Build. 225, 110286. https://doi.org/10.1016/j.enbuild.2020.110286

Chen, Q., Li, B., Liu, X., 2013. An experimental evaluation of the living wall system in hot and humid climate. Energy Build. 61, 298–307. https://doi.org/10.1016/j.enbuild.2013.02.030

Chen, Y., Shu, B., Zhang, R., Amani-Beni, M., 2023. LST determination of different

urban growth patterns: A modeling procedure to identify the dominant spatial metrics. Sustain. Cities Soc. 92, 104459. https://doi.org/10.1016/j.scs.2023.104459

Cheng, C.Y., Cheung, K.K.S.S., Chu, L.M., 2010. Thermal performance of a vegetated cladding system on facade walls. Build. Environ. 45, 1779–1787. https://doi.org/10.1016/j.buildenv.2010.02.005

Cherunova, I. V., Kuleshova, A.A., Kokuashvili, N.B., 2020. The study of urban factors in the human comfort system. IOP Conf. Ser. Mater. Sci. Eng. 962, 1–8. https://doi.org/10.1088/1757-899X/962/3/032086

Cheung, P.K., Jim, C.Y., 2018. Subjective outdoor thermal comfort and urban green space usage in humid-subtropical Hong Kong. Energy Build. 173, 150–162. https://doi.org/10.1016/j.enbuild.2018.05.029

Choi, W., Ranasinghe, D., Bunavage, K., DeShazo, J.R., Wu, L., Seguel, R., Winer, A.M., Paulson, S.E., 2016. The effects of the built environment, traffic patterns, and micrometeorology on street level ultrafine particle concentrations at a block scale: Results from multiple urban sites. Sci. Total Environ. 553, 474–485. https://doi.org/10.1016/j.scitotenv.2016.02.083

Chun, B., Guldmann, J.M.J.-M., 2018. Impact of greening on the urban heat island: Seasonal variations and mitigation strategies. Comput. Environ. Urban Syst. 71, 165–176. https://doi.org/10.1016/j.compenvurbsys.2018.05.006

Coma, J., Pérez, G., Solé, C., Castell, A., Cabeza, L.F., 2014. New green facades as passive systems for energy savings on Buildings. Energy Procedia 57, 1851–1859. https://doi.org/10.1016/j.egypro.2014.10.049

Comesaña, D.F., Steltenpool, S., Carrillo Pousa, G., de Bree, H.-E., Holland, K.R., 2013. Scan and Paint: Theory and Practice of a Sound Field Visualization Method. ISRN Mech. Eng. 2013, 241958. https://doi.org/10.1155/2013/241958

Costa-Carrapiço, I., González, J.N., Raslan, R., Sánchez-Guevara, C., Redondas Marrero, M.D., 2022. Understanding thermal comfort in vernacular dwellings in Alentejo, Portugal: A mixed-methods adaptive comfort approach. Build. Environ. 217. https://doi.org/10.1016/j.buildenv.2022.109084

D'Alessandro, F., Asdrubali, F., Mencarelli, N., 2015. Experimental evaluation and modelling of the sound absorption properties of plants for indoor acoustic applications. Build. Environ. 94, 913–923. https://doi.org/10.1016/j.buildenv.2015.06.004

Daemei, A.B., Azmoodeh, M., Zamani, Z., Khotbehsara, E.M., 2018. Experimental and simulation studies on the thermal behavior of vertical greenery system for temperature mitigation in urban spaces. J. Build. Eng. 20, 277–284. https://doi.org/10.1016/j.jobe.2018.07.024

Daemei, A.B., Eghbali, S.R., Khotbehsara, E.M., 2019. Bioclimatic design strategies: A guideline to enhance human thermal comfort in Cfa climate zones. J. Build. Eng. 25, 100758. https://doi.org/10.1016/j.jobe.2019.100758

Dagmar Schröter, et al., 2005. Ecosystem Service Supply and Vulnerability to Global Change in Europe. https://doi.org/10.1126/science.1115233

Davis, M.J.M., Tenpierik, M.J., Ramírez, F.R., Pérez, M.E., 2017. More than just a Green Facade: The sound absorption properties of a vertical garden with and without plants. Build. Environ. 116, 64–72. https://doi.org/10.1016/j.buildenv.2017.01.010

de Bree, H.-E., Tijs, E., Basten, T., 2007. An Ultra Miniature Measurement Tool to Measure the Reflection Coefficient of Acoustic Damping Materials in Situ, in: SAE 2007 Noise and Vibration Conference and Exhibition. SAE International. https://doi.org/https://doi.org/10.4271/2007-01-2212

de Jesus, M.P., Lourenço, J.M., Arce, R.M., Macias, M., 2017. Green façades and in situ measurements of outdoor building thermal behaviour. Build. Environ. 119, 11–19. https://doi.org/10.1016/j.buildenv.2017.03.041

de Munck, C., Lemonsu, A., Masson, V., Le Bras, J., Bonhomme, M., 2018. Evaluating the impacts of greening scenarios on thermal comfort and energy and water consumptions for adapting Paris city to climate change. Urban Clim. 23, 260–286. https://doi.org/10.1016/j.uclim.2017.01.003

Dede, O.H., Mercan, N., Ozer, H., Dede, G., Pekarchuk, O., Mercan, B., 2021. Thermal insulation characteristics of green wall systems using different growing media. Energy Build. 240, 110872. https://doi.org/10.1016/j.enbuild.2021.110872

Ding, L., Van Renterghem, T., Botteldooren, D., Horoshenkov, K., Khan, A., 2013. Sound absorption of porous substrates covered by foliage: Experimental results and numerical predictions. J. Acoust. Soc. Am. 134, 4599–4609. https://doi.org/10.1121/1.4824830

Dixit, M.K., Fernández-Solís, J.L., Lavy, S., Culp, C.H., 2012. Need for an embodied energy measurement protocol for buildings: A review paper. Renew. Sustain. Energy Rev. 16, 3730–3743. https://doi.org/https://doi.org/10.1016/j.rser.2012.03.021

Djedjig, R., Belarbi, R., Bozonnet, E., 2017. Green wall impacts inside and outside buildings: Experimental study. Energy Procedia 139, 578–583. https://doi.org/10.1016/j.egypro.2017.11.256

Dunnett, N., Kingsbury, N., 2008. Planting Green Roofs and Living Walls. Portland, Or.

E. Tijs, H. E. de Bree, S.S., 2010. Scan and Paint: a novel sound visualization technique, in: Proc. 39th Int. Congr. Noise Control Eng. 2010 (Inter-Noise 2010:

Noise and Sustainability). Lisbon, Portugal. https://doi.org/9781617823961

E. Tijs, 2013. Study and development of an in situ acoustic absorption measurement method. University of Twente.

E. Tijs, H.E. de B., 2008. Recent developments free field PU impedance technique, in: SAPEM 2008, Symp. Acoust. Poro-Elastic Mater. Bradford,, UK.

Erell, E., Pearlmutter, D., Williamson, T., 2012. Urban Microclimate: Designing the Spaces between Buildings. Earthscan, London.

European Commission, 2022. The Vital Role of Nature-Based Solutions in a Nature Positive Economy. https://doi.org/10.2777/307761

European Commission, 2021a. European Mission - 100 Climate neutral and smart cities by 2030.

European Commission, 2021b. SOLUTIONS A Handbook for Practitioners. https://doi.org/10.2777/2498

European Commission, 2014. Horizon 2020 [WWW Document]. URL https://ec.europa.eu/programmes/horizon2020/en

European Commission, 2011. International Reference Life Cycle Data System (ILCD) Handbook - General guide for Life Cycle Assessment - Provisions and Action Steps. https://doi.org/http://dx.doi.org/10.2788/94987

European Commission, Union, P.O. of the E., 2015. Nature-based solutions & re-naturing cities. Final report of the horizon 2020 expert group on 'Nature-based solutions and re-naturing cities' (full version). https://doi.org/10.2777/765301

Europeo, P., 2002. Directiva 2002/49/CE del Parlamento Europeo y del Consejo, de 25 de junio de 2002, sobre evaluación y gestión del ruido ambiental - Declaración de la Comisión ante el Comité de Conciliación de la Directiva sobre evaluación y gestión del ruido ambiental.

Fabbri, K., Ugolini, A., Iacovella, A., Bianchi, A.P., 2020. The effect of vegetation in outdoor thermal comfort in archaeological area in urban context. Build. Environ. 175, 106816. https://doi.org/10.1016/j.buildenv.2020.106816

Fahed, J., Kinab, E., Ginestet, S., Adolphe, L., 2020. Impact of urban heat island mitigation measures on microclimate and pedestrian comfort in a dense urban district of Lebanon. Sustain. Cities Soc. 61. https://doi.org/10.1016/j.scs.2020.102375

Fan, Q., Du, F., Li, H., Zhang, C., 2021. Thermal-comfort evaluation of and plan for public space of Maling Village, Henan, China, PLoS ONE. https://doi.org/10.1371/journal.pone.0256439

Fava, J.A.; Consoli, F.; Dension, R.; Dickson, K.; Mohin, T.; Vigon, B., 1993. A Conceptual Framework for Life-Cycle Impact Assessment. Soc. Environ. Toxicol. Chem. SETAC.

Fava, J.A., 2006. Will the next 10 years be as productive in advancing life cycle approaches as the last 15 years? Int. J. Life Cycle. Assess 11, 6–8.

Fernández-Bregón, N., Urrestarazu, M., Valera, D.L., Fernandez-Bregon, N., Urrestarazu, M., Valera, D.L., Fernández-Bregón, N., Urrestarazu, M., Valera, D.L., 2012. Effects of a vertical greenery system on selected thermal and sound mitigation parameters for indoor building walls. J. Food, Agric. Environ. 10, 1025–1027. https://doi.org/1025-1027. 2012

Fernandez Comesaña, D., Holland, K.R., Fernandez-Grande, E., 2016. Spatial resolution limits for the localization of noise sources using direct sound mapping. J. Sound Vib. 375, 53–62. https://doi.org/https://doi.org/10.1016/j.jsv.2016.04.010

Francis, R.A., Lorimer, J., 2011. Urban reconciliation ecology: The potential of living roofs and walls. J. Environ. Manage. 92, 1429–1437.

https://doi.org/10.1016/j.jenvman.2011.01.012

Francisco Javier Neila González, César Bedoya Frutos, 1997. Técnicas arquitectónicas y constructivas de acondicionamiento ambiental.

Frantzeskaki, N., 2019. Seven lessons for planning nature-based solutions in cities. Environ. Sci. Policy 93, 101–111. https://doi.org/10.1016/j.envsci.2018.12.033

Gago, E.J., Roldan, J., Pacheco-Torres, R., Ordóñez, J., 2013. The city and urban heat islands: A review of strategies to mitigate adverse effects. Renew. Sustain. Energy Rev. 25, 749–758. https://doi.org/10.1016/j.rser.2013.05.057

Galagoda, R.U., Jayasinghe, G.Y., Halwatura, R.U., Rupasinghe, H.T., 2018. The impact of urban green infrastructure as a sustainable approach towards tropical micro-climatic changes and human thermal comfort. Urban For. Urban Green. 34, 1–9. https://doi.org/https://doi.org/10.1016/j.ufug.2018.05.008

GBCe, 2023. Building Life: Cuenta Atras Sector Vivienda.

GBCe, 2021. Informe País GBCe 2021. Sobre el estado de la edificación sostenible en España.

Giordano, R., Montacchini, E., Tedesco, S., 2013. L ' approccio al ciclo di vita nella progettazione , produzione e monitoraggio di una facciata verde 184–190.

Giordano, R., Montacchini, E., Tedesco, S., Perone, A., 2017. Living Wall Systems: A Technical Standard Proposal. Energy Procedia 111, 298–307. https://doi.org/10.1016/j.egypro.2017.03.093

Gourdji, S., 2018. Review of plants to mitigate particulate matter, ozone as well as nitrogen dioxide air pollutants and applicable recommendations for green roofs in Montreal, Quebec. Environ. Pollut. 241, 378–387. https://doi.org/10.1016/j.envpol.2018.05.053

Guan, H., Hu, S., Liu, G., Zhang, L., 2020. The combined effects of temperature and

noise on the comfort perceptions of young people with a normal Body Mass Index. Sustain. Cities Soc. 54, 101993. https://doi.org/10.1016/j.scs.2019.101993

H. E. de Bree, E. Tijs, T.G.H.B., 2006. Two complementary Microflown based methods to determine the reflection coefficient in situ., in: ISMA Int. Conf. Noise Vib. Eng., Heverlee. Belgium.

H. E. de Bree, M. Nosko, E. Tijs, 2008. A handheld device to measure the acoustic absorption in situ, in: Proc. SNVH 2008, 5th Int. Styrian Noise Vib. Harshness Conf. Graz, Austria.

Habitat III Secretariat, United Nations, 2017. The New Urban Agenda, United Nations Publications.

Harris, R.A., Cohn, L.F., 1985. Use of vegetation for abatement of highway traffic noise. J. Urban Plan. Dev. 111, 34–48. https://doi.org/10.1061/(ASCE)0733-9488(1985)111:1(34)

Herath, H.M.P.I.K.M.P.I.K., Halwatura, R.U., Jayasinghe, G.Y., 2018. Evaluation of green infrastructure effects on tropical Sri Lankan urban context as an urban heat island adaptation strategy. Urban For. Urban Green. 29, 212–222. https://doi.org/10.1016/j.ufug.2017.11.013

Héroux, M.E., Babisch, W., Belojevic, G., Brink, M., Janssen, S., Lercher, P., Paviotti, M., Pershagen, G., Waye, K.P., Preis, A., Stansfeld, S., van den Berg, M., Verbeek, J., 2020. WHO environmental noise guidelines for the European Region. Euronoise 2015 2589–2593.

Hoelscher, M.-T., Nehls, T., Jänicke, B., Wessolek, G., 2016. Quantifying cooling effects of facade greening: Shading, transpiration and insulation. Energy Build. 114, 283–290. https://doi.org/https://doi.org/10.1016/j.enbuild.2015.06.047

Hooftman, N., Messagie, M., Van Mierlo, J., Coosemans, T., 2018. A review of the

European passenger car regulations – Real driving emissions vs local air quality. Renew. Sustain. Energy Rev. 86, 1–21. https://doi.org/10.1016/j.rser.2018.01.012

Hornikx, M., Van Renterghem, T., 2012. The potential of vegetation for reducing road traffic noise at urban quiet sides, in: Proceedings - European Conference on Noise Control. pp. 949–954.

Horoshenkov, K.V.. B.H.K.A., Khan, A., Benkreira, H., 2013. Acoustic properties of low growing plants. J. Acoust. Soc. Am. 133, 2554–2565. https://doi.org/10.1121/1.4798671

Horrison, E., Amirtham, L.R., 2016. Role of built environment on factors affecting outdoor thermal comfort - A case of T. Nagar, Chennai, India. Indian J. Sci. Technol. 9, 3–6. https://doi.org/10.17485/ijst/2016/v9i5/87253

Hunter, A.M., Williams, N.S.G., Rayner, J.P., Aye, L., Hes, D., Livesley, S.J., 2014. Quantifying the thermal performance of green façades: A critical review. Ecol. Eng. 63, 102–113. https://doi.org/10.1016/j.ecoleng.2013.12.021

Imran, H.M., Kala, J., Ng, A.W.M., Muthukumaran, S., 2019. Effectiveness of vegetated patches as Green Infrastructure in mitigating Urban Heat Island effects during a heatwave event in the city of Melbourne. Weather Clim. Extrem. 25. https://doi.org/10.1016/j.wace.2019.100217

Ingrao, C., Matarazzo, A., Tricase, C., Clasadonte, M.T., Huisingh, D., 2015. Life Cycle Assessment for highlighting environmental hotspots in Sicilian peach production systems. J. Clean. Prod. 92, 109–120. https://doi.org/https://doi.org/10.1016/j.jclepro.2014.12.053

Ingrao, C., Scrucca, F., Tricase, C., Asdrubali, F., 2016. A comparative Life Cycle Assessment of external wall-compositions for cleaner construction solutions in buildings. J. Clean. Prod. 124, 283–298.

https://doi.org/10.1016/j.jclepro.2016.02.112

International Energy Agency (IEA), 2018. “The Future of Cooling Opportunities for energy- efficient air conditioning”International Energy Agency Website: www.iea.org, 2018.

Iommi, M., 2018. The mediterranean smart adaptive wall. An experimental design of a smart and adaptive facade module for the mediterranean climate. Energy Build. 158, 1450–1460. https://doi.org/https://doi.org/10.1016/j.enbuild.2017.11.025

Irga, P.J., Paull, N.J., Abdo, P., Torpy, F.R., 2017. An assessment of the atmospheric particle removal efficiency of an in-room botanical biofilter system. Build. Environ. 115, 281–290. https://doi.org/10.1016/j.buildenv.2017.01.035

Ismail, M.R., 2013. Quiet environment: Acoustics of vertical green wall systems of the Islamic urban form. Front. Archit. Res. 2, 162–177. https://doi.org/10.1016/j.foar.2013.02.002

Izrael, Y.A., Semenov, S.M., Anisimov, O.A., Anokhin, Y.A., Velichko, A.A., Revich, B.A., Shiklomanov, I.A., 2007. The Fourth Assessment Report of the Intergovernmental Panel on Climate Change: Working Group II contribution, Russian Meteorology and Hydrology. https://doi.org/10.3103/S1068373907090014

Jamei, E., Rajagopalan, P., Seyedmahmoudian, M., Jamei, Y., 2016. Review on the impact of urban geometry and pedestrian level greening on outdoor thermal comfort. Renew. Sustain. Energy Rev. 54, 1002–1017. https://doi.org/10.1016/j.rser.2015.10.104

Javadi, R., 2021. Urban green space and health: The role of thermal comfort on the health benefits from the urban green space; a review study. Build. Environ. 202, 108039. https://doi.org/10.1016/j.buildenv.2021.108039

Jennings, P., Cain, R., 2013. A framework for improving urban soundscapes. Appl.

Acoust. 74, 293–299. https://doi.org/10.1016/j.apacoust.2011.12.003

Jeswani, H.K., Azapagic, A., Schepelmann, P., Ritthoff, M., 2010. Options for broadening and deepening the LCA approaches. J. Clean. Prod. 18, 120–127. https://doi.org/https://doi.org/10.1016/j.jclepro.2009.09.023

Jim, C.Y., 2015a. Cold-season solar input and ambivalent thermal behavior brought by climber greenwalls. Energy 90, 926–938. https://doi.org/10.1016/j.energy.2015.07.127

Jim, C.Y., 2015b. Thermal performance of climber greenwalls: Effects of solar irradiance and orientation. Appl. Energy 154, 631–643. https://doi.org/https://doi.org/10.1016/j.apenergy.2015.05.077

Jim, C.Y., He, H., 2011. Estimating heat flux transmission of vertical greenery ecosystem. Ecol. Eng. 37, 1112–1122. https://doi.org/10.1016/j.ecoleng.2011.02.005

Kabisch, N., Frantzeskaki, N., Pauleit, S., Naumann, S., Davis, M., Artmann, M., Haase, D., Knapp, S., Korn, H., Stadler, J., Zaunberger, K., Bonn, A., 2016. Nature-based solutions to climate change mitigation and adaptation in urban areas : Perspectives on indicators , knowledge ... urban areas : perspectives on indicators , knowledge gaps , barriers , and. Ecol. Soc. 21. https://doi.org/10.5751/ES-08373-210239

Kandelan, S.N., Yeganeh, M., Peyman, S., Panchabikesan, K., Eicker, U., 2022. Environmental study on greenery planning scenarios to improve the air quality in urban canyons. Sustain. Cities Soc. 83, 103993. https://doi.org/10.1016/j.scs.2022.103993

Karakounos, I., Dimoudi, A., Zoras, S., 2018. The influence of bioclimatic urban redevelopment on outdoor thermal comfort. Energy Build. 158, 1266–1274.

https://doi.org/10.1016/j.enbuild.2017.11.035

Khasreen, M.M., Banfill, P.F.G., Menzies, G.F., 2009. Life-cycle assessment and the environmental impact of buildings: A review. Sustainability 1, 674–701. https://doi.org/10.3390/su1030674

Kinsler L. E., Frey A. F., A.B.C. and J.V.S., n.d. Fundamentals of acoustics. John Wiley Sons Inc. New York, United States América. 4º Edición.

Kiss, G., 2012. 19 - Solar energy in the built environment: powering the sustainable city, in: Zeman, F.B.T.-M.S. (Ed.), Woodhead Publishing Series in Energy. Woodhead Publishing, pp. 431–456. https://doi.org/https://doi.org/10.1533/9780857096463.3.431

Klemm, W., Heusinkveld, B.G., Lenzholzer, S., van Hove, B., 2015. Street greenery and its physical and psychological impact on thermal comfort. Landsc. Urban Plan. 138, 87–98. https://doi.org/10.1016/j.landurbplan.2015.02.009

Klingberg, J., Broberg, M., Strandberg, B., Thorsson, P., Pleijel, H., 2017. Influence of urban vegetation on air pollution and noise exposure – A case study in Gothenburg, Sweden. Sci. Total Environ. 599–600, 1728–1739. https://doi.org/10.1016/j.scitotenv.2017.05.051

Kmieć, M., 2014. Green wall technology.

Koch, K., Ysebaert, T., Denys, S., Samson, R., 2020. Urban heat stress mitigation potential of green walls: A review. Urban For. Urban Green. 55, 126843. https://doi.org/10.1016/j.ufug.2020.126843

Köhler, M., 2008. Green facades—A view back and some visions, Urban Ecosystems. https://doi.org/10.1007/s11252-008-0063-x

Kokogiannakis, G., Darkwa, J., Badeka, S., Li, Y., 2019. Experimental comparison of green facades with outdoor test cells during a hot humid season. Energy Build.

185, 196–209. https://doi.org/10.1016/j.enbuild.2018.12.038

Kontoleon, K.J., Eumorfopoulou, E.A., 2010. The effect of the orientation and proportion of a plant-covered wall layer on the thermal performance of a building zone. Build. Environ. 45, 1287–1303. https://doi.org/https://doi.org/10.1016/j.buildenv.2009.11.013

Kosareo, L., Ries, R., 2007. Comparative environmental life cycle assessment of green roofs. Build. Environ. 42, 2606–2613. https://doi.org/10.1016/j.buildenv.2006.06.019

Kottek, M., Grieser, J., Beck, C., Rudolf, B., Rubel, F., 2006. World Map of the Köppen-Geiger climate classification updated. Meteorol. Zeitschrift 15, 259–263. https://doi.org/10.1127/0941-2948/2006/0130

Koyama, T., Yoshinaga, M., Hayashi, H., Maeda, K. ichiro, Yamauchi, A., 2013. Identification of key plant traits contributing to the cooling effects ofgreen façades using freestanding walls. Build. Environ. 66, 96–103. https://doi.org/10.1016/j.buildenv.2013.04.020

Krusche, P., Krusche, M., Althaus, D., Gabriel, I., 1982. Ökologisches Bauen Umweltbundesamt. Vieweg Friedr. + Sohn Ver, Deutschland.

Lacasta, A.M., Peñaranda, A., Cantalapiedra, I.R., 2018. Green streets for noise reduction. Nat. Based Strateg. Urban Build. Sustain. 181–190. https://doi.org/10.1016/B978-0-12-812150-4.00017-3

Lacasta, A.M., Penaranda, A., Cantalapiedra, I.R., Auguet, C., Bures, S., Urrestarazu, M., 2016. Acoustic evaluation of modular greenery noise barriers. Urban For. Urban Green. 20, 172–179. https://doi.org/10.1016/j.ufug.2016.08.010

Lafortezza, R., Sanesi, G., 2019. Nature-based solutions: Settling the issue of sustainable urbanization. Environ. Res. 172, 394–398.

https://doi.org/10.1016/j.envres.2018.12.063

Lee, A.C.K., Jordan, H.C., Horsley, J., 2015. Value of urban green spaces in promoting healthy living and wellbeing: Prospects for planning. Risk Manag. Healthc. Policy 8, 131–137. https://doi.org/10.2147/RMHP.S61654

Lee, L.S.H., Jim, C.Y., 2017. Subtropical summer thermal effects of wirerope climber green walls with different air-gap depths. Build. Environ. 126, 1–12. https://doi.org/10.1016/j.buildenv.2017.09.021

Leuzinger, S., Vogt, R., Körner, C., 2010. Tree surface temperature in an urban environment. Agric. For. Meteorol. 150, 56–62. https://doi.org/10.1016/j.agrformet.2009.08.006

Li, Cuimin, Wei, J., Li, Chunying, 2019a. Influence of foliage thickness on thermal performance of green façades in hot and humid climate. Energy Build. 199, 72–87. https://doi.org/10.1016/j.enbuild.2019.06.045

Ling, T.Y., Chiang, Y.C., 2018. Well-being, health and urban coherence-advancing vertical greening approach toward resilience: A design practice consideration. J. Clean. Prod. 182, 187–197. https://doi.org/10.1016/j.jclepro.2017.12.207

Liu, J., Kang, J., Behm, H., Luo, T., 2014. Effects of landscape on soundscape perception: Soundwalks in city parks. Landsc. Urban Plan. 123, 30–40. https://doi.org/10.1016/j.landurbplan.2013.12.003

Liu, L., Guan, D., Peart, M.R., Wang, G., Zhang, H., Li, Z., 2013. The dust retention capacities of urban vegetation-a case study of Guangzhou, South China. Environ. Sci. Pollut. Res. 20, 6601–6610. https://doi.org/10.1007/s11356-013-1648-3

Loga, T., Hacke, U., Müller, A., Großklos, M., Stein, B., Born, R., Renz, I., Hinz, E., Cischinsky, H., Hörner, M., 2017. Berücksichtigung des Nutzerverhaltens bei energetischen Verbesserungen. https://doi.org/ISSN 1868-0097

Magrini, A., Lisot, A., 2015. Noise Reduction Interventions in the Urban Environment as a form of Control of Indoor Noise Levels. Energy Procedia 78, 1653–1658. https://doi.org/https://doi.org/10.1016/j.egypro.2015.11.246

Malmqvist, T., Glaumann, M., Scarpellini, S., Zabalza, I., Aranda, A., Llera, E., Díaz, S., 2011. Life cycle assessment in buildings: The ENSLIC simplified method and guidelines. Energy 36, 1900–1907. https://doi.org/10.1016/j.energy.2010.03.026

Manso, M., Castro-Gomes, J., Paulo, B., Bentes, I., Teixeira, C.A., 2018. Life cycle analysis of a new modular greening system. Sci. Total Environ. 627, 1146–1153. https://doi.org/10.1016/j.scitotenv.2018.01.198

Manso, M., Castro-Gomes, J.J., 2015. Green wall systems: A review of their characteristics. Renew. Sustain. Energy Rev. 41, 863–871. https://doi.org/10.1016/j.rser.2014.07.203

Manso, M., Castro-Gomes, J.P., 2016. Thermal analysis of a new modular system for green walls. J. Build. Eng. 7, 53–62. https://doi.org/10.1016/j.jobe.2016.03.006

Mariani, L., Parisi, S.G., Cola, G., Lafortezza, R., Colangelo, G., Sanesi, G., 2016. Climatological analysis of the mitigating effect of vegetation on the urban heat island of Milan, Italy. Sci. Total Environ. 569–570, 762–773. https://doi.org/10.1016/j.scitotenv.2016.06.111

Mayrand, F., Clergeau, P., 2018. Green Roofs and Green Walls for Biodiversity Conservation: A Contribution to Urban Connectivity? Sustainability 10, 985. https://doi.org/10.3390/su10040985

Mazhar, N., Brown, R.D., Kenny, N., Lenzholzer, S., 2015. Thermal comfort of outdoor spaces in Lahore, Pakistan: Lessons for bioclimatic urban design in the context of global climate change. Landsc. Urban Plan. 138, 110–117. https://doi.org/10.1016/j.landurbplan.2015.02.007

Mazzali, U., Peron, F., Romagnoni, P., Pulselli, R.M., Bastianoni, S., 2013. Experimental investigation on the energy performance of Living Walls in a temperate climate. Build. Environ. 64, 57–66. https://doi.org/10.1016/j.buildenv.2013.03.005

Mazzucato, M., 2018. Mission-Oriented research and Innovation in the European Union. https://doi.org/10.2777/36546

McKinsey Center for Business and Environment, 2017. Focused acceleration: a strategic approach to climate action in cities in 2030.

Meili, N., Acero, J.A., Peleg, N., Manoli, G., Burlando, P., Fatichi, S., 2021. Vegetation cover and plant-trait effects on outdoor thermal comfort in a tropical city. Build. Environ. 195, 107733. https://doi.org/10.1016/j.buildenv.2021.107733

Mensink, C., De Maerschalck, B., Maiheu, B., Janssen, S., Vankerkom, J., 2011. The role of vegetation in local and Urban air quality, in: HARMO 2011 - Proceedings of the 14th International Conference on Harmonisation within Atmospheric Dispersion Modelling for Regulatory Purposes. pp. 471–475.

Ministerio de Transportes, M. y A.U.-G. de E., 2019. Agenda Urbana Española [WWW Document]. URL https://www.aue.gob.es

Mohtadi, T., 2016. The Complementarity of Improving Quality of Life and Reducing Environmental Footprints in Urban Spaces: The Argument of “hedonisitic Sustainability”. Consilience 16, 20–22.

Morales, P.F.H.Ó.D.R.D.S., 2012. Sistema JARDIN VERTICAL BIOFIVER ®. Vertiarte Jard. Verticales S.L.

Morris, K.I.K.I.J.K., Chan, A., Morris, K.I.K.I.J.K., Ooi, M.C.G.G., Oozeer, M.Y., Abakr, Y.A., Nadzir, M.S.M., Mohammed, I.Y., Al-Qrimli, H.F., 2017. Impact of urbanization level on the interactions of urban area, the urban climate, and human

thermal comfort. Appl. Geogr. 79, 50–72. https://doi.org/10.1016/j.apgeog.2016.12.007

Moya, T.A., van den Dobbelsteen, A., Ottelé, M., Bluyssen, P.M., 2018. A review of green systems within the indoor environment. Indoor Built Environ. 0, 1–12. https://doi.org/10.1177/1420326X18783042

Nadia, S., Noureddine, S., Hichem, N., Djamila, D., 2013. Experimental study of thermal performance and the contribution of plant-covered walls to the thermal behavior of building. Energy Procedia 36, 995–1001. https://doi.org/10.1016/j.egypro.2013.07.113

Nations, U., 2015a. Paris Agreement. Paris.

Nations, U., 2015b. Transforming our world: The 2030 agenda for sustainable development.

Nations, U., 2015c. Sustainable Development Goals (SDG) [WWW Document].

Nesshöver, C., Assmuth, T., Irvine, K.N., Rusch, G.M., Waylen, K.A., Delbaere, B., Haase, D., Jones-walters, L., Keune, H., Kovacs, E., Krauze, K., Külvik, M., Rey, F., Dijk, J. Van, Inge, O., Wilkinson, M.E., Wittmer, H., 2017. Science of the Total Environment The science , policy and practice of nature-based solutions : An interdisciplinary perspective. Sci. Total Environ. 579, 1215–1227. https://doi.org/10.1016/j.scitotenv.2016.11.106

Olivieri, F., 2013. Caracterización experimental y modelo predictivo de las prestaciones termicas de una pared verde. Universidad Politécnica de Madrid.

Olivieri, F., Grifoni, R.C., Redondas, D., Sánchez-Reséndiz, J.A., Tascini, S., 2017. An experimental method to quantitatively analyse the effect of thermal insulation thickness on the summer performance of a vertical green wall. Energy Build. 150, 132–148. https://doi.org/10.1016/j.enbuild.2017.05.068

Olivieri, F., Olivieri, L., Neila, J., 2014. Experimental study of the thermal-energy performance of an insulated vegetal façade under summer conditions in a continental mediterranean climate. Build. Environ. 77, 61–76. https://doi.org/10.1016/j.buildenv.2014.03.019

ONU-Habitat, n.d. Informe mundial sobre asentamientos humanos 2011. Las ciudades y el cambio climático: orientaciones para políticas.

Oquendo-Di Cosola, V., Olivieri, F., Ruiz-García, L., 2022. A systematic review of the impact of green walls on urban comfort: temperature reduction and noise attenuation. Renew. Sustain. Energy Rev. 162, 112463. https://doi.org/10.1016/j.rser.2022.112463

Oquendo-Di Cosola, V., Olivieri, F., Ruiz-García, L., Bacenetti, J., 2020. An environmental Life Cycle Assessment of Living Wall Systems. J. Environ. Manage. 254, 109743. https://doi.org/10.1016/j.jenvman.2019.109743

Oquendo-Di Cosola, V.O., Olivieri, F., Olivieri, L., Sánchez-Reséndiz, J.A., 2021. Towards urban transition: implementing nature-based solutions and renewable energies to achieve the Sustainable Development Goals (SDG). Techne 2, 102–105. https://doi.org/10.13128/techne-10691

Oquendo Di Cosola V., Sánchez-Reséndiz A., Olivieri L., O.F., 2019. Nature Based Solutions for Cities Resilience: opportunities for action in Madrid, in: ICSC-CITIES. Madrid.

Ottelé, M., Perini, K., 2017. Comparative experimental approach to investigate the thermal behaviour of vertical greened façades of buildings. Ecol. Eng. 108, 152–161. https://doi.org/https://doi.org/10.1016/j.ecoleng.2017.08.016

Ottelé, M., Perini, K., Fraaij, A.L.A.L.A.A., Haas, E.M.M., Raiteri, R., 2011. Comparative life cycle analysis for green façades and living wall systems. Energy

Build. 43, 3419–3429. https://doi.org/10.1016/j.enbuild.2011.09.010

Ottelé, M., van Bohemen, H.D., Fraaij, A.L.A., 2010. Quantifying the deposition of particulate matter on climber vegetation on living walls. Ecol. Eng. 36, 154–162. https://doi.org/10.1016/j.ecoleng.2009.02.007

Ow, L.F., Ghosh, S., 2017. Urban cities and road traffic noise: Reduction through vegetation. Appl. Acoust. 120, 15–20. https://doi.org/10.1016/j.apacoust.2017.01.007

P., O., 1997. Encyclopedia of vernacular architecture of the world. Cambridge Univ. Press.

Pan, L., Chu, L.M., 2015. Energy saving potential and life cycle environmental impacts of a vertical greenery system in Hong Kong: A case study, Building and Environment. Elsevier Ltd. https://doi.org/10.1016/j.buildenv.2015.06.033

Pan, L., Wei, S., Chu, L.M., 2018. Orientation effect on thermal and energy performance of vertical greenery systems. Energy Build. 175, 102–112. https://doi.org/10.1016/j.enbuild.2018.07.024

Pedrero, A., Navacerrada, M.Á., de la Prida, D., Iglesias, L., Díaz-Chyla, A., 2020. On the accuracy of the sound absorption measurement with an impedance gun. Appl. Acoust. 158, 107039. https://doi.org/https://doi.org/10.1016/j.apacoust.2019.107039

Pérez-Urrestarazu, L., Fernández-Cañero, R., Franco-Salas, A., Egea, G., 2015. Vertical Greening Systems and Sustainable Cities. J. Urban Technol. 22, 65–85. https://doi.org/10.1080/10630732.2015.1073900

Pérez, Gabriel, Coma, J., Barreneche, C., De Gracia, A., Urrestarazu, M., Burés, S., Cabeza, L.F., 2016a. Acoustic insulation capacity of Vertical Greenery Systems for buildings. Appl. Acoust. 110, 218–226.

https://doi.org/10.1016/j.apacoust.2016.03.040

Pérez, G, Coma, J., Cabeza, L.F., 2018. Vertical greening systems to enhance the thermal performance of buildings and outdoor comfort, in: Nature Based Strategies for Urban and Building Sustainability. pp. 99–108. https://doi.org/10.1016/B978-0-12-812150-4.00009-4

Pérez, Gabriel, Coma, J., Cabeza, L.F., 2018. Vertical greening systems for acoustic insulation and noise reduction. Nat. Based Strateg. Urban Build. Sustain. 157–165. https://doi.org/10.1016/B978-0-12-812150-4.00015-X

Pérez, G., Rincón, L., Vila, A., González, J.M., Cabeza, L.F., 2011. Behaviour of green facades in Mediterranean Continental climate. Energy Convers. Manag. 52, 1861–1867. https://doi.org/10.1016/j.enconman.2010.11.008

Perini, K., Ottelé, M., Giulini, S., Magliocco, A., Roccotiello, E., 2017. Quantification of fine dust deposition on different plant species in a vertical greening system. Ecol. Eng. 100, 268–276. https://doi.org/10.1016/j.ecoleng.2016.12.032

Perini, K., Ottelé, M., Haas, E.M., Raiteri, R., Ungers, O.M., 2011. Greening the building envelope , façade greening and living wall systems. Open J. Ecol. 1, 1–8. https://doi.org/10.4236/oje.2011.11001

Perini, K., Rosasco, P., 2013a. Cost-benefit analysis for green fa??ades and living wall systems. Build. Environ. 70, 110–121. https://doi.org/10.1016/j.buildenv.2013.08.012

Pioppi, B., Pigliautile, I., Piselli, C., Pisello, A.L., 2020. Cultural heritage microclimate change: Human-centric approach to experimentally investigate intra-urban overheating and numerically assess foreseen future scenarios impact. Sci. Total Environ. 703, 134448. https://doi.org/10.1016/j.scitotenv.2019.134448

Piselli, C., Castaldo, V.L., Pigliautile, I., Pisello, A.L., Cotana, F., 2018. Outdoor

comfort conditions in urban areas: On citizens' perspective about microclimate mitigation of urban transit areas. Sustain. Cities Soc. 39, 16–36. https://doi.org/10.1016/j.scs.2018.02.004

Potchter, O., Itzhak Ben-Shalom, H., 2013. Urban warming and global warming: Combined effect on thermal discomfort in the desert city of Beer Sheva, Israel. J. Arid Environ. 98, 113–122. https://doi.org/https://doi.org/10.1016/j.jaridenv.2013.08.006

Price, A., Jones, E.C., Jefferson, F., 2015. Vertical Greenery Systems as a Strategy in Urban Heat Island Mitigation. Water. Air. Soil Pollut. 226. https://doi.org/10.1007/s11270-015-2464-9

Przybysz, A., Sæbø, A., Hanslin, H.M., Gawroński, S.W., 2014. Accumulation of particulate matter and trace elements on vegetation as affected by pollution level, rainfall and the passage of time. Sci. Total Environ. 481, 360–369. https://doi.org/10.1016/j.scitotenv.2014.02.072

Pugh, T.A.M., MacKenzie, A.R., Whyatt, J.D., Hewitt, C.N., 2012. Effectiveness of green infrastructure for improvement of air quality in urban street canyons. Environ. Sci. Technol. 46, 7692–7699. https://doi.org/10.1021/es300826w

Razzaghmanesh, Mostafa, Razzaghmanesh, Morteza, 2017a. Thermal performance investigation of a living wall in a dry climate of Australia. Build. Environ. 112, 45–62. https://doi.org/10.1016/j.buildenv.2016.11.023

Renewable, I., Agency, E., 2018. Opportunities to accelerate national energy transitions through advanced deployment of renewables.

Romanova, A., Horoshenkov, K. V., Hurrell, A., 2019. An application of a parametric transducer to measure acoustic absorption of a living green wall. Appl. Acoust. 145, 89–97. https://doi.org/10.1016/j.apacoust.2018.09.020

Rueda, S., 2010. Sistema de indicadores y condicionantes para ciudades grandes y medianas.

Ruggeri, G., Mazzocchi, C., Corsi, S., 2016. Urban gardeners' motivations in a Metropolitan city: The case of Milan. Sustain. 8. https://doi.org/10.3390/su8111099

Ruiz-Páez, R., Díaz, J., López-Bueno, J.A., Asensio, C., Ascaso, M.S., Saez, M., Luna, M.Y., Barceló, M.A., Navas, M.A., Linares, C., 2023. Short–term effects of air pollution and noise on emergency hospital admissions in Madrid and economic assessment. Environ. Res. 219, 115147. https://doi.org/https://doi.org/10.1016/j.envres.2022.115147

Saaroni, H., Amorim, J.H., Hiemstra, J.A., Pearlmutter, D., 2018. Urban Green Infrastructure as a tool for urban heat mitigation: Survey of research methodologies and findings across different climatic regions. Urban Clim. 24, 94–110. https://doi.org/10.1016/j.uclim.2018.02.001

Sachs, J.D., Schmidt-Traub, G., Mazzucato, M., Messner, D., Nakicenovic, N., Rockström, J., 2019. Six Transformations to achieve the Sustainable Development Goals. Nat. Sustain. 2, 805–814. https://doi.org/10.1038/s41893-019-0352-9

Safikhani, T., Abdullah, A.M., Ossen, D.R., Baharvand, M., 2014. Thermal impacts of vertical greenery systems. Environ. Clim. Technol. 14, 5–11. https://doi.org/10.1515/rtuect-2014-0007

Salmond, J.A., Williams, D.E., Laing, G., Kingham, S., Dirks, K., Longley, I., Henshaw, G.S., 2013. The influence of vegetation on the horizontal and vertical distribution of pollutants in a street canyon. Sci. Total Environ. 443, 287–298. https://doi.org/10.1016/j.scitotenv.2012.10.101

Sánchez-Reséndiz, J.A., Ruiz-García, L., Olivieri, F., Ventura-Ramos, E., 2018.

Experimental assessment of the thermal behavior of a living wall system in semi-arid environments of central Mexico. Energy Build. 174, 31–43. https://doi.org/https://doi.org/10.1016/j.enbuild.2018.05.060

Säumel, I., Weber, F., Kowarik, I., 2015. Toward livable and healthy urban streets: Roadside vegetation provides ecosystem services where people live and move. Environ. Sci. Policy 62, 24–33. https://doi.org/10.1016/j.envsci.2015.11.012

Scarpa, M., Mazzali, U., Peron, F., 2014. Modeling the energy performance of living walls: Validation against field measurements in temperate climate. Energy Build. 79, 155–163. https://doi.org/10.1016/j.enbuild.2014.04.014

Schindler, B.Y., Blank, L., Levy, S., Kadas, G., Pearlmutter, D., Blaustein, L., 2016. Integration of photovoltaic panels and green roofs: review and predictions of effects on electricity production and plant communities. Isr. J. Ecol. Evol. 62, 68–73. https://doi.org/10.1080/15659801.2015.1048617

Sendra-Arranz, R., Oquendo, V., Olivieri, L., Olivieri, F., Bedoya, C., Gutiérrez, A., 2020. Monitorization and statistical analysis of south and west green walls in a retrofitted building in Madrid. Build. Environ. 183. https://doi.org/10.1016/j.buildenv.2020.107049

Serra, V., Bianco, L., Candelari, E., Giordano, R., Montacchini, E., Tedesco, S., Larcher, F., Schiavi, A., 2017. A novel vertical greenery module system for building envelopes: The results and outcomes of a multidisciplinary research project. Energy Build. 146, 333–352. https://doi.org/https://doi.org/10.1016/j.enbuild.2017.04.046

Shafiee, E., Faizi, M., Yazdanfar, S.A., Khanmohammadi, M.A., 2020. Assessment of the effect of living wall systems on the improvement of the urban heat island phenomenon. Build. Environ. 181, 106923.

https://doi.org/10.1016/j.buildenv.2020.106923

Sharifi, A., Khavarian-Garmsir, A.R., 2020. The COVID-19 pandemic: Impacts on cities and major lessons for urban planning, design, and management. Sci. Total Environ. 749, 1–3. https://doi.org/10.1016/j.scitotenv.2020.142391

Sheweka, S., Magdy, N., 2011. The living walls as an approach for a healthy urban environment. Energy Procedia 6, 592–599. https://doi.org/10.1016/j.egypro.2011.05.068

Sheweka, S.M., Mohamed, N.M., 2012. Green facades as a new sustainable approach towards climate change. Energy Procedia 18, 507–520. https://doi.org/10.1016/j.egypro.2012.05.062

Siano, D., Viscardi, M., Panza, M.A., 2016. Automotive Materials: An Experimental Investigation of an Engine Bay Acoustic Performances. Energy Procedia 101, 598–605. https://doi.org/https://doi.org/10.1016/j.egypro.2016.11.076

Sierra-Pérez, J., Boschmonart-Rives, J., Gabarrell, X., 2016. Environmental assessment of façade-building systems and thermal insulation materials for different climatic conditions. J. Clean. Prod. 113, 102–113. https://doi.org/10.1016/j.jclepro.2015.11.090

Smith, C., Levermore, G., 2008. Designing urban spaces and buildings to improve sustainability and quality of life in a warmer world. Energy Policy 36, 4558–4562. https://doi.org/10.1016/j.enpol.2008.09.011

Stone Jr., B., 2012. The City and the Coming Climate. Climate Changes in the Places We Live. Cambridge University Press.

Šuklje, T., Medved, S., Arkar, C., 2016. On detailed thermal response modeling of vertical greenery systems as cooling measure for buildings and cities in summer conditions. Energy 115, 1055–1068. https://doi.org/10.1016/j.energy.2016.08.095

Susorova, I., Azimi, P., Stephens, B., 2014. The effects of climbing vegetation on the local microclimate, thermal performance, and air infiltration of four building facade orientations. Build. Environ. 76, 113–124. https://doi.org/10.1016/j.buildenv.2014.03.011

Taleghani, M., 2018a. Outdoor thermal comfort by different heat mitigation strategies-A review. Renew. Sustain. Energy Rev. 81, 2011–2018. https://doi.org/10.1016/j.rser.2017.06.010

Tallis, M.J., Amorim, J.H., Calfapietra, C., Freer-Smith, P., Grimmond, S., Kotthaus, S., 2015. The impacts of green infrastructure on air quality and temperature. Handb. Green Infrastruct. 30–49. https://doi.org/10.4337/9781783474004.00008

Tamási, A., Dobszay, G., 2015. Requirements for Designing Living Wall Systems – Analysing System Studies on Hungarian Projects 78–87. https://doi.org/10.3311/PPar.8337

Tan, C.L., Wong, N.H., Jusuf, S.K., 2014a. Effects of vertical greenery on mean radiant temperature in the tropical urban environment. Landsc. Urban Plan. 127, 52–64. https://doi.org/10.1016/j.landurbplan.2014.04.005

Tan, C.L., Wong, N.H., Jusuf, S.K., Chiam, Z.Q., 2015. Impact of plant evapotranspiration rate and shrub albedo on temperature reduction in the tropical outdoor environment. Build. Environ. 94, 206–217. https://doi.org/10.1016/j.buildenv.2015.08.001

Tang, X., Yan, X., 2017. Acoustic energy absorption properties of fibrous materials: A review. Compos. Part A Appl. Sci. Manuf. 101, 360–380. https://doi.org/10.1016/j.compositesa.2017.07.002

Tedesco, S., Giordano, R., Montacchini, E., 2016. How to Measure the Green Façade Sustainability? A Proposal of a Technical Standard. Energy Procedia 96, 560–567.

https://doi.org/10.1016/j.egypro.2016.09.100

Teotónio, I., Silva, C.M., Cruz, C.O., 2021. Economics of green roofs and green walls: A literature review. Sustain. Cities Soc. 69. https://doi.org/10.1016/j.scs.2021.102781

Tong, Z., Baldauf, R.W., Isakov, V., Deshmukh, P., Max Zhang, K., 2016. Roadside vegetation barrier designs to mitigate near-road air pollution impacts. Sci. Total Environ. 541, 920–927. https://doi.org/10.1016/j.scitotenv.2015.09.067

UICN, 2020. Estándar Global de la UICN para soluciones basadas en la naturaleza. Un marco sencillo para la verificación, el diseño y la extensión de SbN 30.

UK Green Wall Association, 2013. UK Guide to Green Walls.

United Nations, 1987. Report of the World Commission on Environment and Development: Our Common Future. United Nations General Assembly document A/42/427.

United Nations - Department of Economic and Social Affairs-Population Division, 2018. The World ’s Cities in 2018 - Data Booklet.

United States Environmental Protection Agency (EPA), 2008. Reducing Urban Heat Islands: Compendium of Strategies. Urban HeatIsland Basics.

van de Wouw, P.M.F., Ros, E.J.M., Brouwers, H.J.H., 2017. Precipitation collection and evapo(transpi)ration of living wall systems: A comparative study between a panel system and a planter box system. Build. Environ. 126, 221–237. https://doi.org/10.1016/j.buildenv.2017.10.002

Van Den Berg, M., 2007. Night noise guidelines for Europe. Turkish Acoust. Soc. - 36th Int. Congr. Exhib. Noise Control Eng. INTER-NOISE 2007 ISTANBUL 7, 5016–5025.

Van Renterghem, T., Botteldooren, D., Verheyen, K., 2012. Road traffic noise shielding

by vegetation belts of limited depth. J. Sound Vib. 331, 2404–2425. https://doi.org/https://doi.org/10.1016/j.jsv.2012.01.006

Van Renterghem, T., Dekoninck, L., Botteldooren, D., 2020. Multi-stage sound planning methodology for urban redevelopment. Sustain. Cities Soc. 62, 102362. https://doi.org/10.1016/j.scs.2020.102362

Van Renterghem, T., Forssén, J., Attenborough, K., Jean, P., Defrance, J., Hornikx, M., Kang, J., 2015. Using natural means to reduce surface transport noise during propagation outdoors. Appl. Acoust. 92, 86–101. https://doi.org/10.1016/j.apacoust.2015.01.004

Van Renterghem, T., Hornikx, M., Forssen, J., Botteldooren, D., 2013. The potential of building envelope greening to achieve quietness. Build. Environ. 61, 34–44. https://doi.org/10.1016/j.buildenv.2012.12.001

Voogt, J.A., Oke, T.R., 2003. Thermal remote sensing of urban climates. Remote Sens. Environ. 86, 370–384. https://doi.org/10.1016/S0034-4257(03)00079-8

Vuckovic, M., Kiesel, K., Mahdavi, A., 2017. Studies in the assessment of vegetation impact in the urban context. Energy Build. 145, 331–341. https://doi.org/10.1016/j.enbuild.2017.04.003

Vujcic, M., Tomicevic-Dubljevic, J., Grbic, M., Lecic-Tosevski, D., Vukovic, O., Toskovic, O., 2017. Nature based solution for improving mental health and well-being in urban areas. Environ. Res. 158, 385–392. https://doi.org/10.1016/j.envres.2017.06.030

Wai, K.M., Yuan, C., Lai, A., Yu, P.K.N., 2020. Relationship between pedestrian-level outdoor thermal comfort and building morphology in a high-density city. Sci. Total Environ. 708, 134516. https://doi.org/10.1016/j.scitotenv.2019.134516

Wang, C., mohd-rahim, F., Chuing Loo, S., Miswan, N., 2014. Vertical greenery

systems (VGS) in urban tropics, Open House International.

Weerakkody, U., Dover, J.W., Mitchell, P., Reiling, K., 2018a. Quantification of the traffic-generated particulate matter capture by plant species in a living wall and evaluation of the important leaf characteristics. Sci. Total Environ. 635, 1012–1024. https://doi.org/10.1016/j.scitotenv.2018.04.106

Weerakkody, U., Dover, J.W., Mitchell, P., Reiling, K., 2018b. Evaluating the impact of individual leaf traits on atmospheric particulate matter accumulation using natural and synthetic leaves. Urban For. Urban Green. 30, 98–107. https://doi.org/10.1016/j.ufug.2018.01.001

Weerakkody, U., Dover, J.W., Mitchell, P., Reiling, K., 2018c. The impact of rainfall in remobilising particulate matter accumulated on leaves of four evergreen species grown on a green screen and a living wall. Urban For. Urban Green. 35, 21–31. https://doi.org/10.1016/j.ufug.2018.07.018

Wei, D., Yang, L., Bao, Z., Lu, Y., Yang, H., 2022. Variations in outdoor thermal comfort in an urban park in the hot-summer and cold-winter region of China. Sustain. Cities Soc. 77. https://doi.org/10.1016/j.scs.2021.103535

Weinmaster, M., 2009. Are green walls as “green” as they look? an introduction to the various technologies and ecological benefits of green walls. J. Green Build. 4, 1–18. https://doi.org/http://dx.doi.org/10.3992/jgb.4.4.3

Weißenberger, M., Jensch, W., Lang, W., 2014. The convergence of life cycle assessment and nearly zero-energy buildings: The case of Germany. Energy Build. 76, 551–557. https://doi.org/10.1016/j.enbuild.2014.03.028

Wernet, G., Bauer, C., Steubing, B., Reinhard, J., Moreno-Ruiz, E., and Weidema, B., 2016. The ecoinvent database version 3 (part I): overview and methodology.

WHO, 2003. Health Aspects of Air Pollution with Particulate Matter , Ozone and

Nitrogen Dioxide. Rep. a WHO Work. Gr. Bonn, Ger. 13–15 January 2003 98. https://doi.org/10.2105/AJPH.48.7.913

Wong, N.C.N.H., Kwang Tan, A.Y., Chen, Y., Sekar, K., Tan, P.Y., Chan, D., Chiang, K., Wong, N.C.N.H., 2010. Thermal evaluation of vertical greenery systems for building walls. Build. Environ. 45, 663–672. https://doi.org/10.1016/j.buildenv.2009.08.005

Wong, N H, Kwang Tan, A.Y., Tan, P.Y., Chiang, K., Wong, N.C., 2010. Acoustics evaluation of vertical greenery systems for building walls. Build. Environ. 45, 411–420. https://doi.org/10.1016/j.buildenv.2009.06.017

Wong, P.P.-Y., Lai, P.-C., Low, C.-T., Chen, S., Hart, M., 2016. The impact of environmental and human factors on urban heat and microclimate variability. Build. Environ. 95, 199–208. https://doi.org/10.1016/j.buildenv.2015.09.024

Xiao, X.D., Dong, L., Yan, H., Yang, N., Xiong, Y., 2018. The influence of the spatial characteristics of urban green space on the urban heat island effect in Suzhou Industrial Park. Sustain. Cities Soc. 40, 428–439. https://doi.org/10.1016/j.scs.2018.04.002

Xing, Y., Jones, P., Donnison, I., 2017. Characterisation of nature-based solutions for the built environment. Sustain. 9, 1–20. https://doi.org/10.3390/su9010149

Yahia, M., Johansson, E., 2014. Landscape interventions in improving thermal comfort in the hot dry city of Damascus, Syria–The example of residential spaces with detached buildings, Landscape and Urban Planning. https://doi.org/10.1016/j.landurbplan.2014.01.014

Yahia, M.W., Johansson, E., Thorsson, S., Lindberg, F., Rasmussen, M.I., 2018. Effect of urban design on microclimate and thermal comfort outdoors in warm-humid Dar es Salaam, Tanzania. Int. J. Biometeorol. 62, 373–385.

https://doi.org/10.1007/s00484-017-1380-7

Yang, F., Yuan, F., Qian, F., Zhuang, Z., Yao, J., 2018. Summertime thermal and energy performance of a double-skin green facade: A case study in Shanghai. Sustain. Cities Soc. 39, 43–51. https://doi.org/10.1016/j.scs.2018.01.049

Yilmaz, N.G., Lee, P.J., Imran, M., Jeong, J.H., 2023. Role of sounds in perception of enclosure in urban street canyons. Sustain. Cities Soc. 90, 104394. https://doi.org/10.1016/j.scs.2023.104394

Yin, H., Kong, F., Middel, A., Dronova, I., Xu, H., James, P., 2017. Cooling effect of direct green façades during hot summer days: An observational study in Nanjing, China using TIR and 3DPC data. Build. Environ. 116, 195–206. https://doi.org/10.1016/j.buildenv.2017.02.020

Yin, Y., Zhang, D., Zhen, M., Jing, W., Luo, W., Feng, W., 2022. Combined effects of the thermal-acoustic environment on subjective evaluations in outdoor public spaces. Sustain. Cities Soc. 77, 103522. https://doi.org/10.1016/j.scs.2021.103522

Zaid, S.M., Perisamy, E., Hussein, H., Myeda, N.E., Zainon, N., 2018. Vertical Greenery System in urban tropical climate and its carbon sequestration potential: A review. Ecol. Indic. 91, 57–70. https://doi.org/10.1016/j.ecolind.2018.03.086

Zhang, L., Deng, Z., Liang, L., Zhang, Y., Meng, Q., Wang, J., Santamouris, M., 2019. Thermal behavior of a vertical green facade and its impact on the indoor and outdoor thermal environment. Energy Build. 204. https://doi.org/10.1016/j.enbuild.2019.109502

Zhang, X.X., Wu, P.F., Chen, B., 2010. Relationship between vegetation greenness and urban heat island effect in Beijing City of China, in: Procedia Environmental Sciences. pp. 1438–1450. https://doi.org/10.1016/j.proenv.2010.10.157